GEOLOGICAL SURVEY OF CANADA
OPEN FILE 6547

Borehole Geophysical Logging in the Flin Flon Mining Camp

C.J. Mwenifumbo and A.L. Mwenifumbo

2012

Natural Resources Canada | Ressources naturelles Canada

Canada

GEOLOGICAL SURVEY OF CANADA
OPEN FILE 6547

Borehole Geophysical Logging in the Flin Flon Mining Camp

C.J. Mwenifumbo and A.L. Mwenifumbo

2012

doi:10.4095/291534

This publication is available from the Geological Survey of Canada Bookstore (http://gsc.nrcan.gc.ca/bookstore_e.php).
It can also be downloaded free of charge from GeoPub (http://geopub.nrcan.gc.ca/).

Recommended citation:
Mwenifumbo, C.J. and Mwenifumbo, A.L., 2012. Borehole Geophysical Logging in the Flin Flon Mining Camp; Geological Survey of Canada, Open File 6547, 75 p. doi:10.4095/291534

Publications in this series have not been edited; they are released as submitted by the author.

TABLE OF CONTENTS

1 INTRODUCTION

The Geological Survey of Canada (GSC) conducted multisensor borehole geophysical measurements in five drillholes ranging in depths from 200 m to 1790 m (Table 1) in the Flin Flon mining camp as part of the Targeted Geosciences Initiative 3 (TGI-3). The parameters that were measured included natural gamma ray spectrometry (total count gamma, potassium, uranium and thorium), spectral gamma-gamma density, full waveform sonic, magnetic susceptibility, inductive conductivity, and temperature. Magnetic susceptibility, conductivity, temperature and total count gamma were acquired with the IFG multiparameter probes/data acquisition system. Natural gamma ray spectrometry, spectral gamma-gamma density and temperature were acquired with the GSC probes/data system. The full waveform sonic data were acquired with the Mount Sopris probe.

Table 1: *Coordinates of the five drillholes that were geophysically logged by the Geological Survey of Canada in 2006. 4Q66W3 was drilled to 2134 m but logged to 1060 m because of a blockage.*

Borehole	Easting	Northing	Elevation	Angle	Hole	Casing	Depth
FFM001	52883.84	-18923.16	256000	-85	BQ	3.66	1793
4Q66W3	51292.23	-18021.67	2532.93	-85	BQ	0.30	2134
FFS039	49711.66	-18650.57	2547.71	-55	BQ	3.00	1121
4Q62	3+50W	85+99N		-55	BQ	1.98	212
FS036	-508.00	-4772.00	2560.00	-55	NQ	3.50	1265

The locations of the drillholes are presented in Figures 1 and 2. Not all of the parameters mentioned above were logged in each of these drillholes.

The two primary objectives of the logging program were:

(1) to collect acoustic physical rock property data (density, P-wave velocity and acoustic impedance) for the seismic sub-project to aid in the modelling and interpretation of seismic surveys.

(2) to collect physical rock properties to characterize the different lithology, alteration and mineralization in the mining camp.

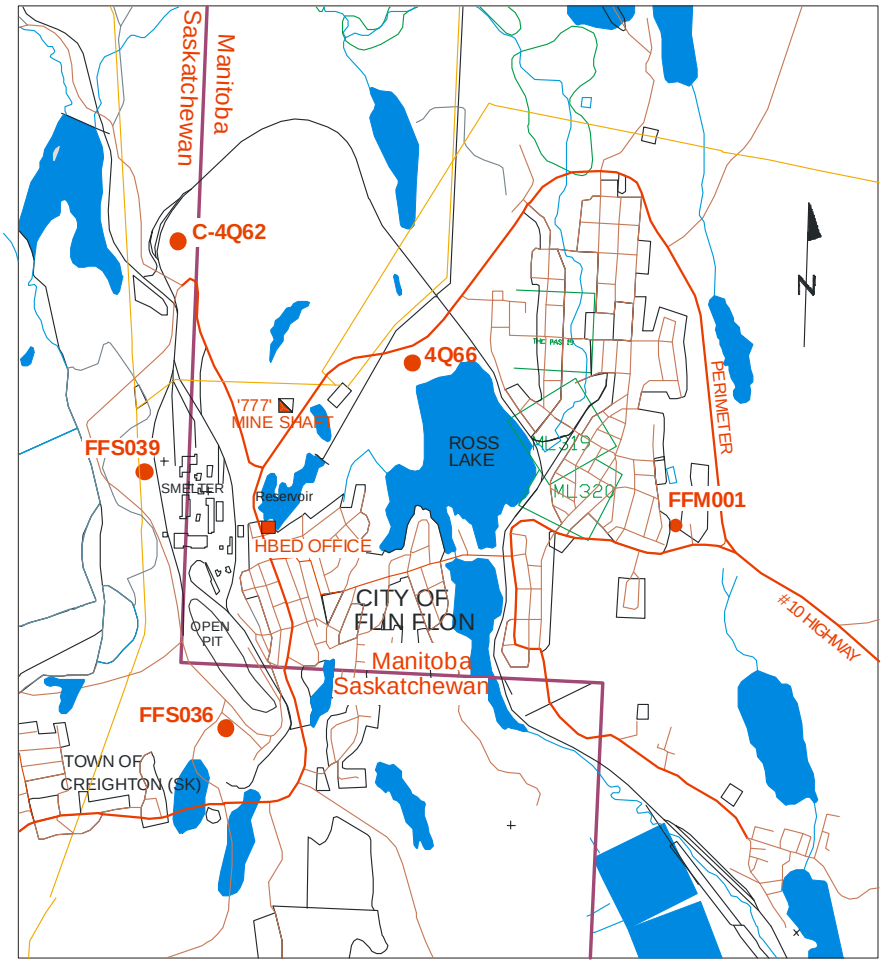

Figure 1: *Location of the 2006 physical property logging, Flin Flon area, Manitoba. NTS: 63K12NW, 13SW. Scale: 1:25000 (after Alan Vowles, Hudson Bay Exploration and Development Ltd, 2008)*

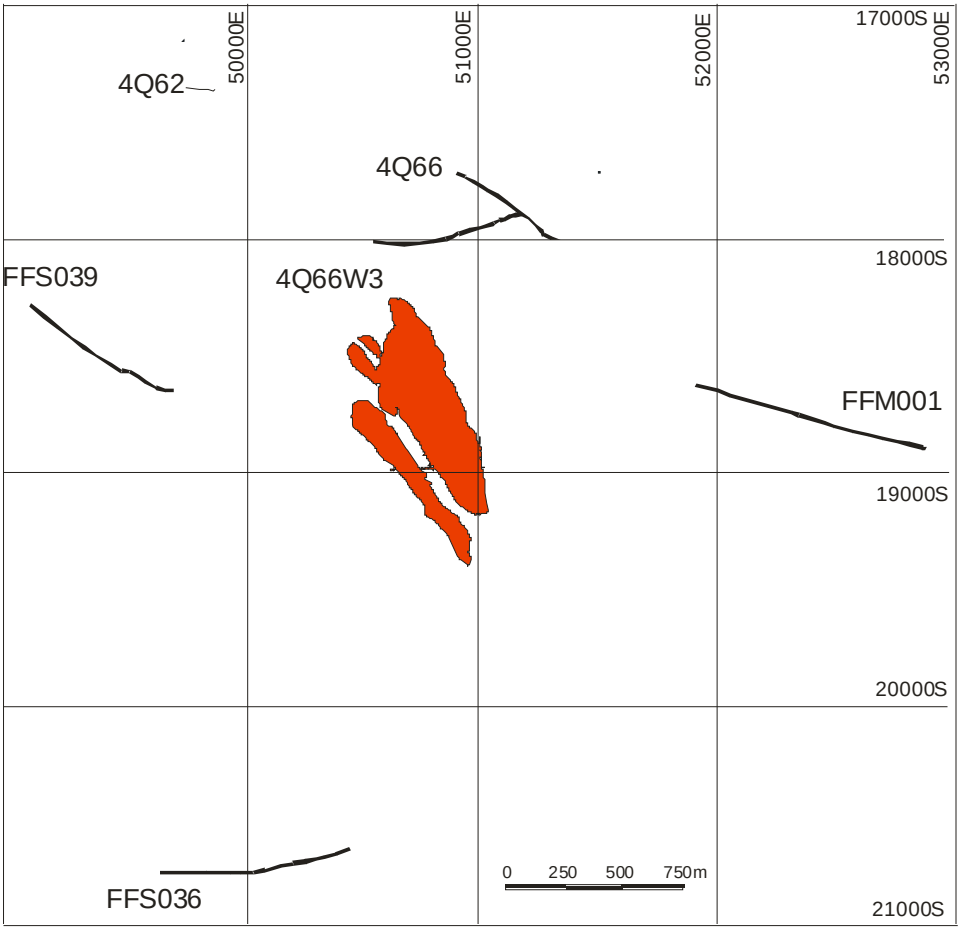

Figure 2. *Surface projection of the drillholes that were geophysically logged for physical properties in relation to the plan view of the Triple 7 orebody (after Alan Vowles, Hudson Bay Exploration and Development Ltd, 2008)*

2 GEOLOGY OF THE FLIN FLON MINING CAMP

The dominant units in the Flin Flon camp include: ca. 1.85 Ga Missi group sediments that consist of arkose, greywacke and conglomerate; and older ca. 1.88 Ga igneous rocks of the Flin Flon assemblage (Gibson et la., 2011). The latter comprises basalt-basaltic andesite flows/volcaniclastics, rhyolite flows, domes and volcaniclastics, synvolcanic gabbro and diorite. Younger intrusive rocks include mafic intrusions of the Boundary suite (Gibson et la., 2011) and quartz feldspar porphyry of the Phantom intrusive suite. An informal stratigraphy of the Flin Flon district, developed under the TGI I and TGI III, comprises four formations; the Flin Flon, Hidden, Louis and Douglas formations. Figure 3 shows the geological map of the Flin Flon mining camp. Also included on the map are the locations of the drillholes that were geophysically logged.

The Flin Flon formation is subdivided into three members; the Club member that consists of massive rhyolites, rhyolite breccias, and rhyolite-clast-bearing mafic volcaniclastic and bedded tuff; the Blue Lagoon member, that lies conformably on the Club member, consisting of plagioclase phyric flows and plagioclase crystal-rich volcaniclastics; and the Millrock member. The Millrock member is host to massive sulphides in the Flin Flon mining camp. Several lithofacies are recognized in this member including plagioclase porphyritc basaltic pillowed flows that are intercalated with amoeboid breccias, basaltic scoria, and quartz-feldspar phyric rhyolite and rhyolite breccias. Massive sulphides are generally localized within felsic volcanic units (rhyolite and rhyolite volcaniclastics) and capped with bedded tuffs (Figure 9, in Gibson et la., 2011).

The Hidden formation is composed of mafic flows, sills and volcaniclastic rocks with lesser basaltic-andesite flows, rhyolite flows and felsic volcaniclastic rocks (Gibson et la., 2011). Its base, the basaltic andesite flows, is placed at the last occurrence of tuff and/or rhyolite of the Hidden formation. Several members have been recognized in the Hidden formation including 1920 member, Reservoir member, Stockwell member and Carlisle Lake member (refer to Gibson et la., 2011 for a detailed description of these lithofacies).

The Louis formation is composed of basalt flows and mafic volcaniclastic rocks with minor amounts of rhyolite flows and felsic volcaniclastic rocks. The rhyolites form the base of the Louis formation.

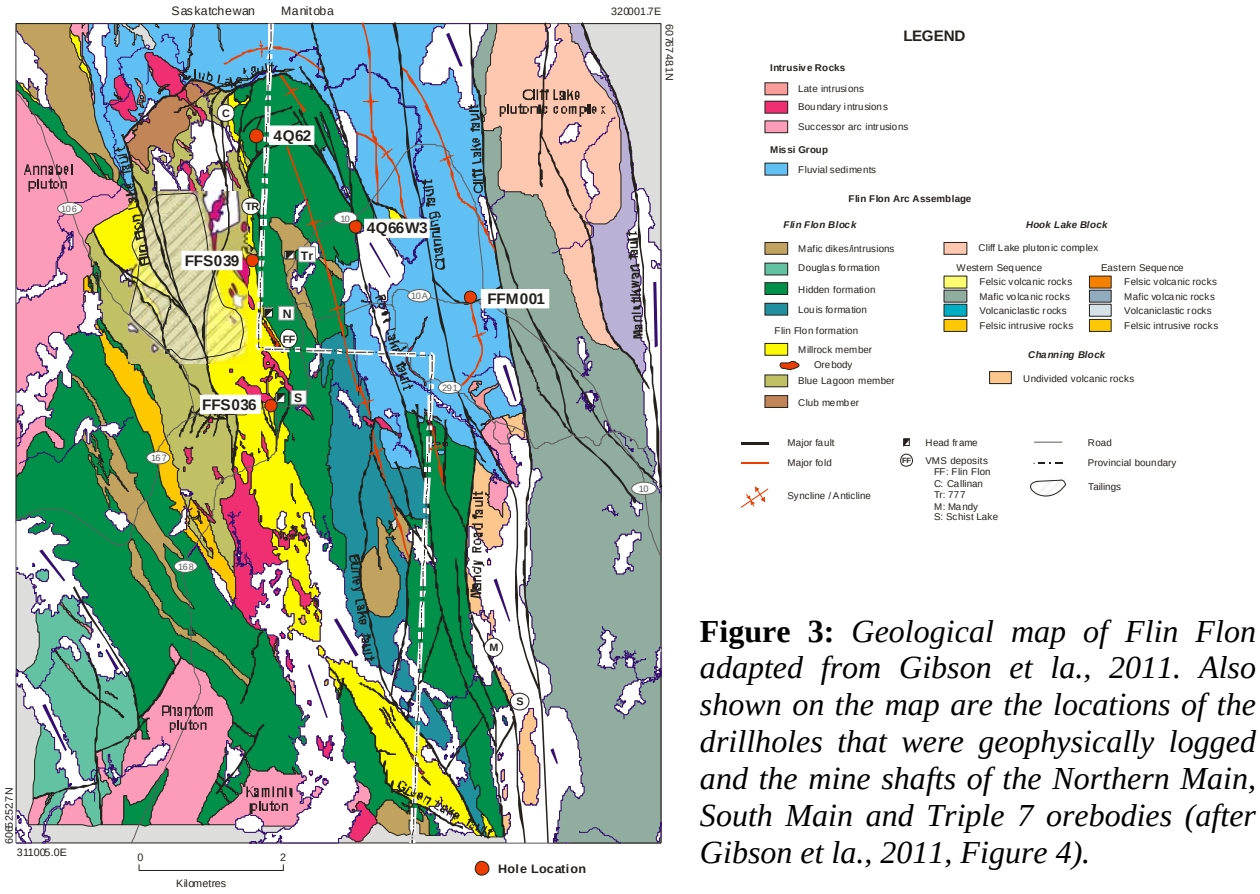

Figure 3: *Geological map of Flin Flon adapted from Gibson et la., 2011. Also shown on the map are the locations of the drillholes that were geophysically logged and the mine shafts of the Northern Main, South Main and Triple 7 orebodies (after Gibson et la., 2011, Figure 4).*

Figure 4 shows an east-west geological section across the Flin Flon mining camp with the approximate locations of the two deep drillholes, FFM001 and 4Q66W3. FFM001 was drilled through thick Missi sediments and the bottom section of the hole intersects an aphyric member that consists of basalt flows and fragmentals, diorites and feldspar-quartz porphyry. 4Q66W3 was drilled through the porphyritic member of the Hidden Formation. 4Q66W3 is depicted to intersect the Ross Lake fault.

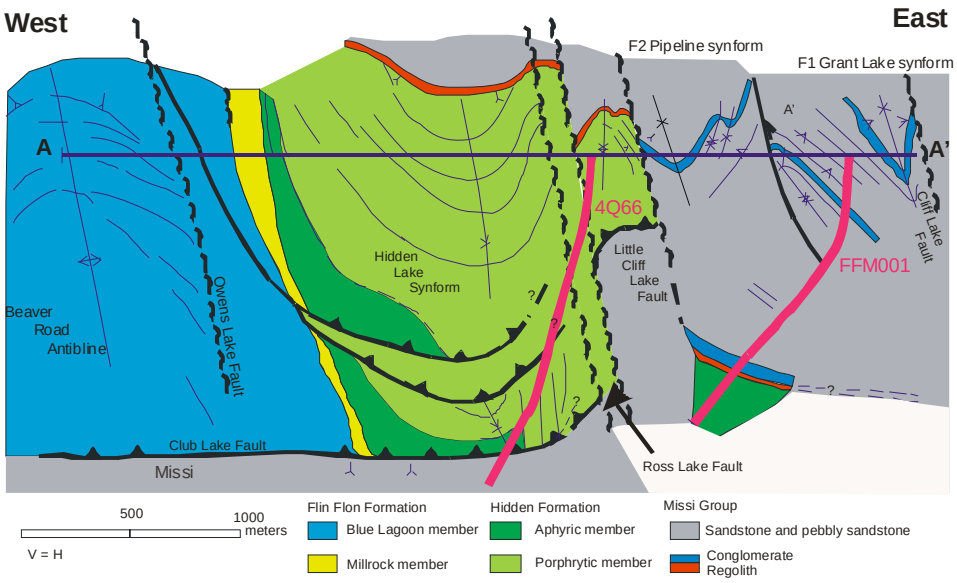

Figure 4: *East-west geological section across the Flin Flon mining camp showing the locations of FFM001 drilled through the thick Missi group and that of 4Q66W3 (after Sally Pehrsson, 2007)*

Drill core geology for the five drillholes is presented in the following sections in the form of lithology columns for each hole. These brief descriptions are summarized from the drill core logging conducted by the Hudson Bay Exploration and Development Company.

2.1 Geology Intersected in FFM001

Drillhole FFM001 was drilled to investigate a possible occurrence of volcanogenic massive sulphide deposits located under a thick cover of younger Missi sediments. The following significant rock units are intersected by FFM001:

(1) Missi sedimentary rocks consisting of a sequence of arkosic sandstone, greywacke and pebble conglomerates between 2.8 m and 883.13 m,
(2) amygdaloidal basalts (883.13 m – 974.0 m),
(3) Missi sedimentary rocks (arkose, greywacke and pebble conglomerates) (974.0 m– 1162.24 m), and
(4) an amygdaloidal and feldspar-phyric basalt package (1162.34 m - 1793.0 m) that includes feldspar-quartz porphyry, diorite, mafic tuffs and basalts.

A rhyolite – chloritic and carbonitized quartz-porphyry, intersected between 1231.5 m and 1237.5 m, is of particular significance in terms of mineralization.

There is extensive fracturing/faulting and alteration within the Missi sedimentary rocks. Alteration observed in the Missi sediments comprises hematite, carbonate and chlorite and is mainly confined to the faulted/sheared/ fractured sections. Primary (detrital) and secondary (alteration) magnetite is prevalent within the sediments.

The major alteration in the amygdaloidal and feldspar-phyric basalt package includes carbonate, quartz and chlorite (quartz-calcite-chlorite veining is prevalent). There are traces of mineralization that include disseminated pyrite, pyrrhotite, chalcopyrite and magnetite.

Figure 5 shows a generalized geologic column of FFM001 from 800 m -1793 m of Missi sediments, Hidden formation basalt flows, diorites, feldspar quartz porphyry and volcaniclasitics. The section above 800 m is all Missi sediments. An expanded section from 1550 to 1793 m (Figure 5b) shows intermixed feldspar-quartz porphyry, diorite and basalts with thick mafic volcaniclastics. Silicification and carbonatization are the major alteration in this rock package.

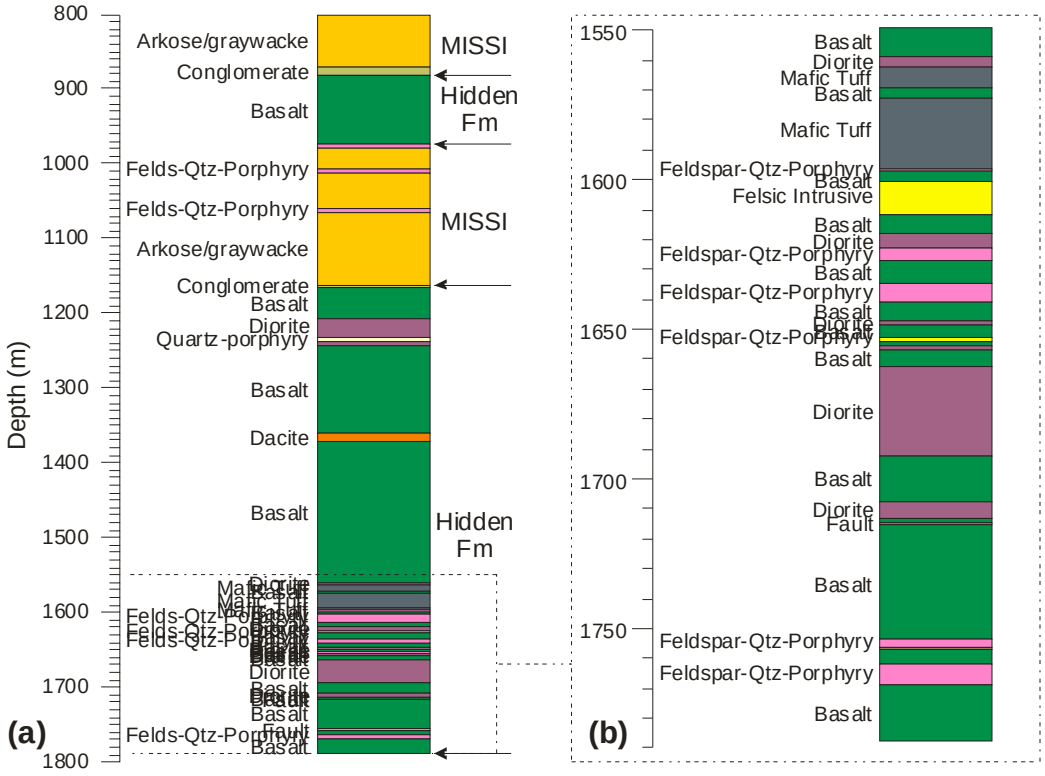

Figure 5: (a) *Lithology column of drillhole FFM001 presented from 800 to the bottom of the drillhole. The upper 800 m is all Missi sediments. (b) An expanded section from 1500 to the bottom of the drillhole is presented in the right hand column. Lithology summarized from Hudson Bay Exploration and Development Company Limited diamond drill log report, 1998.*

2.2 Geology Intersected in 4Q66W3

4Q66W3 was drilled to 2134 m (wedged at 880 m). The lithology columns presented in Figure 6 only show the geophysically logged interval (0–1070m). The drillhole intersects mostly Hidden formation rocks consisting of porphyritic basalt flows and fragmentals with occasional gabbros, diorite and rhyolite in this interval. There are several sections with missing drill core. This drillhole is a good candidate for using borehole geophysical logs to fill-in the missing lithology.

The rhyodacite intrusives are slightly mineralized with disseminated pyrite and pyrrhotite. The basalt flows and fragmentals are highly altered.

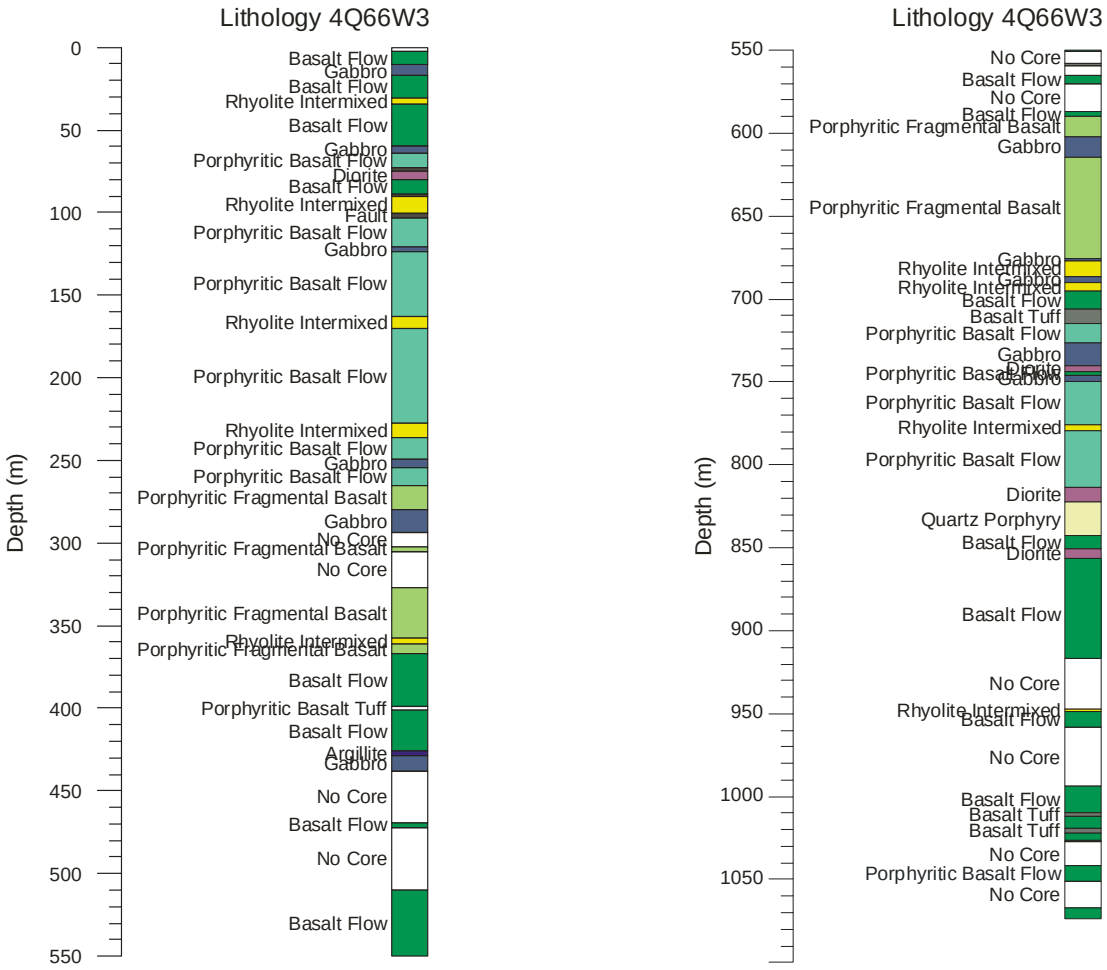

Figure 6: *Lithology columns for drillhole 4Q66W3 from 0 to 550 m and 550 m to 1070 m. 4Q66W3 is wedge # 3 from 4Q66 drillhole starting at 880 m and drilled to a depth of 2134m. The lithology column is presented to the geophysically logged depth. The hole was plugged beyond 1070 m. Lithology summarized from Hudson Bay Exploration and Development Company Limited diamond drill log report for hole 4Q66W3, 1994.*

2.3 Geology Intersected in FFS039

Drillhole FFS039 is located west of the smelter and west of the Triple 7 orebody. This hole was drilled to test the possible faulted duplication of the Flin Flon mine horizon. The major lithology/stratigraphy intersected in FFS039 is shown in Figure 7. The upper gabbro unit that is not magnetite-rich (125 m – 162 m) has several feldspar-porphyritic and potassic altered rhyolite dykes. Both the gabbroic boundary intrusion and the basalts are highly altered. Quartz, carbonate, potassic, epidote and chlorite alteration are the most prevalent (Ames et la., 2002). The bottom of the hole intersects the felsic intrusions and diorite that belong to the Flin Flon horizon. No significant mineralization is intersected in this hole. However, disseminated pyrite in all lithology is a product of the alteration.

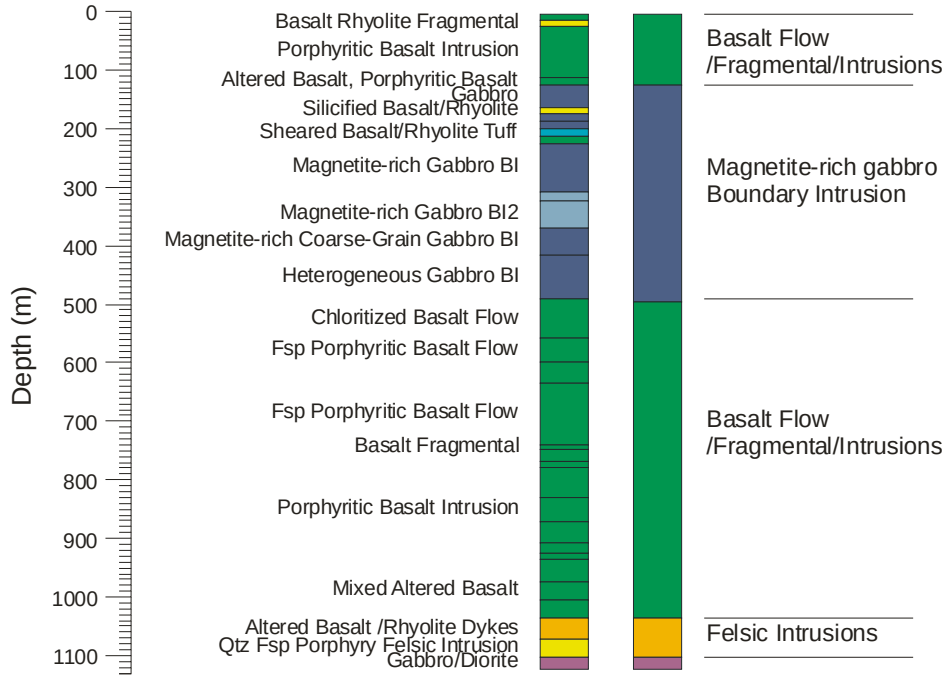

Figure 7: *Lithology column of drillhole FFS039. The right hand column is generalized lithology. Late magnetite-rich boundary intrusion gabbros intrude through the basalt flows and fragmentals. Lithology summarized from Hudson Bay Exploration and Development Company Limited diamond drill log report for hole FFS039, 2006.*

2.4 Geology Intersected in 4Q62

Drillhole 4Q62 is located north of the Calliman deposit and intersects significant mineralization. Figure 8 shows the lithology and visual estimates of the five main sulphide minerals: pyrite, pyrrhotite, sphalerite, and chalcopyrite. The Flin Flon rhyolite flows and tuffs are hosts to mineralization. Chlorite and carbonate alteration are prevalent in all the lithologies intersected in this drillhole.

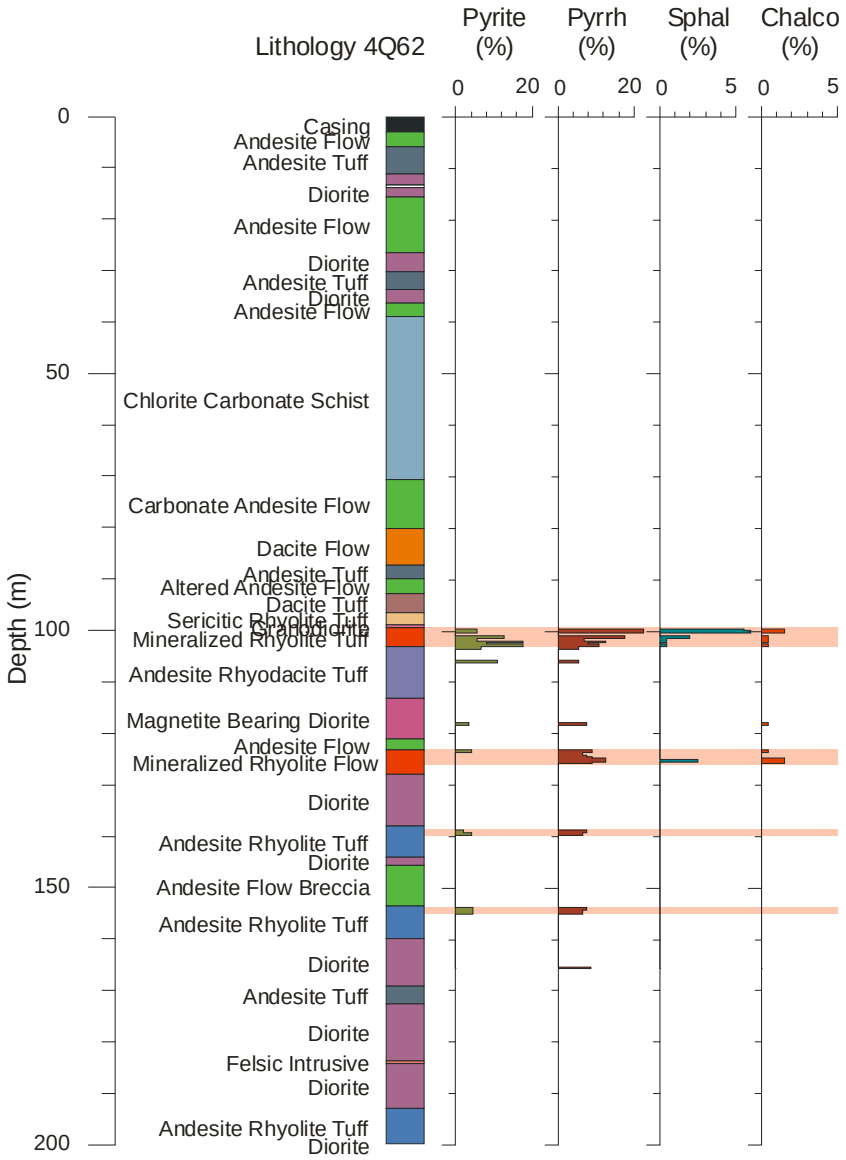

Figure 8: *Lithology column of drillhole 4Q62. The visual percent sulphide mineralization is presented on the right hand side. Pyrrh=pyrrhotite, Sphal=sphalerite, Chalco=chalcopyrite.*

2.5 Geology Intersected in FFS036

Drillhole FFS036 is located north of the south main shaft of the Flin Flon mine. FFS036 was drilled to test the possible faulted duplication of the Flin Flon mine horizon. The major lithologies intersected in FFS036 include basalts, rhyolites, gabbro and granodiorite belonging to the three major stratigraphic units: the Flin Flon Footwall stratigraphy, the Blue Lagoon member and the Mill Rock member (Figure 9)

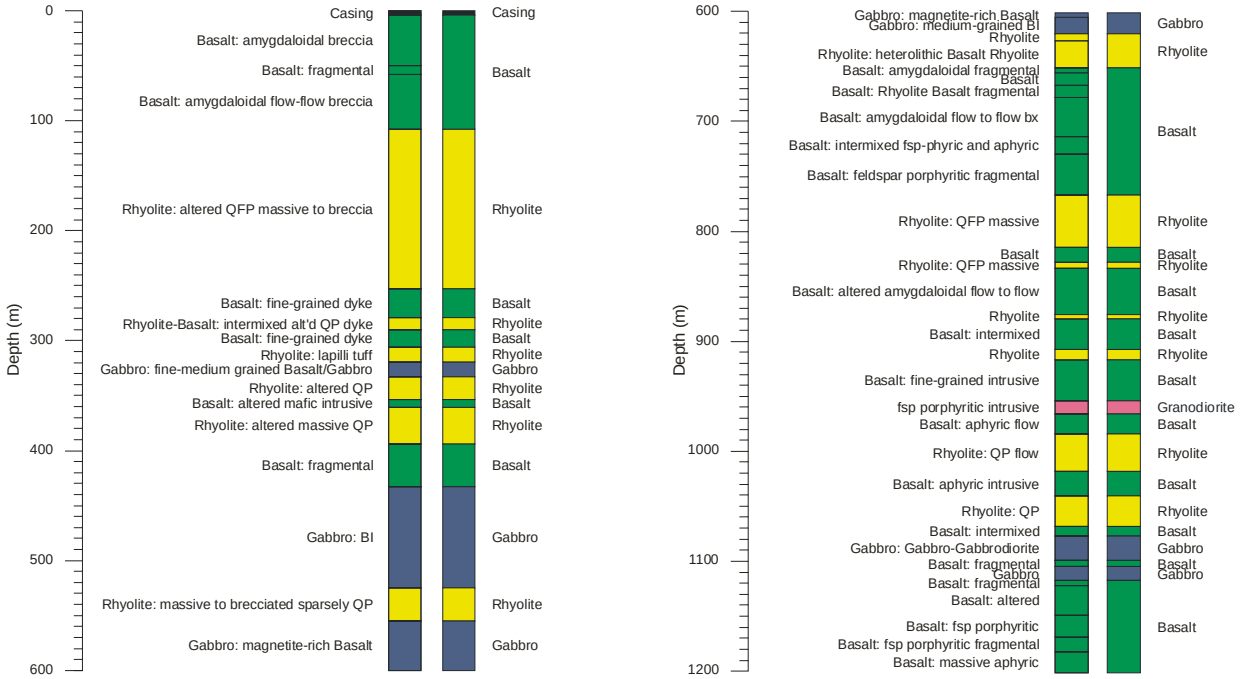

Figure 9: *Lithology columns generated from the drill core geology: for 0 m to 600 m and 600 m to 1200 m. The left hand lithology column is a detailed geological description of the intersected lithology and the right-hand column represents a generalized geology column. Lithology summarized from Hudson Bay Exploration and Development Company Limited diamond drill log report for hole FFS036, 2005.*

3 BOREHOLE GEOPHYSICAL LOGGING

The suite of geophysical logs acquired in the Flin Flon mining camp included natural gamma ray spectrometry, spectral gamma-gamma density, full waveform sonic, magnetic susceptibility, conductivity, total count gamma and temperature. Magnetic susceptibility, conductivity, temperature, natural gamma ray (total count) and resistivity were acquired with the IFG multiparameter probe. Only the magnetic susceptibility, conductivity, temperature and total count gamma ray logs will be presented here. As the conductivity measurements were not calibrated, they are presented as voltages.

Four drillholes were logged with the GSC logging system with a combined total depth of 2.43 km. Two drillholes, FF001 and FFS036, were logged under contract to DGI Geosciences Inc. DGI logging in FFM001 consisted of total count gamma, density, magnetic susceptibility and temperature logs to a total depth of 1766 m (drillhole depth 1793m). The density log is not calibrated and is presented as arbitrary units (AU). Drillhole FFS039 was logged to a depth of 1269 m with magnetic susceptibility and neutron logging tools.

The results of the borehole geophysical logging are presented, for each hole, as geophysical signatures that are characteristic for mapping lithology and alteration, and for delineating mineralization. This suite of geophysical logs can be grouped into two categories:

- Rock properties of interest for characterizing lithology, alteration and mineralization that include radiometric logs (K, U, and Th), magnetic susceptibility, and resistivity/ conductivity.
- Rock properties that affect seismic wave propagation and are of interest for mapping structures/ faults include compressional wave velocity and density logs.

3.1 FFM001 Borehole Geophysical Logs

Borehole geophysical logging was initially carried out by DGI Geosciences who collected total count gamma, density, magnetic susceptibility and temperature logs. FFM001 was revisited with the GSC logging system. Borehole FFM001 intersects 1600 m of Missi sediments consisting of arkosic sandstone, greywacke and conglomerate. There is a basaltic wedge between 870 and 970 m.

3.1.1 Lithology and alteration signatures

Hanging wall rocks

Figure 10 shows total count gamma, magnetic susceptibility, density and P-wave velocity logs over a section of borehole from 1100 m to 1400 m. The rocks intersected in this section constitute the hanging wall rocks that consist mainly of the Missi sediments and basalt flows with minor igneous rocks that include felsic rocks (quartz porphyry) and basic rocks (dacite flows and diorite).

All four geophysical logs show relatively uniform responses within the Missi sediments. These Missi sedimentary rocks exhibit high gamma ray activity, relatively low magnetic susceptibility compared to the igneous rocks, low density, and low P-wave velocities. Alteration zones of disseminated magnetite are depicted by increased magnetic susceptibility. The Missi conglomerates exhibit lower gamma ray activity than what is observed in the upper Missi sediments. The conglomerates also have higher densities and velocities as compared to the Missi sediments.

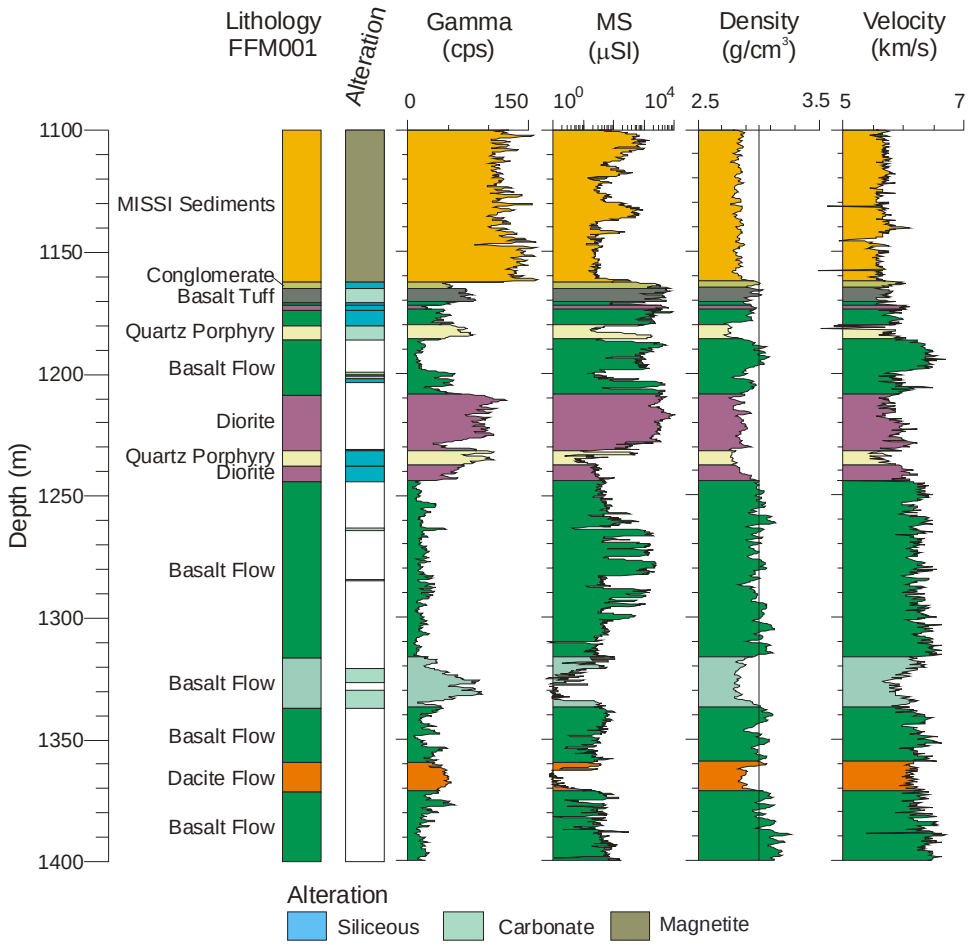

Figure 10 *Lithology and alteration columns, total count natural gamma ray, magnetic susceptibility, density and velocity logs from 1500 m to 1750 m in FFM001. Magnetic susceptibility is plotted on a logarithmic scale. The lithology is superimposed on the geophysical logs.*

The basalt flow package is characterized by low natural gamma ray activity; its densities and velocities are higher than those observed in all the other rock types. The basalt wedge between Missi sediments, at 880 m – 980 m (not shown in Figure 10) consists mainly of amygdaloidal basalts that are highly magnetic. There are also foliated, veined and altered basalts that exhibit lower magnetic susceptibilities. Some basalt dykes are non-magnetic and hence exhibit low magnetic susceptibilities.

The quartz-phyric basalts with carbonate alteration have higher potassium content, lower densities and lower velocities than unaltered basalts (e.g., 1320 m - 1340 m). The epidote alteration zones show higher magnetic susceptibility (e.g., 1260 m - 1300 m) due to the development of secondary magnetite.

The diorites have high natural gamma ray activity due, mainly, to high K content (as opposed to U or Th, see radiometric section). Here the densities and velocities are lower than in the basalts.

Lower volcanic rocks

Figure 11 shows lithology, alteration and mineralization columns, total count gamma, magnetic susceptibility, density and P-wave velocity logs over a section of the borehole from 1550 to 1750 m. This section is composed of flow and fragmental basalts, diorites, rhyolites and feldspar porphyries.

The gamma ray log clearly distinguishes between the different types of lithology. The feldspar porphyry has the highest gamma ray activity, followed by the diorites and rhyolite intrusion. The lowest gamma ray activity is observed in the basalts. However, there are some variations in the gamma ray activity in these basalts that is more likely due to alteration (e.g., basalt between 1693 and 1709 m that exhibits decreasing gamma ray activity and increasing magnetic susceptibility towards the underlying diorite suggests depletion of potassic minerals and increase in magnetite). Carbonate alteration was identified in the drill core within this basalt unit. The geophysical response characteristics in the diorite also vary along the different intersections primarily due to alteration. The diorite intersection at 1708 m -1714 m, for instance, exhibits higher density, higher velocity, and extremely low gamma ray values compared to other diorites (e.g., 1663 m – 1693 m). This diorite may have been misidentified in the drillcore lithology logging and could represent a different type of intrusion.

There are also some distinct changes in magnetic susceptibility, density and P-wave velocity among the different lithologies. The rhyolites and feldspar porphyries are characterized by very low susceptibilities, densities and P-wave velocities. The basalts exhibit higher susceptibilities, densities and P-wave velocities.

Alteration consists primarily of carbonatization and silicitization. Silicified zones have higher natural gamma ray values compared to carbonatized zones implying that quartz alteration is accompanied by sericite alteration.

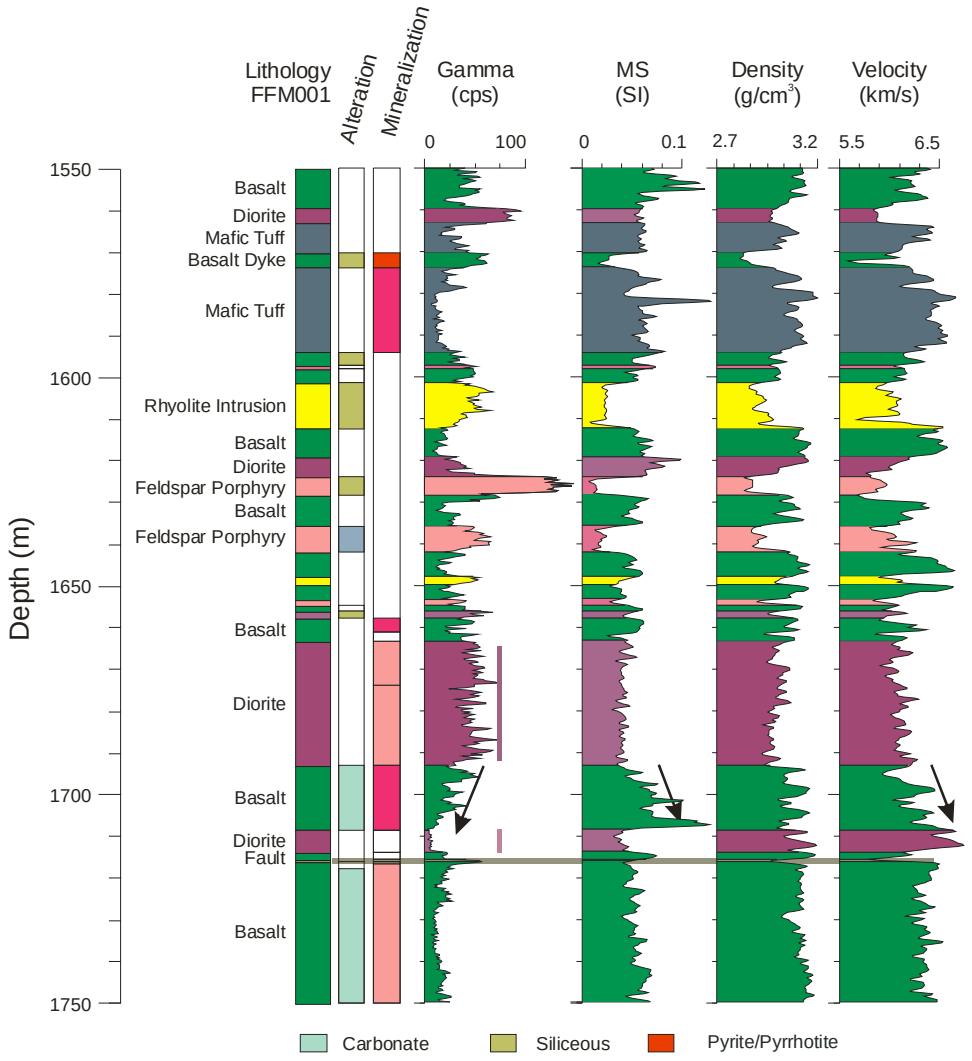

Figure 11: *Lithology, alteration and mineralization columns, total count natural gamma ray, magnetic susceptibility, density and P-wave velocity logs plotted from 1500 m to 1750 m in FFM001. The lithology is superimposed on the geophysical logs.*

An interesting geophysical response to alteration is observed in the basalt flow between 1693 m and 1708 m. This basalt intersection is carbonate altered and mineralized with disseminated pyrite and pyrrhotite. The gamma ray response shows decreasing activity towards the diorite below, whereas the magnetic susceptibility and P-wave velocity response show increasing values towards the diorite. Pyrrhotite may be responsible for the increases in magnetic susceptibility.

3.1.2 Radiometric signature

Four logs are determined from the gamma ray spectral data: the total count log (count rate summed up in an energy window from ~ 0.1 to 3.0 MeV), and the K, eU and eTh logs. The prefix 'e' in eU and eTh denotes equivalent trace element radioelement determination because these measurements are made indirectly by counting gamma-rays from daughter isotopes of U and Th, assuming radioactive equilibrium. The total count gamma-ray log monitors the overall gamma-ray activity and does not discriminate between the different sources of radioactivity.

Figures 12 and 13 show the four radiometric logs determined from the gamma-ray spectrometric data (Total count gamma, K, eU, and eTh) from 1100m to 1400 m and 1550 to 1750 m, respectively. In the Missi sediments all the three radioelements are present and contribute to the overall radioactivity. The high K, eU and eTh in Missi sediments suggest the arkoses and greywacke are late stage felsic intrusions.

One interesting observation is that the diorite between 1210 m and 1240 m (Figure 12) has elevated K and eTh which suggests that this is a lithology characteristic and not a function of alteration. There is also a distinct difference in the radiometric signature of the feldspar porphyries between 1520 m and 1550 m (Figure 13). The upper porphyry unit has high K and Th whereas the lower porphyry unit only has elevated K content. This difference suggests that we may be looking at two different intrusions. This idea is also supported by the differences between diorites (1570 m – 1720 m, Figure 13).

The porphrytic basalt flows have low radioelement content except where there is potassic alteration (1315 m -1335 m, Figure 12)). This zone is indicated as a carbonate alteration zone but the high K content suggests sericitization is the major alteration in this zone.

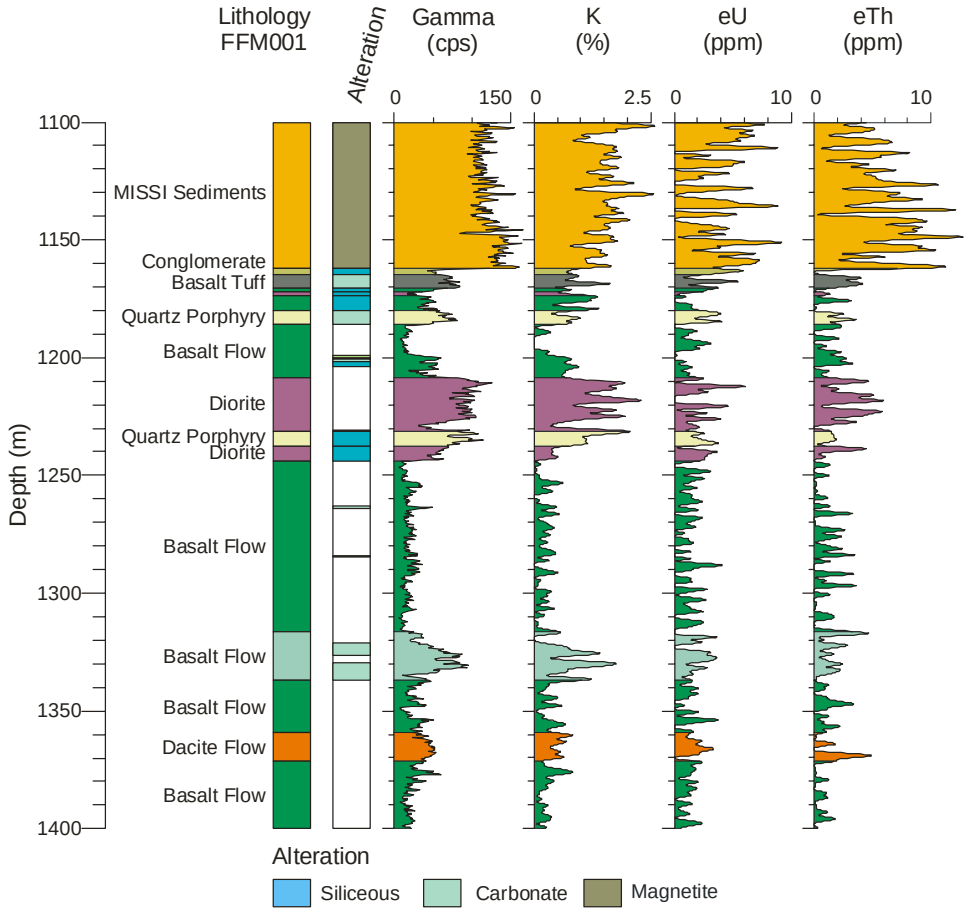

Figure 12*: Lithology and alteration columns, and the four radiometric logs; total count gamma, K, equivalent U (eU) and equivalent Th (eTh) acquired in FFM001 plotted from 1100 m to 1400 m. The lithology is superimposed on the geophysical logs. The Missi sediments above 1100m have the same radiometric signature and hence are not plotted.*

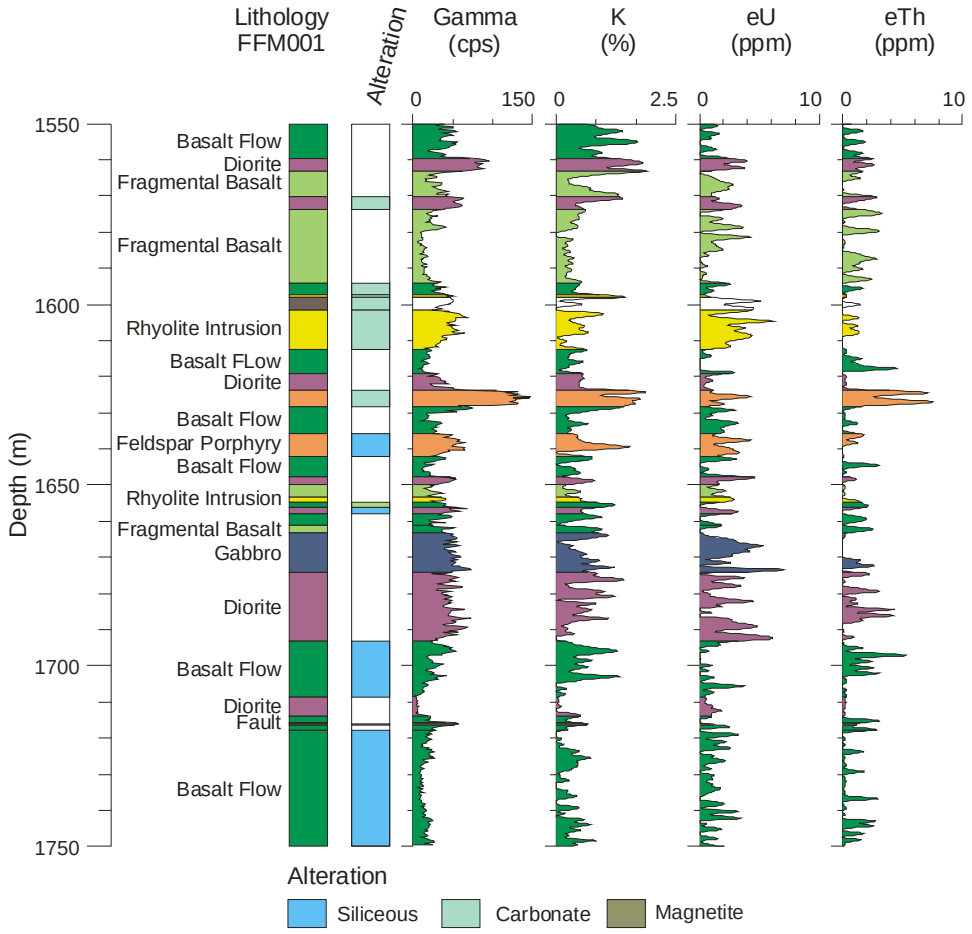

Figure 13: *Lithology and alteration columns and the radiometric logs (Gamma, K, eU and eTh) acquired in FFM001 and plotted from 1550 m to 1750 m. The lithology is superimposed on the geophysical logs.*

3.1.3 In-situ acoustic properties

It has been demonstrated that acoustic logs, (i.e., density, P-wave velocity and impedance (density x velocity)) can be used in lithology mapping, ore delineation, detection/ characterization of permeable zones and the interpretation of reflection and tomography surveys carried out in the mining and mineral exploration industry. One of our objectives for acquiring acoustic logs in the Flin Flon mining camp was to provide acoustic rock property data for the interpretation of seismic surveys. Interpretation of seismic reflection data requires knowledge of the acoustic impedances of the rocks. Seismic reflections occur when there is a change in acoustic impedance.

Figure 14 shows the acoustic logs from FFM001. FFM001 intersects a thick sequence of Missi sediments, basalt flows and fragmentals with various thicknesses of diotite, dacites, rhyolites and quartz-feldspar porphyries. The Missi sediments have fairly uniform densities that are lower when compared to the basalt package. Basaltic flows have the highest densities and velocities

whereas the basalt fragmental, diorite, rhyolite, and quartz-feldspar porphyry are characterized by lower velocities. It is interesting to note that the velocities gradually decrease towards the basalts; (e.g. from 750 m to 890 m and from 1000 m to 1170 m). This suggests that the basalt interval between 890 m and 980 m is a wedge that has been thrust into the Missi sediments.

There is a very high contrast between the Missi sediments and the basalt. The interface between these two rock types should act as an excellent reflector.

Figures 15 and 16 show the distributions of density and P-wave velocity in a histogram format and also cross plots of velocity versus density for the entire FFM001 hole.

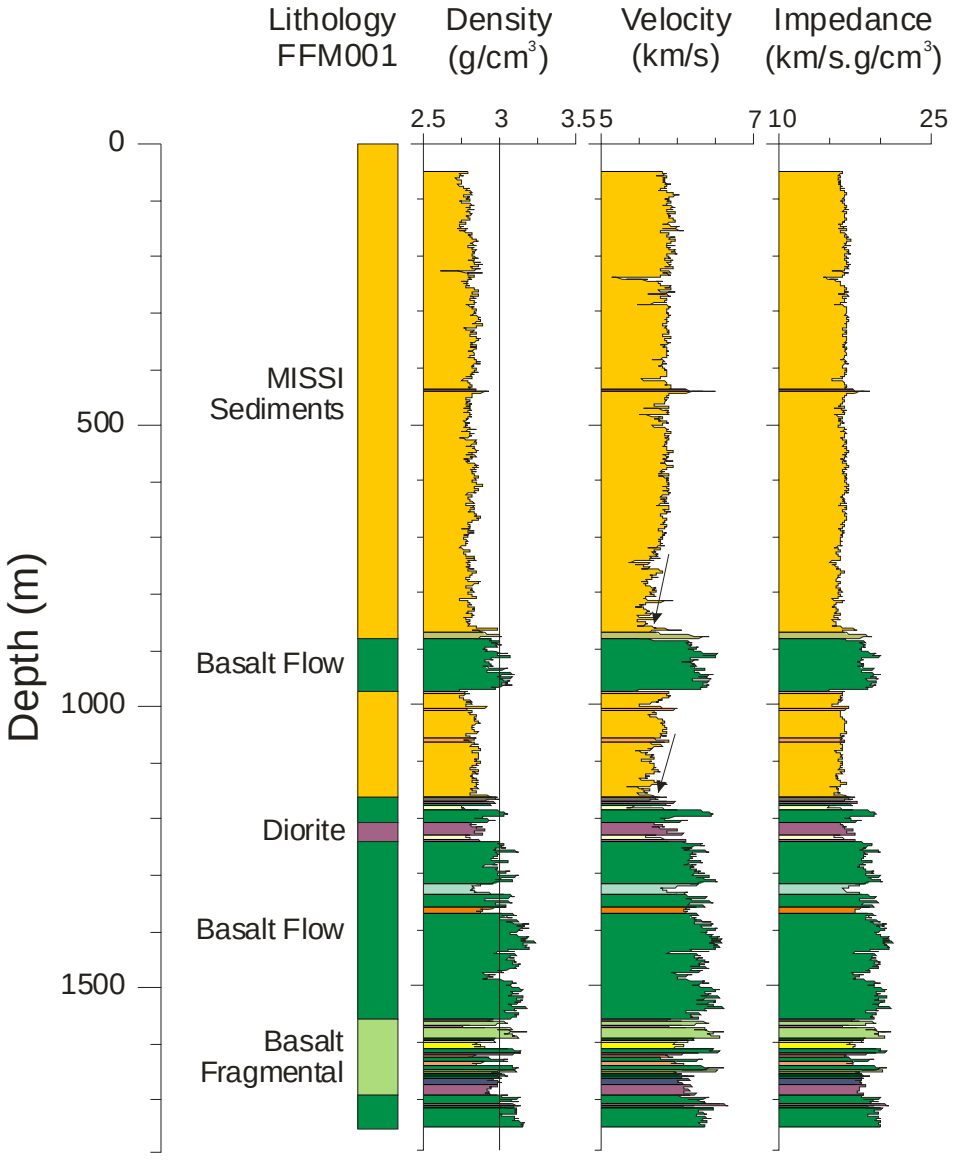

Figure 14: *Density, P-wave velocity and acoustic impedance logs from FFM001. The acoustic impedance contrasts are associated with changes in lithology and cause seismic reflections.*

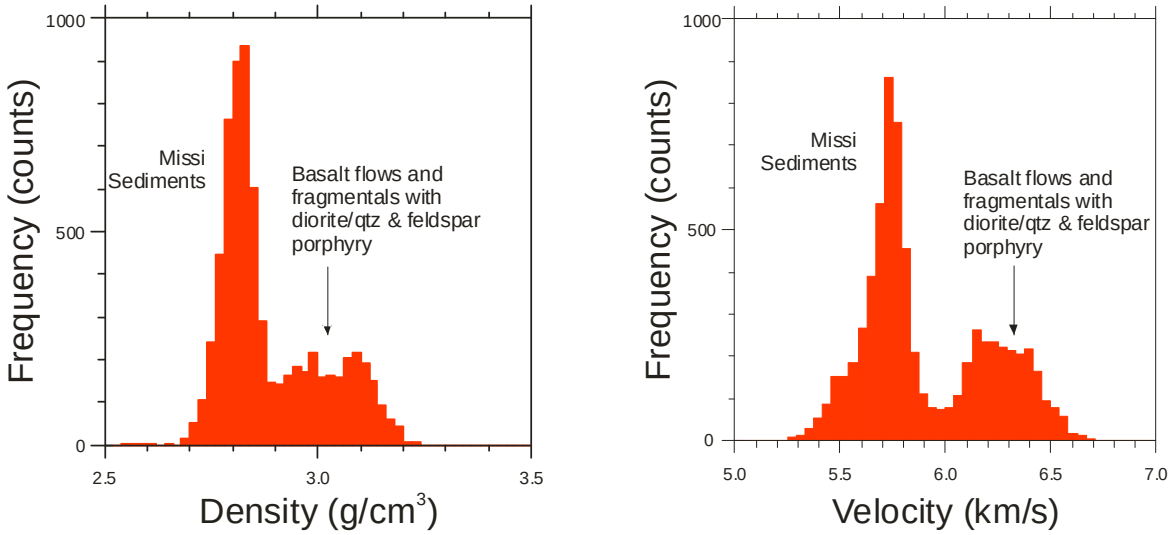

Figure 15*: Histograms of in-situ density and velocity from FFM001.*

The distributions of both the density and velocity data are bimodal (representing mainly the (1) Missi sediments (density <2.9 g/cm^3 and velocity <6.0 km/s) and (2) basalt flows and fragmental with diorite/quartz and feldspar porphyry (density >2.9 g/cm^3 and velocity >6.0 km/s). Missi sediments have a tight distribution whereas the basaltic package is wide spread primarily because the "basalt" group includes flows, fragmentals, dacites, diorites, rhyolites, and quartz and feldspar porphyries.

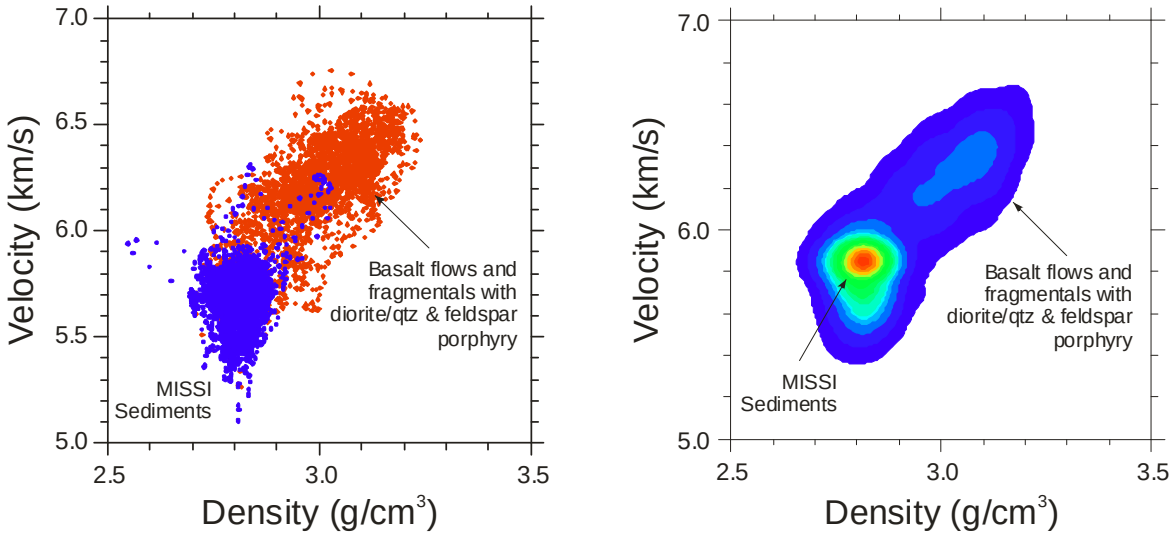

Figure 16*: Cross plot and the kernel density estimate of the in-situ velocity versus density logging data from FFM001. The density increases as velocity increases in the basalt flows and fragmental rock package.*

The data in the cross plot are grouped into two main lithology classes: the Missi sediments, and the basalt flows and fragmentals. The two main lithology units form two distinct clusters. The Missi sediments form an elliptical cluster that is elongate along the velocity axis, i.e., the density is fairly constant while the velocity shows some variation.

3.2 4Q66W3 Borehole Geophysical Logs

3.2.1 Lithology and alteration signatures

Figures 17 and 18 show the gamma, magnetic susceptibility, density and P-wave velocity logs from 4Q66W3 plotted from 100 m to 500 m and from 600 m and 1000 m, respectively. The gamma ray log correlates well with the lithology. There are several sections in this drillhole that were not cored and this is where the gamma log can fill-in the geology gaps. For example, the section without drill core from 440 m to 500 m can be interpreted as basalt flows with slightly anomalously high gamma ray activity that is due to basalt tuffs.

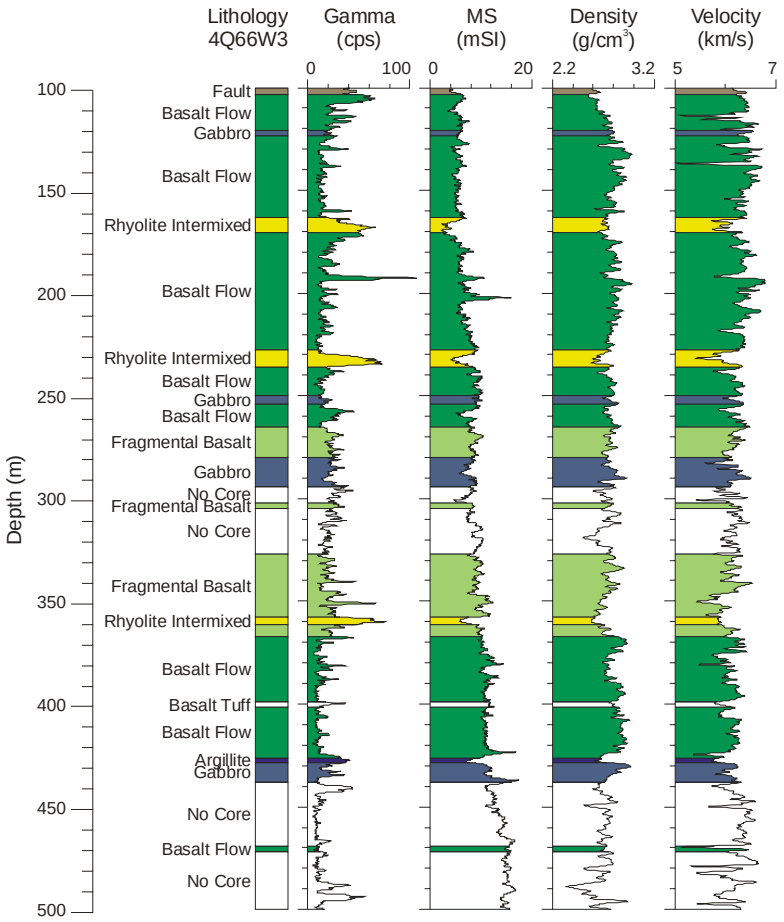

Figure 17: Total count *gamma, magnetic susceptibility, density and P-wave velocity from 4Q66W3 plotted from 100 m to 500 m. There are several sections that were not cored in this drillhole.*

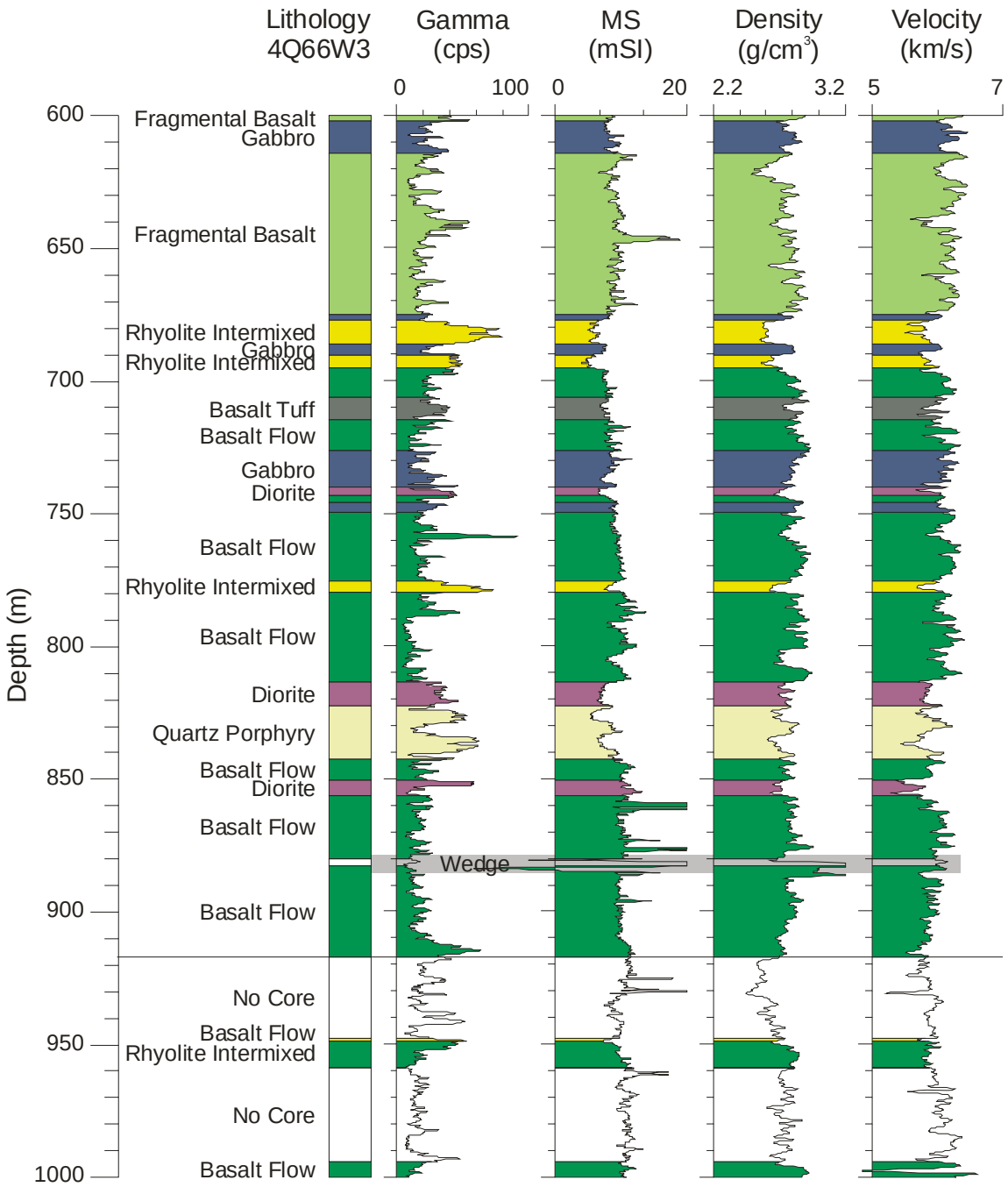

Figure 18: *Gamma, magnetic susceptibility, density and P-wave velocity from 4Q66W3 plotted from 550m to 1000m. Anomalous susceptibilities and densities between 880 and 890 m are due to wedges.*

3.2.2 Radiometric signature

Basalt flows exhibit low radioelement concentrations. There are a few sections that have elevated K and U content (e.g., around 190 m, Figure 19). These elevated radioelement content are caused by sericitic alteration. Rhyolite exhibits the highest gamma ray activity due to increased K and uranium content. There some differences in the radiometric characteristics of the intermixed rhyolite rock package. Some have a corresponding increase in thorium (see Figure 20).

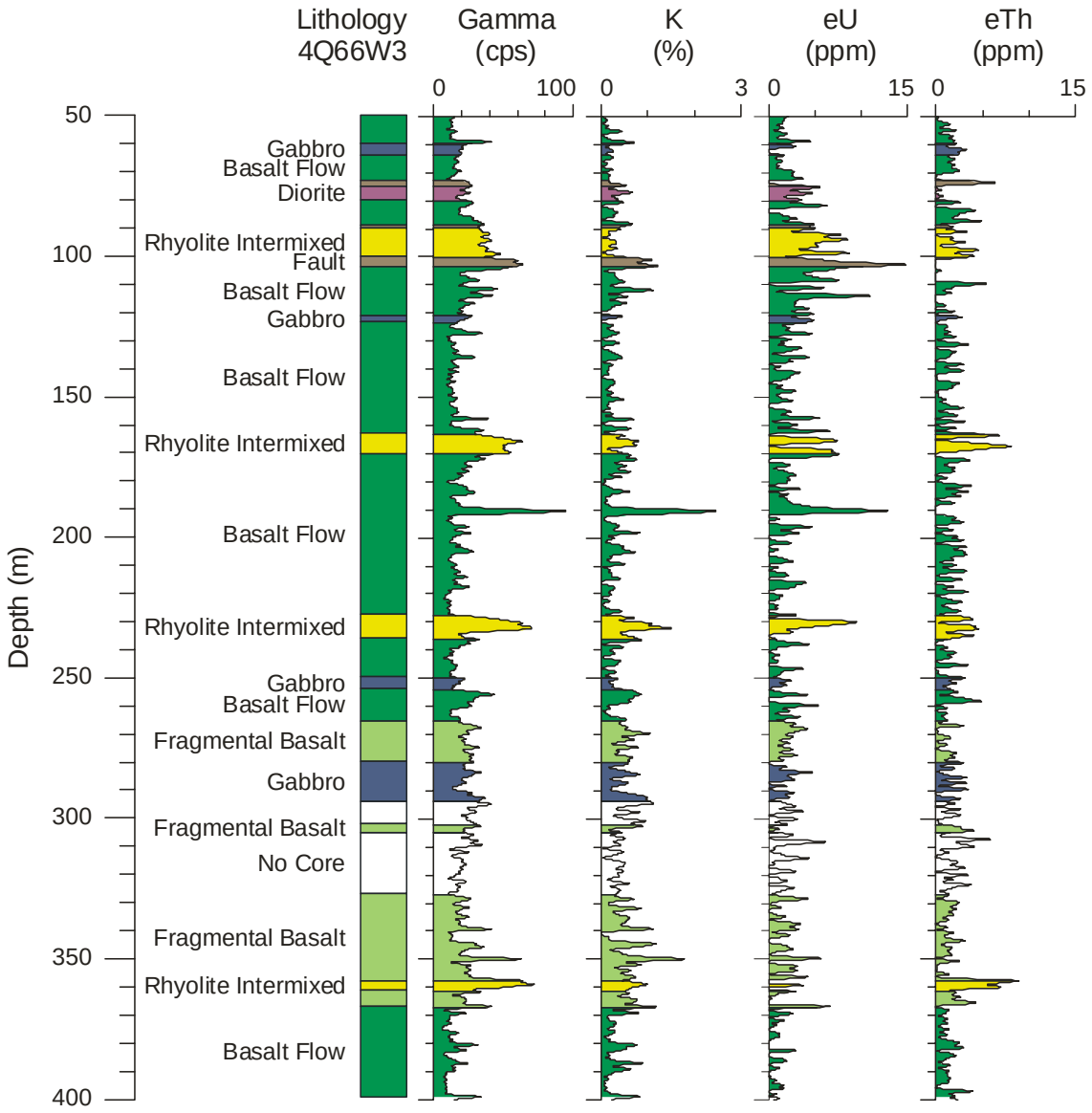

Figure 19: *Radiometric logs: total count gamma, K, equivalent U (eU) and equivalent Th (eTh) acquired in 4Q66W3 plotted from 50 m to 400 m.*

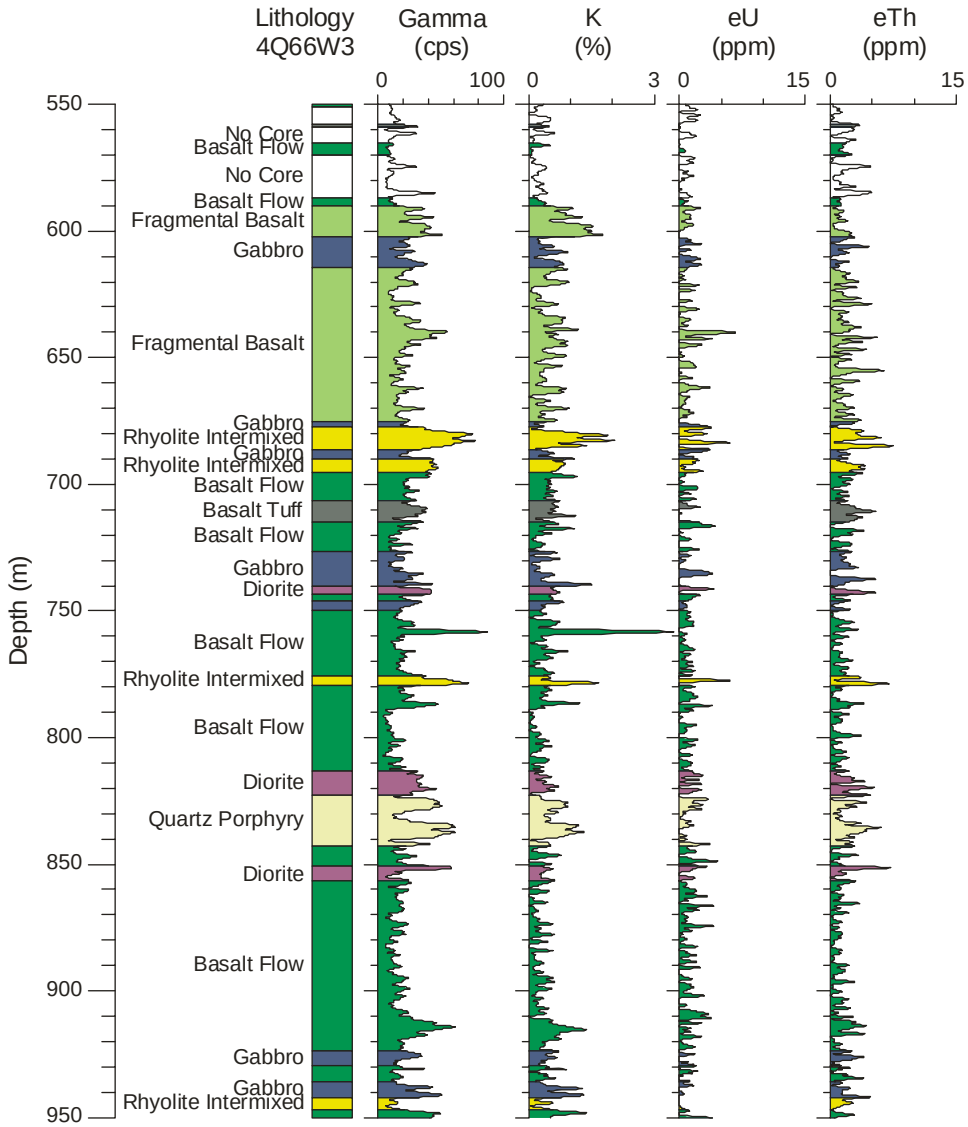

Figure 20: *Radiometric logs: total count gamma, K, equivalent U (eU) and equivalent Th (eTh) acquired in 4Q66W3 plotted from 550 m to 950 m.*

3.2.2 In-situ acoustic properties

The acoustic data (density, velocity, impedance and VDL) are presented in two sections: section 1 from 50 m to 550 m (Figure 21) and section 2 from 550 m to 1050 m (Figure 22). There is variation in the acoustic properties that is a function of lithology. The rhyolitic rocks have the lowest acoustic impedance followed by the fragmental basalts. The porphyritic basalt flows have high density, velocity and acoustic impedance. The variation in the acoustic properties within the basalt flows is caused by alteration.

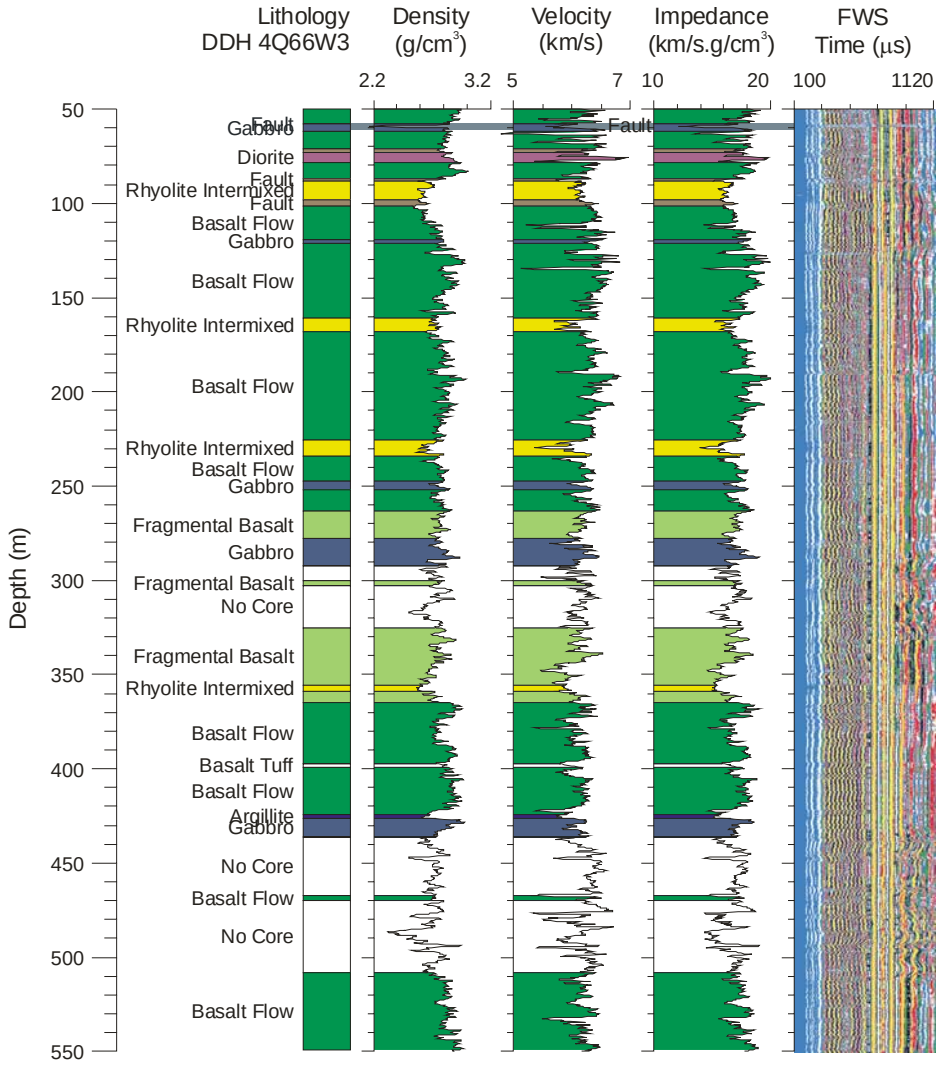

Figure 21: *Density, P-wave velocity, impedance and variable density (VDL) logs from 4Q66W3.*

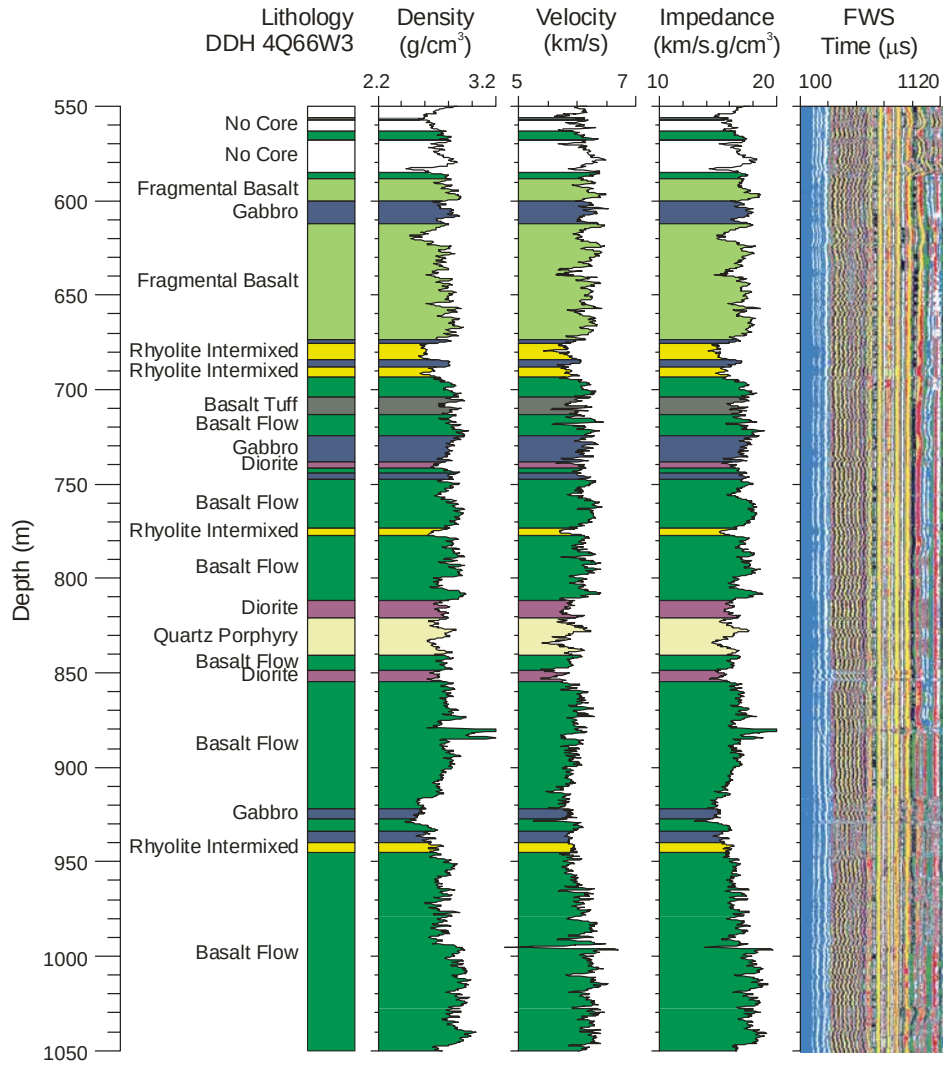

Figure 22: *Density, P-wave velocity, impedance and variable density (VDL) logs from 4Q66W3. The VDL is a method of displaying the full acoustic waveform at a single receiver with different amplitudes represented by different colours.*

3.3 FFS039 Borehole Geophysical Logs

3.3.1 Lithology and alteration signatures

Figure 23 shows the gamma, magnetic susceptibility, resistivity, density and velocity logs acquired in drillhole FFS039. This hole intersects porphrytic fragmental and flow basalts, gabbros that are altered and sheared (grouped as boundary intrusions), and diorites, porphyritic rhyolite intrusions at the bottom of the hole.

The basalts have low gamma ray activity (except where there is potassic alteration; e.g., 110 m - 117 m, 520 m - 546 m, 980 m - 999 m, 1018 m - 1030 m), low magnetic susceptibility, fairly uniform density and uniform velocity. Again variations in density and velocity are due to alteration. The high resistivity correlates with silicified zones.

The low resistivity, low density, low velocity and high gamma section within the magnetite-rich sheared gabbro (172 m – 186 m) immediately below the rhyolite (162 m – 172 m) correlates with a fault zone that is strongly altered and clay/mud rich. The high velocity in the rhyolite is due to silicification.

The boundary intrusion gabbros (125 m – 490 m) have unusual physical rock properties. Their radiometric signature is uncharacteristic of gabbros: high gamma ray activity. The magnetic susceptibility is variable although these sections are geologically identified as magnetite-rich. The most prominent feature of the magnetic susceptibility log is the extremely high values in the sheared and chloritized magnetite-rich gabbro (310 m – 370 m). This is caused by alteration and not primary magnetic minerals as there is a corresponding low gamma ray activity. The low gamma ray activity suggests that during the process of magnetite enrichment, most of the radioelements were depleted. This zone appears to be the centre of alteration because the resistivity, density and velocity are decreasing towards it from above and below. The centre of this high magnetic susceptibility zone exhibits high resistivity, density and P-wave velocity.

The diorites and quartz-feldspar porphyritic rhyolite intrusion intersected near the bottom of the borehole (1035 m – 1120 m) exhibits high gamma ray activity with the highest being observed in the quartz-feldspar porphyry. The porphyry is characterized by high magnetic susceptibility, low density and low velocity.

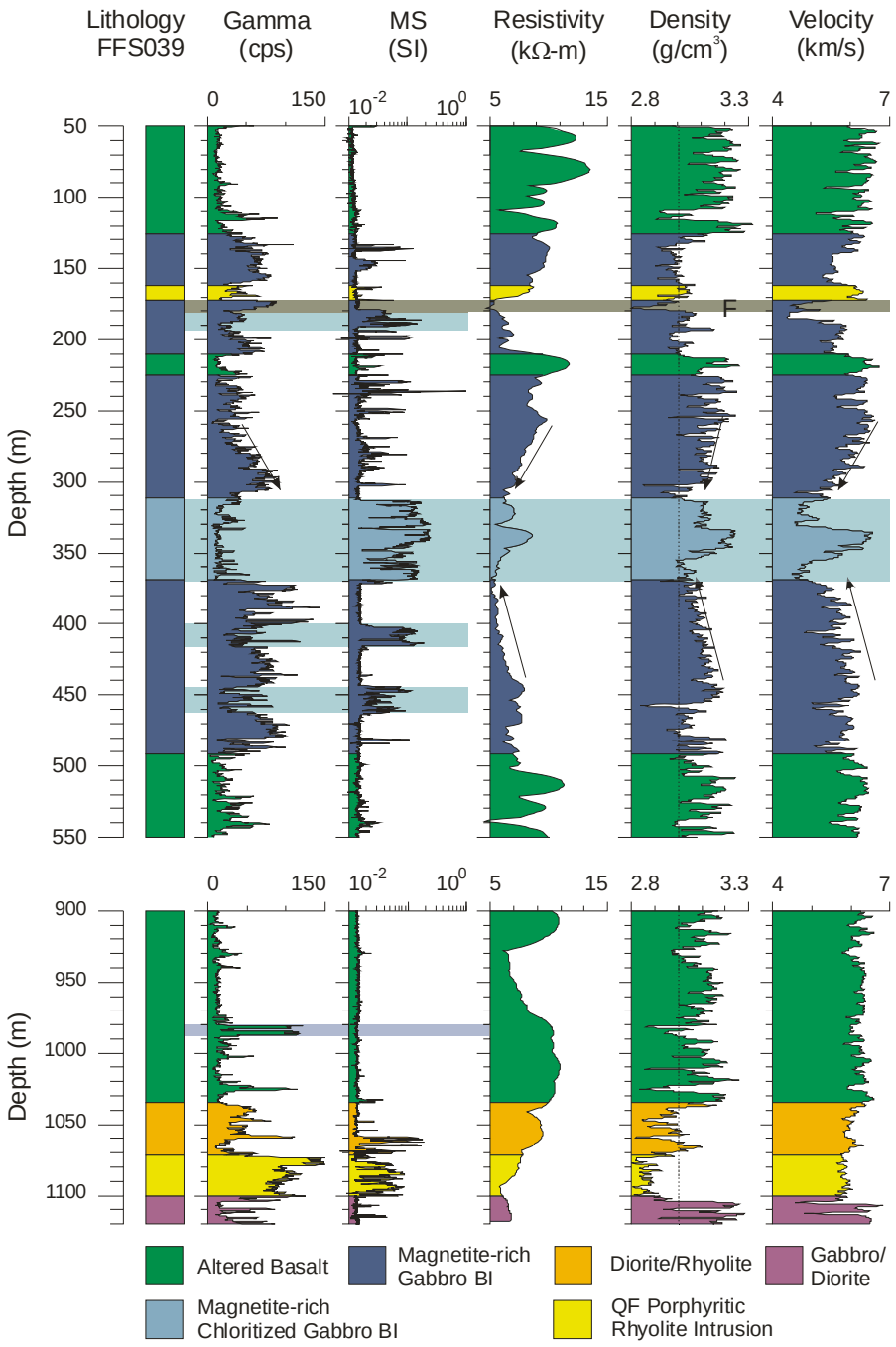

Figure 23: *Total count gamma, magnetic susceptibility, resistivity, density and, P-wave velocity logs from FFS039. The logs are plotted in two sections: 50m to 550m and 900m to 1120m. The section between 550m to 900m is comprised of basalt flows and fragmentals that have geophysical characteristics similar to basalts displayed in the plot.*

3.3.2 Radiometric signature

The gabbroic boundary intrusions have unusual radiometric signatures. All the radioelement concentrations (^{40}K, U, Th) are elevated. These significant variations in the radioelement concentrations are interpreted to be primarily due to alteration as the geochemistry of unaltered intrusions indicate no significant amounts of potassium (^{40}K) (Syme and Forester, 1976). Also the concentrations of ^{40}K, U, and Th are extremely low in basalts and gabbros (Larsen and Gottfried, 1960). Sericite altered zones in the gabbros have high K content. Increases in U content appear to be associated with fault/fracture zones. Uranium is quite mobile in nature and tends to be deposited under reducing conditions. The chloritized magnetite rich gabbros show a marked decrease in radioelement content (310 m – 370 m). Chloritization appears to deplete/remove radioelements. There is a corresponding increase in the magnetite in this zone (see Figure 24). The basalts intersected in this hole are highly altered but generally have low gamma ray activity compared to the gabbroic intrusions. An altered zone (sericitized zone) between 510 m to 560 m exhibits high K content. The high gamma ray activity at approximately 980 m is due to high uranium and thorium content. The detailed geological log indicates that this is quartz-feldspar porphyry.

The diorite/rhyolite rocks below the basalts show distinct radiometric signatures from the quartz-feldspar porphyritic rocks. They have high potassium and uranium whereas the QFP's show all the radioelemetnts (k, U, and Th) as high. Figure 25 shows an expanded section of the drillhole with gamma, K, U, Th and magnetic susceptibility. The QFP can be divided into two main sections: the upper third of the QFP has very high gamma ray activity but low magnetic susceptibility whereas the bottom two-thirds of this rock unit has high magnetic susceptibility.

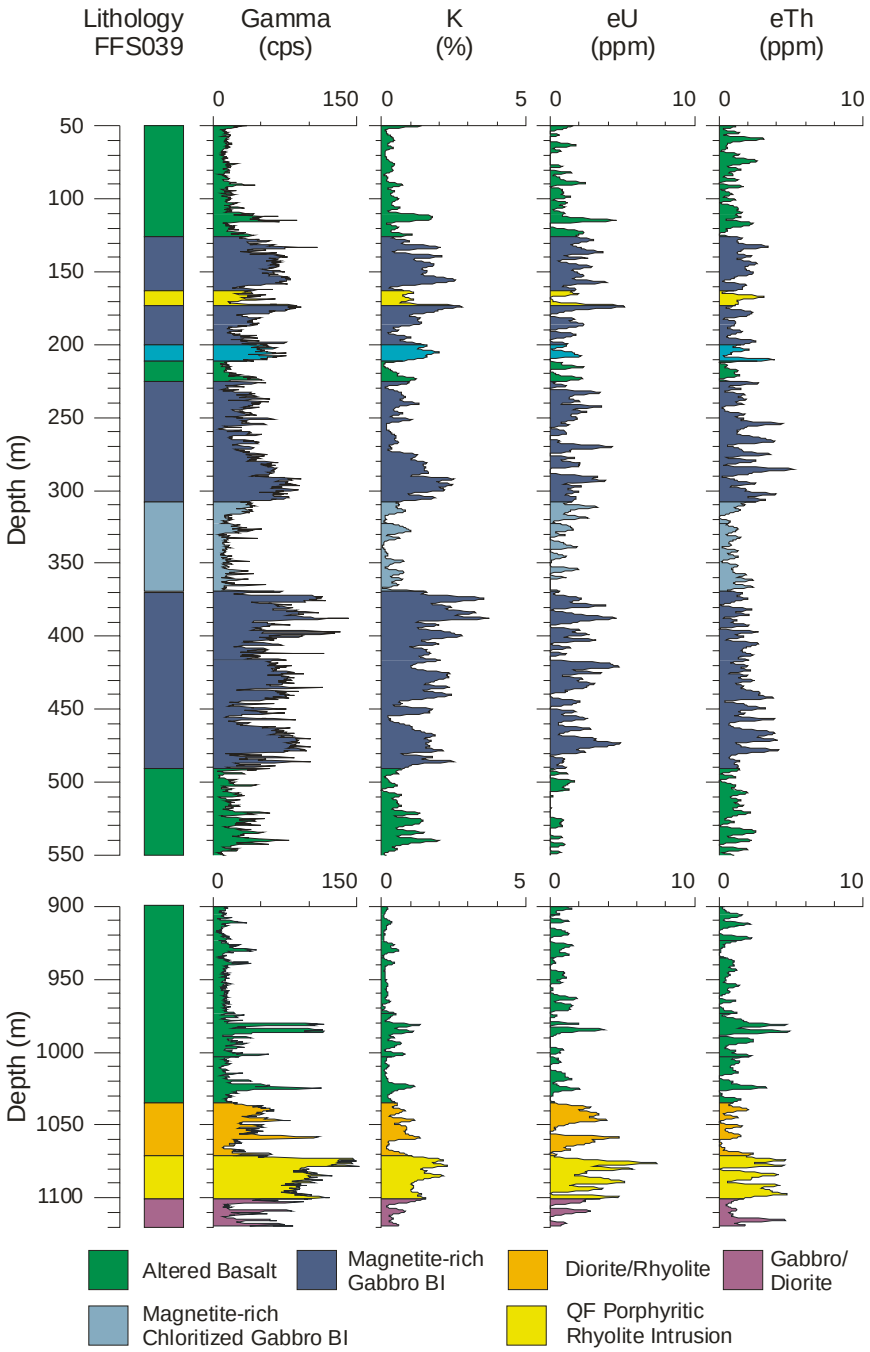

Figure 24: *Radiometric logs: total count gamma, K, equivalent U (eU) and equivalent Th (eTh) from FFS039. The logs are plotted in two sections: 50 to 550m and 900 m to 1120m. The borehole section between 550m to 900m consists of basalt flows and fragmentals that have similar geophysical characteristics to the basalts that are displayed in the plot.*

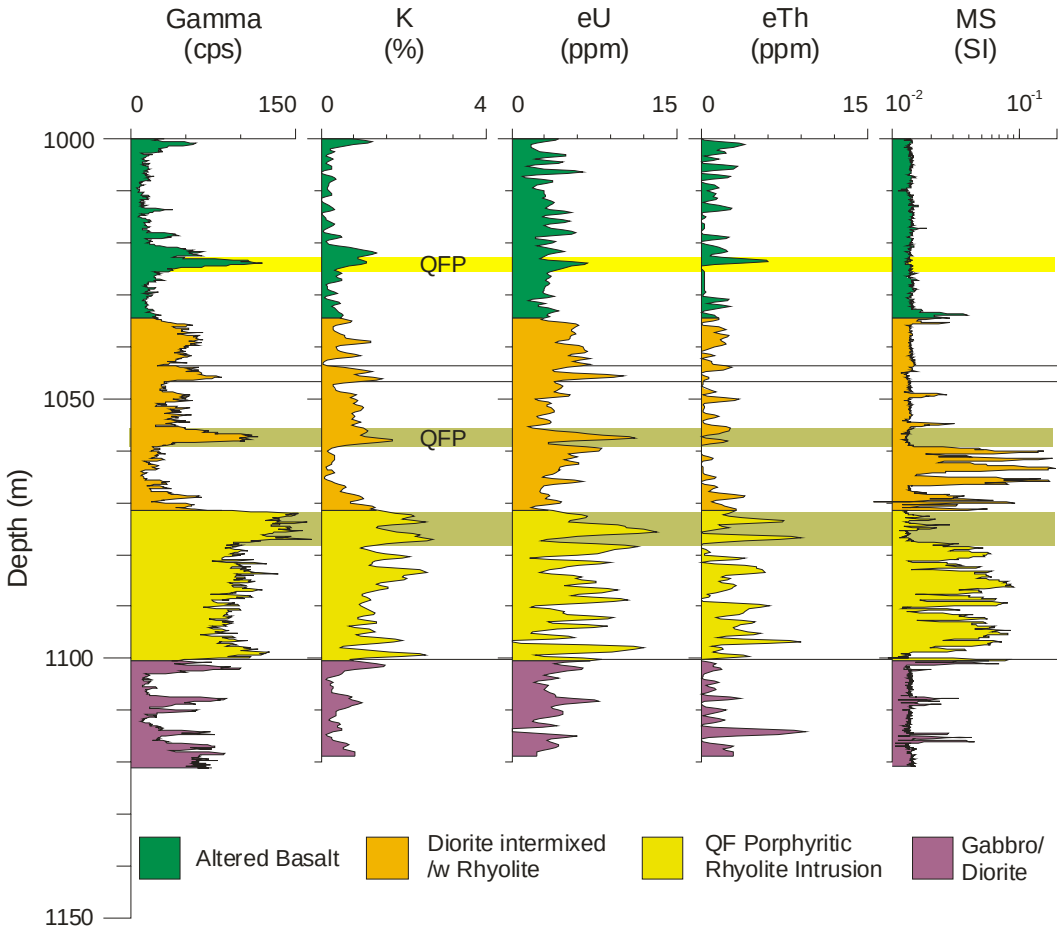

Figure 25: *Radioelement logs (Gamma, K, eU and eTh) and magnetic susceptibility log for the bottom section of FFS039. There is a quartz-feldspar(QF) porphyritic rhyolite within the altered basalt with elevated K, U, and Th.*

3.3.3 In-situ acoustic properties

All four acoustic logs correlate well with the lithology and alteration (Figure 26). The lowest densities, velocities and acoustic impedance are seen in the quartz-feldspar porphyries. The amplitudes of these parameters are similar to those observed in the basalts and boundary intrusion gabbros; lower values are also observed in highly sheared/fractured and altered zones. There appear to be different phases in the magnetite-rich boundary intrusion gabbros (Syme and Forester, 1976). The average densities in the upper gabbro units (125 - 210m) are lower than those in the lower gabbros.

There are a few interfaces where there are significant changes in the acoustic impedance. These include changes that are associated with alteration (e.g., 332 m, 356 m) and those associated with lithology (e.g., 1100 m). In particular, the sheared/chlorite gabbroic zone between 332 m and 356 m has higher acoustic impedance than the rocks above and below it, which should make it visible with seismic techniques.

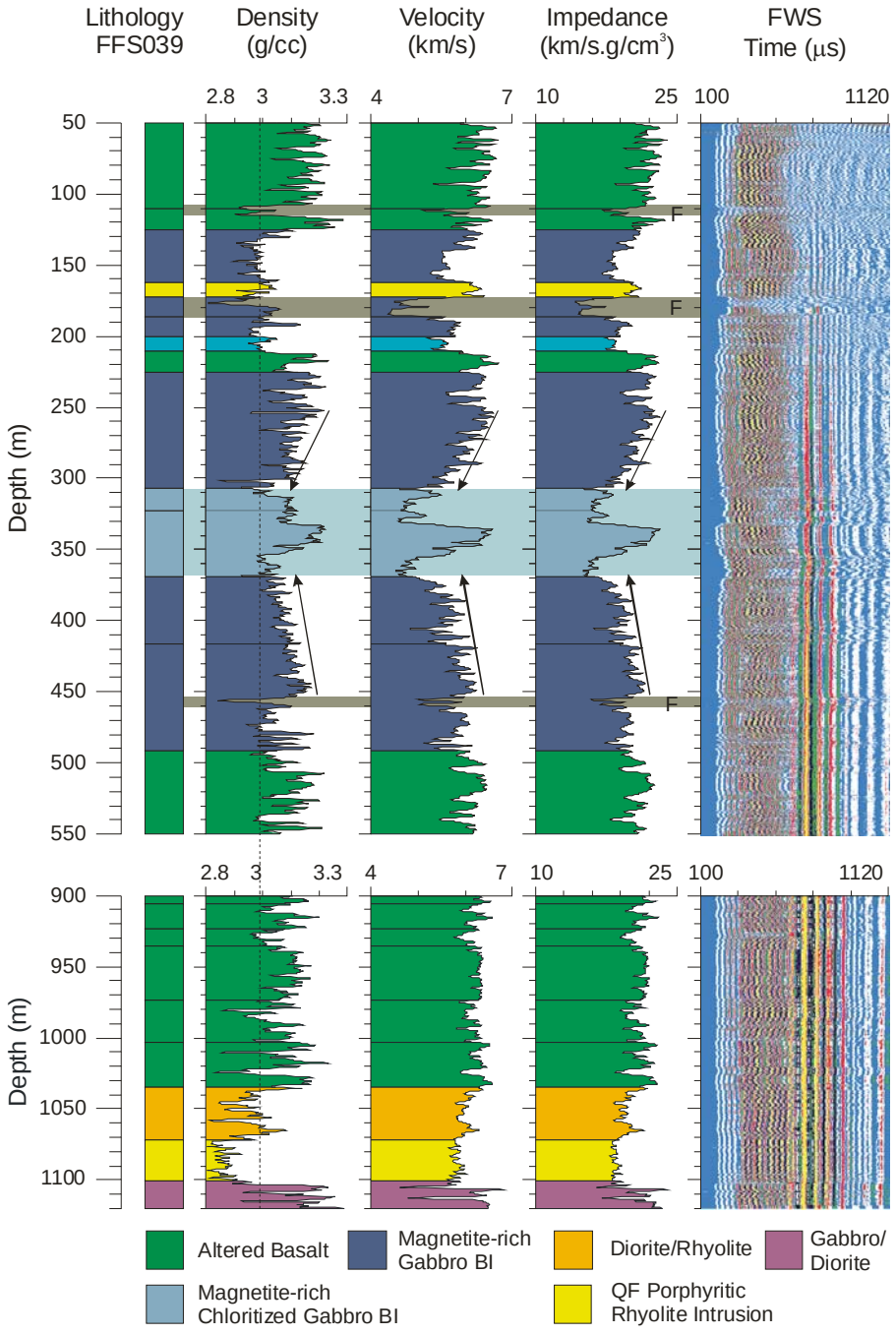

Figure 26: *Density, P-wave velocity, impedance and variable density (VDL) logs from FFS039. The VDL is a method of displaying the full acoustic waveform at a single receiver with different amplitudes represented by different colours. The logs are plotted in two sections: 50 to 550m and 900 m to 1120m. The section between 550m to 900m has basalt flows and fragmentals that have geophysical characteristics that are similar to the basalts. BI = boundary intrusion, QF=quartz feldspar.*

Figures 27 and 28 show the distributions in a histogram format and box-and-whisker plots of P-wave velocity and density for hole FFS039, respectively. The logging data has been classified according to the five major lithologies intersected in the drillhole. The distributions indicate that there is not much separation in the velocities between the different lithologies with the exception of the basalts that are on the average higher than the other lithologies. From a seismic interpretation viewpoint, one has to look at the interfaces between different lithologies in their emplacement sequence. For instance, there is a significant acoustic impedance contrast at the interface between the rhyolite intrusion and the gabbro/diorite (at 1100 m, see figure 26). Gabbros and basalts have similar densities. The rhyolites have significantly lower densities than the basalts, gabbros or diorites.

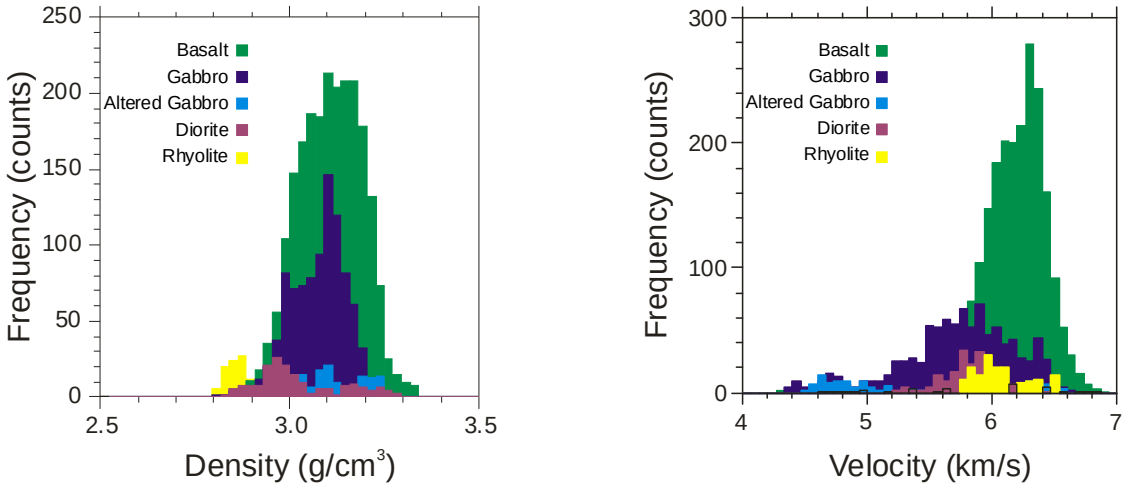

Figure 27: *Density and velocity and distributions for five main lithology/ alteration units intersected in FFS039.*

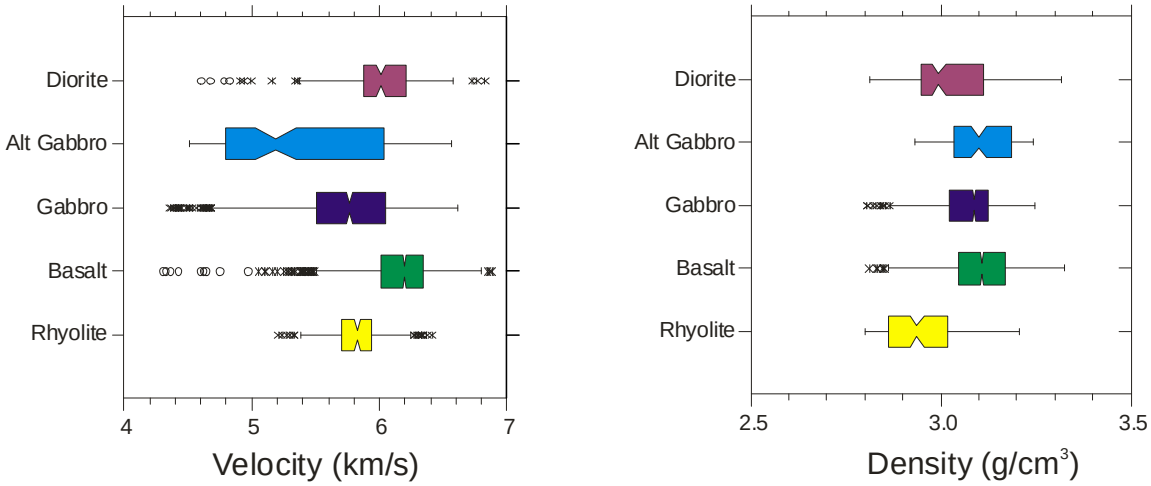

Figure 28: *Box-and-whisker plots of velocity and density for five main lithology/alteration units intersected in FFS039. Alt=altered.*

Basalts and gabbro have similar densities. The rhyolites have slightly lower densities (2.90 g/cm^3 median density) compared to basalt and gabbros (~3.1 g/cm^3) median density). The densities of diorites are slightly higher than those of the rhyolites, but are lower than the basalts and gabbros (see also histogram, Figure 27). The P-wave velocities are fairly similar except that those of the basalts appear to be slightly higher.

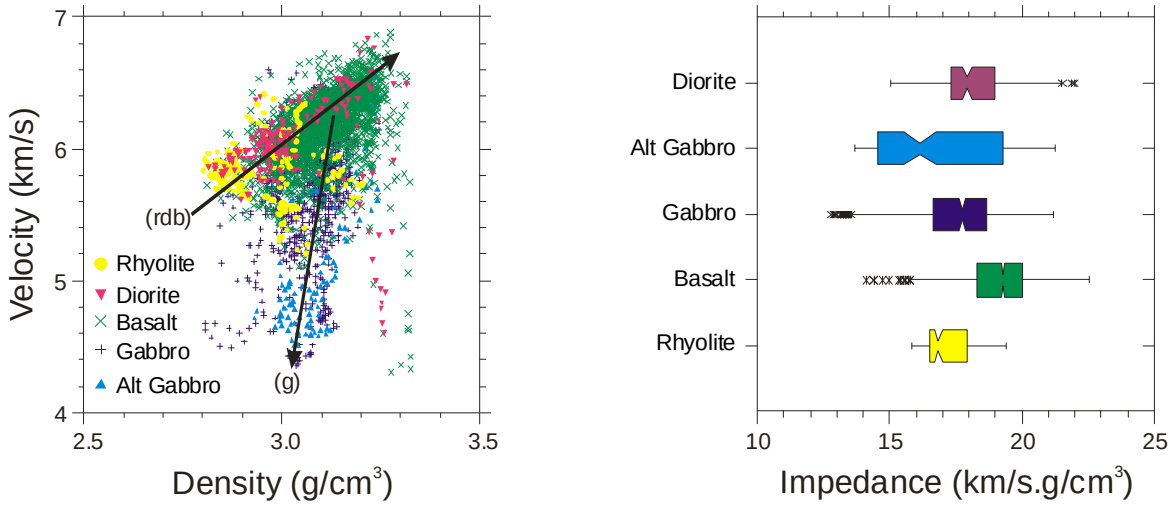

Figure 29: *Cross-plot of the in-situ velocity versus density logging data from FFS039. Alt-altered. (rdb) – trend for rhyolite, diorite and basalts. (g) – trend for gabbros. The box-and-whisker plots of the acoustic impedance are shown on the right.*

The velocity-density cross-plot (Figure 29) shows that a slight decrease in density for the gabbros results into a large change in the velocity.

The density within gabbros is fairly uniform. However, the velocity varies significantly within the gabbros as a function of alteration.

3.4 4Q62 Borehole Geophysical Logs

Borehole geophysical logging was carried out in 4Q62 to look at the mineralization and host rock geophysical characteristics. The mineralization consists of pyrite, pyrrhotite, chalcopyrite, and sphalerite. The host rocks are the Flin Flon formation. These observations would be essential in determining the best exploration strategies.

3.4.1 Lithology and alteration signatures

The gamma ray log is very characteristic of the lithology intersected in 4Q62 (see Figure 30). The volcanic flows, andesite, dacite and diorite, exhibit the lowest gamma ray activity due to their low radioelement content. However, the tuff equivalents (andesitic, dacitic and rhyodacite tuffs) exhibit slightly higher activity. The ryholite tuffs are highly altered, sercite being the main

alteration mineral and hence exhibit the highest gamma ray activity. Magnetic susceptibility appears to be positively correlated with the gamma ray signature in the volcanics.

The chlorite carbonate schist has higher gamma activity as compared to the underlying andesite. The degree of alteration in the schist increases towards the lower andesite flow as indicated in the gamma, resistivity and velocity logs.

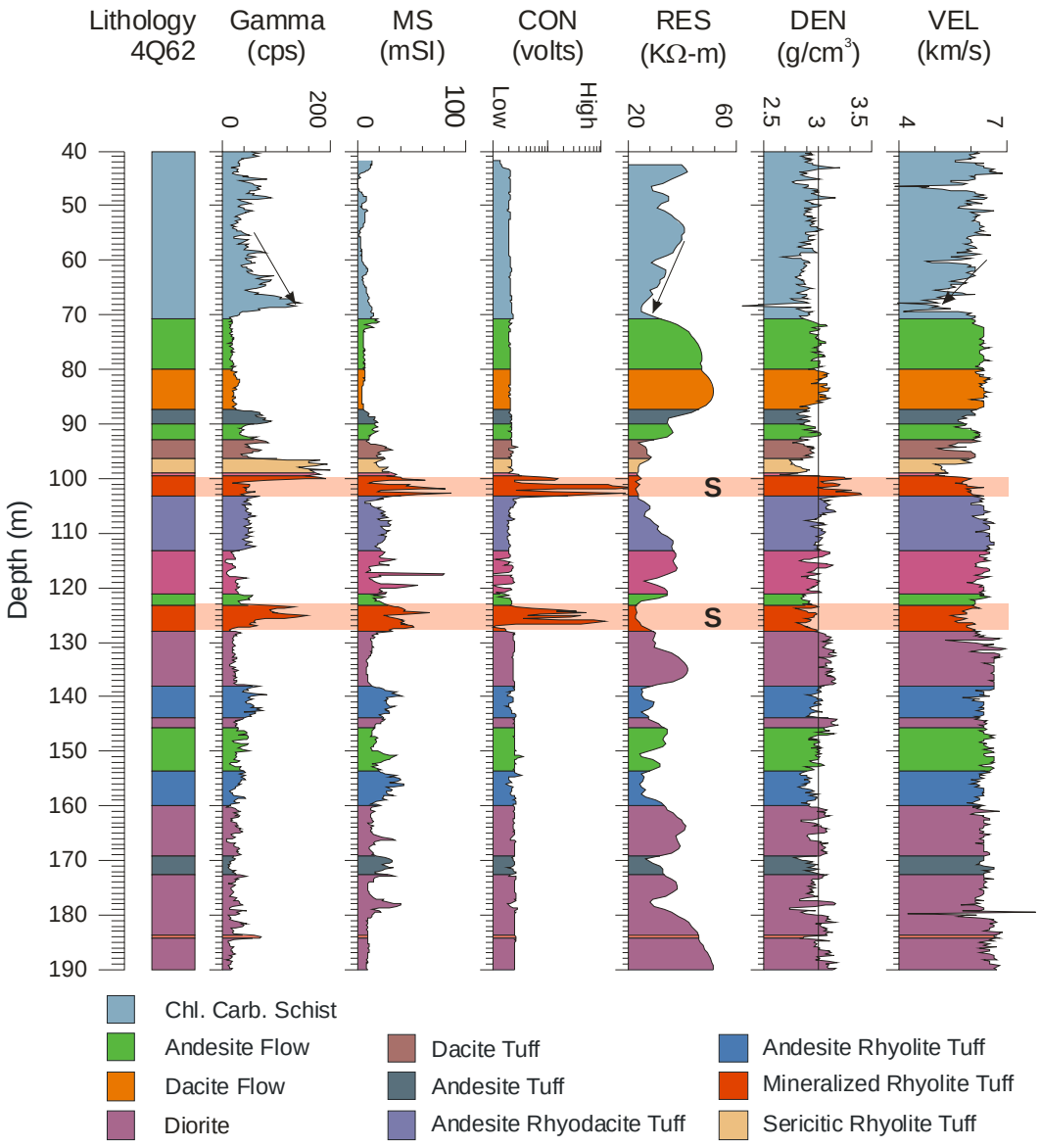

Figure 30: *Gamma, magnetic susceptibility (MS), conductivity (CON), resistivity (RES), density (DEN) and P-wave velocity (VEL). The conductivity log is uncalibrated and presented in units of volts. The resistivity is a 16-inch normal array resistivity log.*

3.4.2 Radiometric signature

Figure 31 shows the radiometric logs: total count gamma, potassium (K), equivalent uranium (eU) and equivalent thorium (eTh). The ryholite tuffs (96.5 m – 98.8 m) above the upper mineralized zone are sericitic and hence exhibit elevated K content. There is also very high U content.

The mineralized rhyolite tuffs show high K and U content. Rhyolites generally have high K content but the corresponding increase in U suggests that alteration during the mineralization process was responsible for the increases in both K and U. Strong sericite and carbonate alteration is observed in the rhyolite tuffs. This observation suggests that increases in the radioelements, K and U, are good indicators of proximity to mineralization.

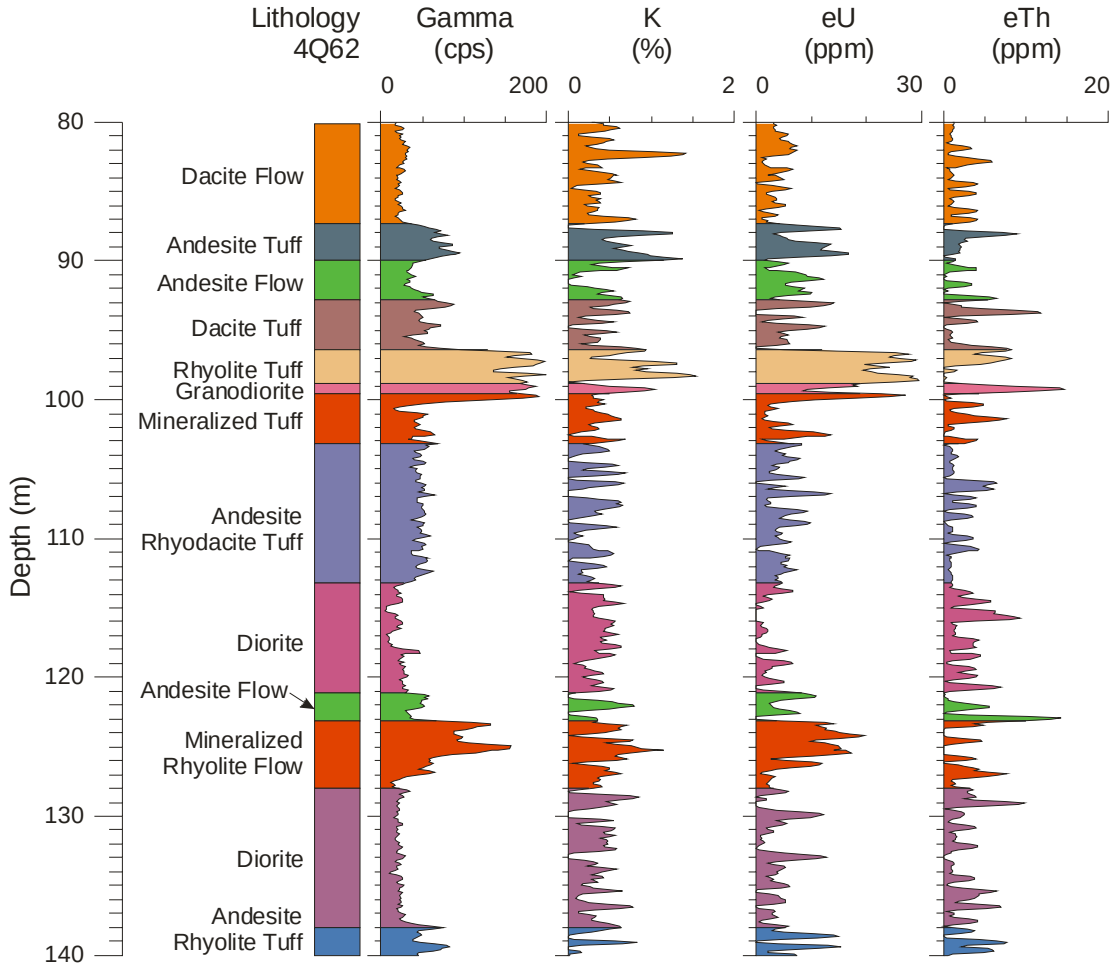

Figure 31: *Radiometric logs: total count gamma, K, equivalent U (eU) and equivalent Th (eTh) from 4Q62.*

3.4.3 In-sSitu acoustic properties

Figure 32 shows density, velocity, acoustic impedance and the full waveform log plotted as a variable density log (VDL). All the logs correlate well with lithology and structure. The volcanic tuffs are characterized by lower acoustic impedance, whereas the basalt flows are characterized by higher impedances. Although the mineralized rhyolite tuffs exhibit higher densities (99.5 m - 103 m) than the host rocks, the velocity log does not show a corresponding high velocity. Hence, the acoustic impedance does not clearly distinguish mineralized from unmineralized host rocks. Because of the highly altered nature of the mineralized zones, the disseminated sulphide zones (mineralized rhyolite tuffs, 123 m – 128 m) show low acoustic impedance.

Full waveform acoustic logging is an important technique for in-situ fracture characterization and permeability estimation. Open fractures intersecting a drillhole disrupt the propagation of acoustic energy along the hole and result in a reduction in the amplitude of all arrivals in the full waveform. A major fracture zone around 66m is clearly evident on all the four logs and is characterized by low density, low velocity, and hence low acoustic impedance. The full waveform log also clearly shows this zone with low amplitude across the entire wave train. The acoustic impedance shows a decreasing trend towards mineralization in the host rocks above. This is an indication of the increasing content of low-velocity alteration minerals such as sericite and chlorite. This characteristic response is a possible vector towards mineralization.

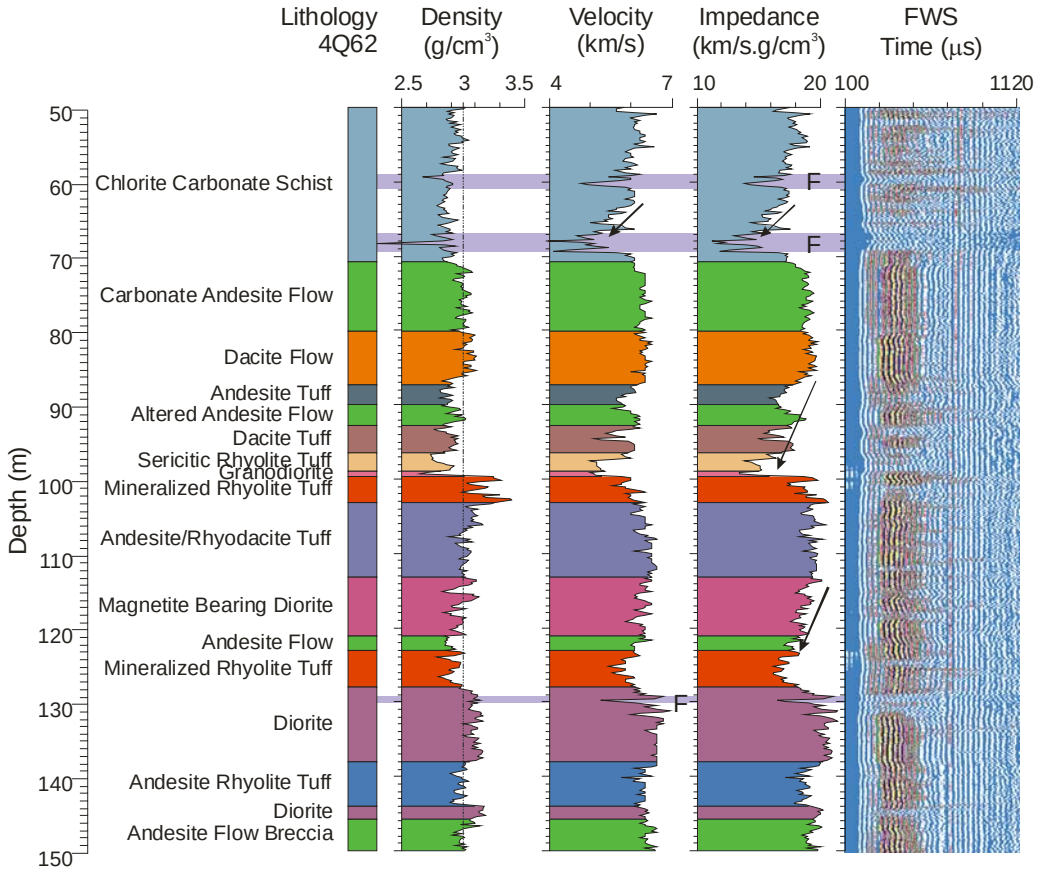

Figure 32: *Density, P-wave velocity, impedance and variable density (VDL) logs from 4Q62. The VDL is a method of displaying the full acoustic waveform at a single receiver with different amplitudes represented by different colours. The fault zones are evident in all four logs.*

3.4.4 Mineralization signature

Figure 33 shows the spectral gamma gamma, conductivity and magnetic susceptibility logs from 4Q62. Also shown is mineralization intersected in this drillhole that consists of the following sulphide minerals: pyrrhotite, pyrite, chalcopyrite and sphalerite. Magnetite is also a major oxide in the mineralized zones.

Mineralized zones exhibit high conductivity and magnetic susceptibility (e.g. 99.5 – 104 m). The high susceptibilities are primarily due to increases in the pyrrhotite content as it is correlated with an increase in conductivity. The zone between 123 m – 126 m is not as conductive. The major alteration in this mineralized zone is sericite, which is associated with an increase in U (Figure 33).

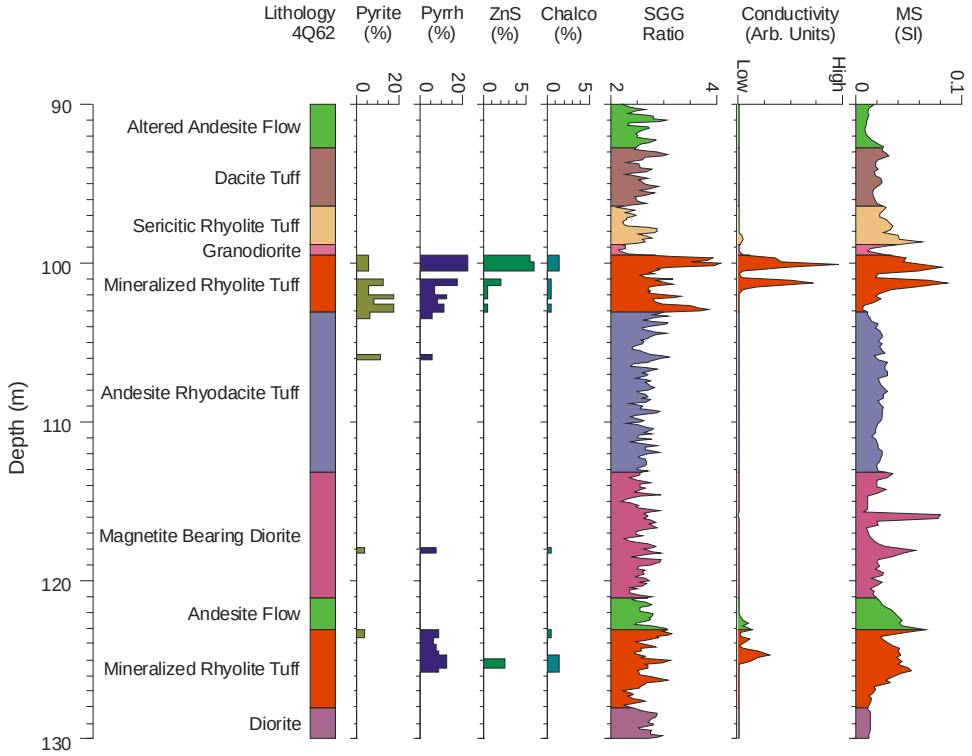

Figure 33: *Lithology column, sulphide minerals (Pyrite, Pyrrhotite (Pyrrh), and Sphalerite (ZnS)), spectral gamma gamma ratio, conductivity and magnetic susceptibility (MS) logs from 4Q62. The SGG ratio, a ratio of a low energy window (100-200 keV to 200-500 keV) to a high energy window, is a heavy element indicator derived from the spectral gamma gamma data. The conductivity log is uncalibrated and is presented in arbitrary units.*

3.5 FFS036 Borehole Geophysical Logs

Figure 34 shows magnetic susceptibility and neutron logs acquired in FFS036. Also included is a simplified geological column of the main lithology units. The uncalibrated, dead time corrected neutron log is presented as counts per second. The three main lithologies intersected in FFS036 (basalt, rhyolite and gabbro) have quite distinct neutron responses. There is a very clear distinction between the rhyolite and basalts/gabbros. The rhyolites have a higher neutron response compared to the basalts/gabbros. It is worth noting the relative increase in the neutron response for all the lithologies from 650 m to the bottom of hole. However, the relative difference between rhyolites and basalts/gabbros is the same – higher porosities in rhyolites. The neutron response is quite varied in all the lithologies because it is a function of the free hydrogen in the water molecule and/or minerals.

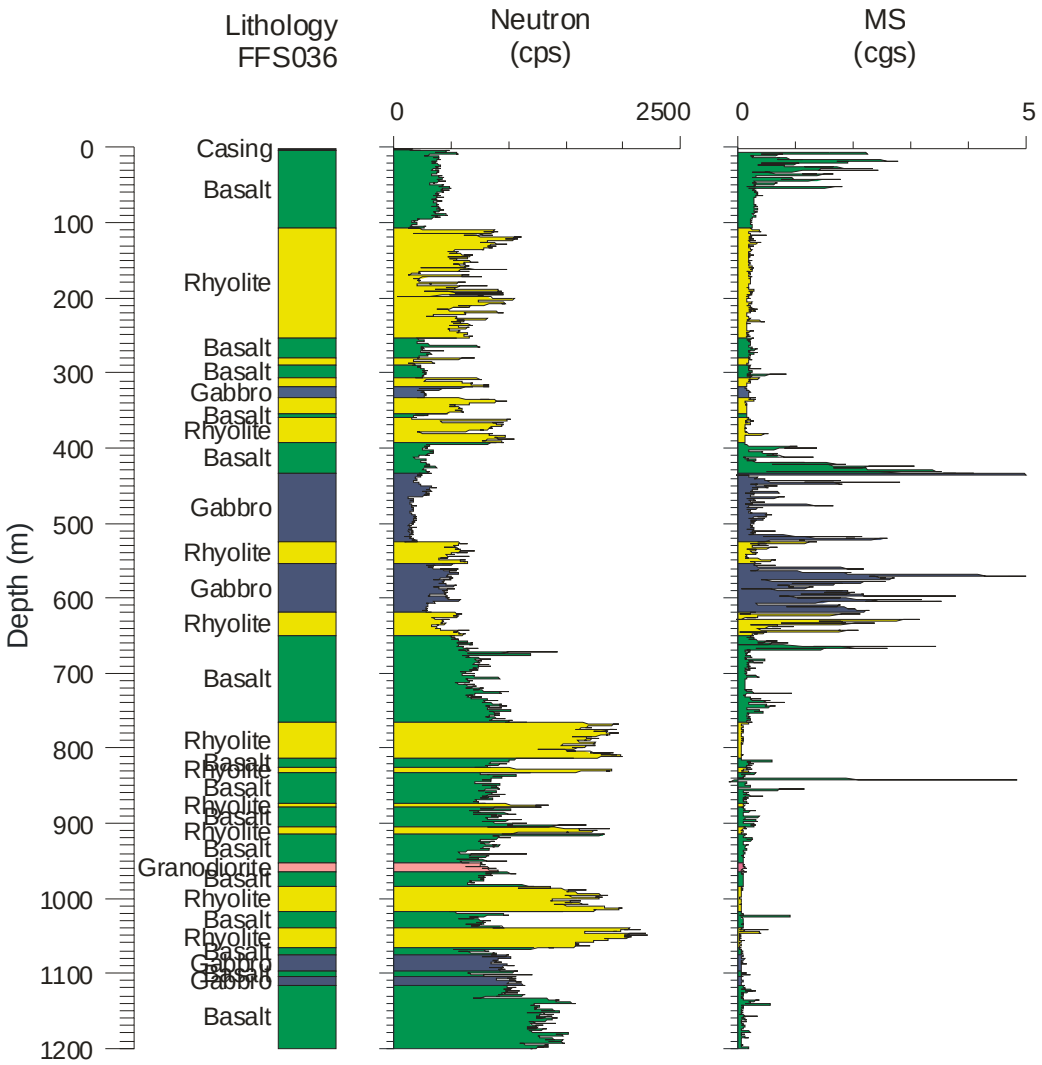

Figure 34: *Lithology, neutron porosity and magnetic susceptibility logs acquired in FFS036. The lithology is superimposed on the geophysical logs.*

The magnetic susceptibility log shows responses that are not well correlated with lithology. Generally, high susceptibilities are observed in the fragmental basalts and gabbros (boundary intrusion). However, one occasionally sees high susceptibilities within the rhyolites (e.g., 620 m – 680 m). This could be due to the development of secondary magnetite or rhyolite mixed in with fragments of magnetic gabbro.

Figure 35 shows the upper 500 m of FFS036 with a detailed geological description. The neutron log clearly distinguishes rhyolite from the basalts and gabbros. The basalts from 3.50m – 107.68m consist of amygdaloidal/ fragmental basalt flows/breccias. The low neutron response (high porosity) near the bottom of this unit is due to a high degree of fracturing and shearing. There is also a preponderance of hydrous alteration minerals, epidote and sercite, that gives a low neutron counts (high porosity) response. It is interesting to note that there are variations within the rhyolite (110-250m) that exhibit low neutron response (high porosity) equivalent to those observed in the gabbro and basalts (255 – 285 m). The detailed geological log indicates there are numerous basalt gabbro dykes within this predominantly rhyolite unit that are epidotized (epidote – a calcium aluminium iron silicate hydroxide). This is due to alteration and/or variation of hydrous alteration minerals.

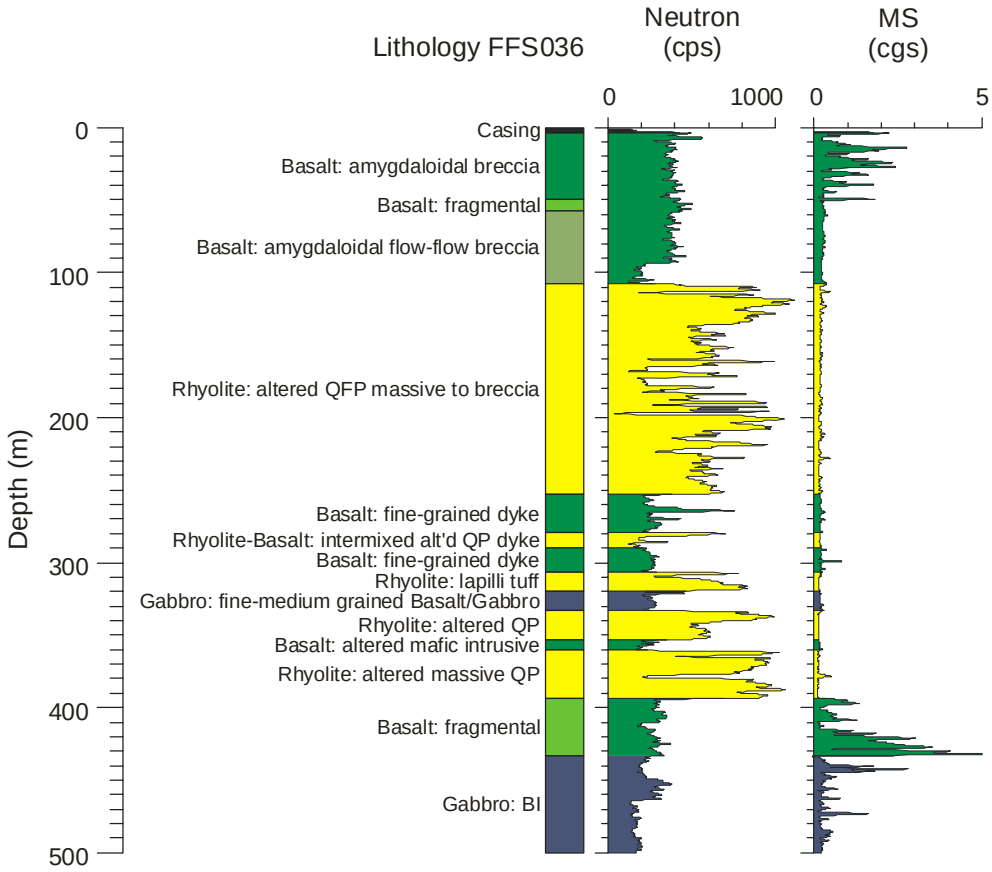

Figure 35: *Lithology, neutron porosity and magnetic susceptibility logs acquired in FFS036. The logs are shown from 0 to 500 m to show the detailed neutron response characteristics of the rhyolitic rock package. The lithology is superimposed on the geophysical logs.*

4 FLIN FLON MINING CAMP GEOTHERMAL PROFILE

Figure 36 shows the temperature-depth profiles for drillholes FFM001, FFS039, 4Q66W3 and 4Q62. The temperature-depth profiles are influenced by drilling and its takes several years for the geothermal gradient to approach that of the true geothermal gradient (Mwenifumbo, 1993). Thus, the most recently drilled hole, FFS039, is far from approaching geothermal equilibrium. The anomalous high temperature between 150 and 200 suggests warmer drilling fluids had permeated into a porous fracture/fault zone and this temperature anomaly should subside with time. This zone is within a sheared boundary intrusion gabbro and exhibits low resistivity. The minor blips, e.g., at ~410 m also suggest a similar scenario (contact between coarse grained and heterogeneous gabbro that is more likely porous).

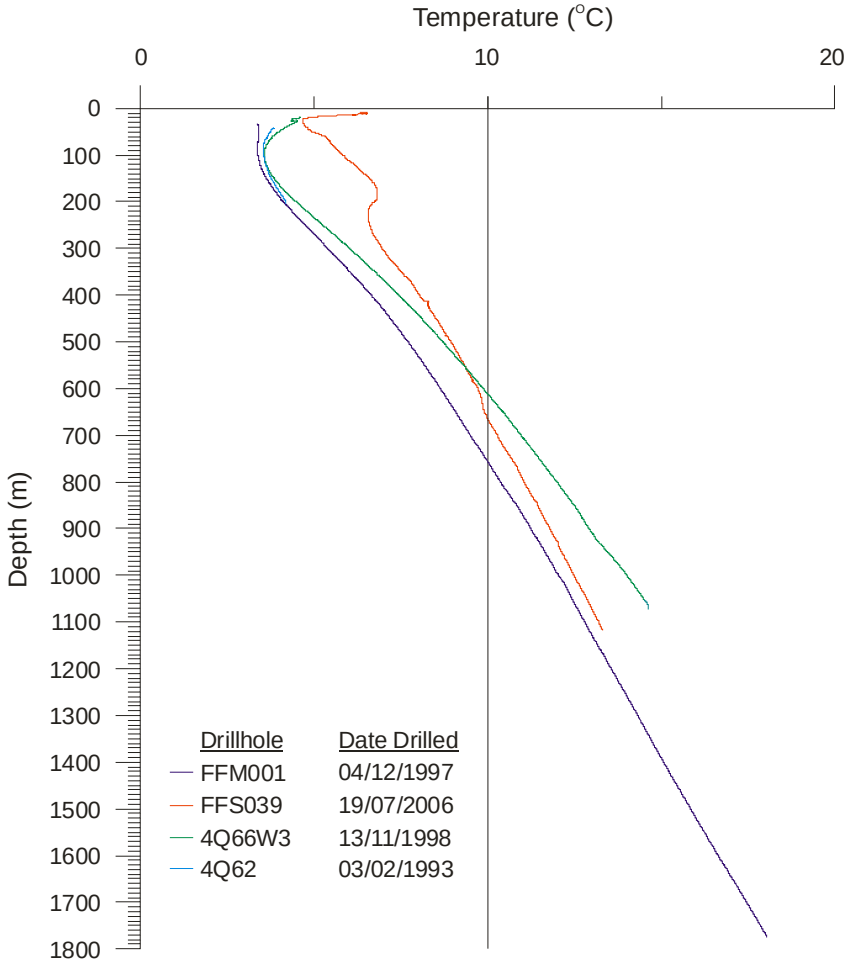

Figure 36: *Temperature logs acquired in four drillholes; FFM001, FFS039, 4Q66W3 and 4Q62.*

5 SUMMARY OF THE GEOPHYSICAL LOGGING

This summary is organized according to lithology, alteration and mineralization. The borehole geophysical signature is primarily a function of lithology and not of formations. Formations with the same rock types will generally exhibit the same geophysical signatures.

5.1 Lithology

The rocks intersected in the drillholes that were geophysically logged are here grouped into five main suites; (1) Missi sediments and conglomerates; (2) gabbros, (3) basalts, (4) diorites and (5) felsic volcanics and volcanoclasitsc (rhyolite flows and tuffs).

5.1.1 Missi sediments and conglomerates

The characteristic signatures of the Missi sediments are as follows:

- High radioelement content (K, U and Th)
- Acoustic properties are fairly uniform.
- Low velocities and densities in fracture/fault zones.
- Disseminated hematite alteration zones show increased magnetic susceptibility.

The Missi conglomerates exhibit distinctively different geophysical characteristics from the Missi sediments. The radioelement content is lower than in Missi sediments and the densities and velocities are higher than the Missi sediments.

5.1.2 Gabbros

Unusual physical rock properties are observed in the Boundary Intrusion (BI) Gabbros.

- The radioelement concentration (K, U, Th) is generally high and this is an uncharacteristic signature of gabbros.
- The magnetic susceptibility in BI gabbros is quite variable but generally they are highly magnetic.
- Sheared and altered gabbros exhibit the highest susceptibilities and low gamma ray activity suggesting secondary enrichment of magnetic minerals and depletion of the radioelement, potassium.

5.1.3 Basaltic Rocks

- Most of the basalts have the lowest natural gamma ray values. However, quartz-phyric basalts exhibit higher K content, lower densities and lower velocities than unaltered basalts
- Generally the densities and velocities are higher than what is observed in the Missi sediments and other volcanics.

- The amygdaloidal basalts have high magnetic susceptibilities compared to the rest of basalts whereas foliated, veined and altered basalts show lower magnetic susceptibilities.
- Some basalt dykes are non-magnetic and exhibit low magnetic susceptibilities.

5.1.4 Diorites

- High natural gamma ray values mostly due to elevated K content
- Densities and velocities are lower than in basalts.
- There is significant variability in some of the geophysical signatures in diorites. Some diorite intersections have higher density, higher velocity, and extremely low gamma ray values whereas others have fairly high gamma ray values.

5.1.5 Felsic volcanic flows and volcanoclastics

- The most characteristic geophysical signature in the felsic volcanics is high gamma ray activity that is due primarily to high K content.
- Most these volcanics have undergone sericitic alteration and this alteration is generally accompanied by elevated uranium content.
- The densities and P-wave velocities are low compared to the basic intrusives and other basic volcanics.

5.2 Alteration

There are several types of alteration observed in the Flin Flon mining camp that are associated with mineralization and include sericitization, silicification, carbonatization and chloritization. The major alteration that is closely associated with mineralization is sericitization and it is characterized by elevated K content. There is also generally an associated increase in U.

Most of the silicified zones have high radiometric signatures (high gamma ray activity) because they are associated with sericitic alteration. Carbonate altered zones are characterized by extremely low gamma ray activity and also the magnetic susceptibility signature is low. There is a depletion of potassium and probably oxidation of magnetic minerals to non-magnetic oxides during the alteration process.

Fault zones with chlorite and carbonate alteration have elevated K and U.

Epidote alteration; however, appears to be characterized by higher magnetic susceptibility mostly due to the development of secondary magnetic.

The acoustic properties of the rocks are highly affected by alteration. Generally, altered zones exhibit low densities and low P-wave velocities.

5.3 Mineralization

Major sulphide minerals in the Flin Flon mining camp include pyrrhotite, pyrite, chalcopyrite and sphalerite. Magnetite is a major oxide in mineralized zones. Only one of the drillholes intersected significant mineralization.

The mineralized zones are highly conductive and hence form a good target for various electrical and electromagnetic surveying techniques. The zones also exhibit high magnetic susceptibilities because of their association with magnetite and pyrrhotite.

6.0 CONCLUSIONS

Based on the results obtained from geophysical logging a recommendation was made that sufficient impedance differences exist in the Flin Flon camp stratigraphy to merit conducting a seismic experiment. Promise in differentiating different stratigraphic units is also shown.

7.0 ACKNOWLEDGEMENTS

We wish to thank Bill Hyatt and Yves Blanchard, formally of the GSC borehole logging section, for the excellent job they did in the data acquisition. Special thanks are also due to Barbara Elliott, who working as a volunteer, did the data processing. Many thanks go to Hudbay Minerals Inc. and Alan Vowles for providing and expediting the logistics during the data acquisition and also for providing the geological data. DGI Geosciences collected some of the datasets presented in this report under contract to Hudbay. This report is a contribution to the Targeted Geoscience Initiative (TGI-3 Flin Flon geological mapping project) 2005–2010.

8 REFERENCES

Ames, D.E., Tardif, N., MacLachlan, K., and Gibson, H.L., 2002. Geology and hydrothermal alteration of the Flin Flon-Triple 7-Callinan VMS Horizon hanging-wall stratigraphy: Flin Flon Targeted Geoscience Initiative; in Summary of Investigations 2002, Volume 2, Industry Resources, Misc. Rep. 2002-4.2, CD-ROM, Paper B-3, 12p.

Bristow, Q. and Bernius, G., 1984. Field evaluation of a magnetic susceptibility logging tool; in Current Research, Part A, Geological Survey of Canada, Paper 84-1A, p. 453-462.

Bristow, Q. and Conaway, J.G., 1984. Temperature gradient measurements in boreholes using low noise high resolution digital techniques; *in* Current Research, Part B, Geological Survey of Canada, Paper 84-1B, p. 101-108.

Bristow, Q., 1985. A digital processing unit for the GeoInstruments magnetic susceptibility sensors, with analogue and RS-232C outputs; *in* Current Research, Part B, Geological Survey of Canada, Paper 85-1B, p. 463-466.

Gibson, H.L., Pehrsson, S., Lafrance, B., DeWolfe, Y.M., Syme, R-L., Bailes, A., Gilmore, K., Devine, C., Simard, R., MacLachlan, K., and Pearson, B., 2011. The volcanological and structural evolution of the paleoproterozoic and structural evolution of the Flin Flon and Snow Lake Mining districts; *in* Field Trip Guidebook, Field Trip 3B, GAC-MAC-SEG-SGA Joint Annual Meeting, Ottawa, Ontario.

Killeen, P.G., 1982. Borehole logging for uranium by measurement of natural gamma radiation - a review; International Journal of Applied Radiation and Isotopes, Vol. 34, No. 1, p. 231-260.

Killeen, P.G., 1986. A system of deep test holes and calibration facilities for developing and testing new borehole geophysical techniques; *in* Borehole Geophysics for Mining and Geotechnical Applications, *ed.* P.G. Killeen, Geological Survey of Canada , Paper 85-27, 1986, p. 29-46.

Killeen, P.G. and Mwenifumbo, C.J., 1988. Downhole assaying in Canadian mineral deposits with the spectral gamma-gamma method; in Current trends in nuclear borehole logging techniques for elemental analysis, IAEA-ECDOC-464, p. 23-29.

Larsen, E.S. and Gottfried, D., 1960. Uranium and thorium in selected suites of igneous rocks. American Journal of Science, Bradley Volume, Vol. 258_A, 1960, p.151-169

Mwenifumbo, C.J., 1989. Optimization of logging parameters in continuous, time-domain induced polarization measurements. *in* Proceedings of the Third International Symposium on Borehole Geophysics form Mineral, Geotechnical, and Groundwater Applications, Oct. 2-5, Las Vegas, Nevada, vol. 1, p. 201-232.

Mwenifumbo, C.J., 1993. Temperature logging in mineral exploration. Journal of Applied Geophysics, 30:297-313.

Mwenifumbo, C.J. and Killeen, P.G., 1987. Natural gamma ray logging in volcanic rocks: the Mudhole and Clementine base metal prospects; *in* Buchans Geology, Newfoundland, ed. R.V. Kirkham; Geological Survey of Canada, Paper 86-24, Report 16, p. 263-272.

Paillet, F.L. and Cheng, C.H., 1991. Acoustic Waves in Boreholes. CRC Press, Boca Raton, Florida, 264 p.

Pehrsson, Sally. 2007. Personal communication

Pflug, K.A., Killeen, P.G. and Mwenifumbo, C.J., 1994. Acoustic velocity logging at the McConnell nickel deposit, Sudbury area, Ontario: preliminary in-situ measurements; *in* Current Research 1994-C, Geological Survey of Canada, p. 279-286.

Vowles, A., 2007. Drill hole logs and reports, Hudson Bay Exploration and Development Company Limited. Personal communication

Wilson, H.C., Michel, F.A., Mwenifumbo, C.J. and Killeen, P.G. 1989. Application of borehole geophysics to groundwater energy resources; *in* Proceedings of the 3rd International Symposium on Borehole Geophysics for Minerals and Geotechnical Logging, 2-5 Oct., 1989, Las Vegas, Nevada, pp. 317-336.

Syme, E.C. and Forester, R.W. 1977: Petrogenesis of the Boundary Intrusions in the Flin Flon area of Saskatchewan and Manitoba; Canada Journal of Earth Sciences, v. 14, n. 3, p. 444-455

9.1 APPENDIX A – GSC Logging Tools

BOREHOLE GEOPHYSICAL LOGGING SYSTEM

The primary components of the GSC digital logging system are:

1. The borehole probe containing the geophysical sensor
2. The logging cable and winch for sending the signal to the surface instruments, and for sending power down to the probe
3. The depth counter attached to the wellhead pulley for keeping track of the location of the probe in the hole
4. The up-hole analogue-to-digital converter (ADC) to convert the analogue signal to digital form for recording (specific to individual parameters)
5. The PC-based data acquisition system to acquire, display and store the data

Most modern 'slim-hole' tools, like the GSC system, are 38 to 50 mm in diameter and designed to run in BQ holes or larger. Their logging speed is usually about 6 m/minute and can be run in air- and/or water-filled holes depending on the sensor. The data sampling rate ranges from 1 to 5 samples per second and provides a measurement every 2 to 10 cm along the hole.

The GSC truck-mounted system is equipped with several logging tools (probes) with different sensors that can measure twelve parameters in total. The characteristics of these logging tools and their measuring principles are briefly described below.

A1 SPECTRAL GAMMA-RAY LOGGING

A1.1 Geological Interpretation of Spectral Gamma Ray Logs

Gamma-ray measurements detect variations in natural radioactivity originating from changes in concentrations of the trace elements uranium (U) and thorium (Th) as well as changes in concentration of the major rock forming element potassium (K). Since the concentrations of these naturally occurring radioelements vary between different rock types, natural gamma-ray logging provides an important tool for lithology mapping and stratigraphic correlation (Mwenifumbo and Killeen, 1987). Gamma-ray logs are also important for detecting alteration zones, and for providing information on rock types. For example, in sedimentary rocks, sandstones can be easily distinguished from shale due to the low potassium content of the sandstones as compared to the shales.

In sedimentary rocks, potassium (primarily originating from clay minerals such as illite and montmorillonite) is generally the principal source of natural gamma radiation. In igneous and metamorphic geologic environments, there are three sources of natural radiation (U, Th and K) that may contribute equally to the total number of gamma rays detected by the gamma probe. Often in base metal and gold exploration areas, the principal source of the natural gamma

radiation is potassium because alteration, characterized by the development of sericite (sericitization), is prevalent in some of the lithology units. This results in an increase in the element potassium in these units. This renders sericitized zones excellent targets for gamma-ray logging. Feldspar porphyry sills that contain higher concentrations of K-feldspar minerals also show higher than normal radioactivity in the gamma-ray logs.

The distribution of uranium and thorium is generally linked to the metamorphism and alteration processes. During metamorphism and hydrothermal alteration processes, uranium and thorium may be preferentially concentrated in certain lithology units.

A1.2 Principle of Spectral Gamma-Ray Logging

A gamma-ray probe's sensor is usually a sodium iodide or caesium iodide scintillation detector. Unlike an ordinary gamma-ray tool that only counts the total gamma rays, the spectral gamma-ray tool also measures the energy of each gamma ray detected. K, U and Th produce gamma rays with characteristic energies and thus the individual concentrations of these three radioelements can be estimated.

Potassium emits gamma rays with energies of 1.46 MeV and decays into two stable isotopes (argon and calcium) that are no longer radioactive. Uranium and thorium; however, decay into daughter-product isotopes that are unstable (i.e. radioactive). In nature, uranium decays into a series of about a dozen radioactive elements that finally decay into a stable form of lead. The decay of thorium forms a similar series of radioelements. As each radioelement in the disintegration series decays, it is accompanied by emissions of alpha or beta particles or gamma rays. These gamma rays have specific energies associated with the particular decaying radioelement. The most prominent of the gamma rays in the uranium series originates from the decay of ^{214}Bi (bismuth), and in the thorium series originates from the decay of ^{208}Tl (thallium).

Because there should be an equilibrium relationship between the daughter product and parent, it is possible to compute the quantity (concentration) of parent uranium (^{238}U) and thorium (^{232}Th) in a decay series by counting gamma rays from ^{214}Bi and ^{208}Tl respectively (if the probe has been properly calibrated, Killeen, 1982).

During each second while the probe is moving along the hole, the gamma rays are sorted by energy into an energy spectrum. The number of gamma rays in three pre-selected energy windows centred over ^{40}K, ^{214}Bi and ^{208}Tl peaks in the spectrum is computed, as is the total gamma-ray count. These four numbers represent gamma rays originating from potassium, uranium, thorium and Total Count (TC) detected during that one second of counting time.

These data are recorded along with the depth and displayed on a chart recorder to produce gamma-ray spectral logs. The raw gamma-ray spectral logs (Total Count log, K log, U log and Th log) provide more information than a non-spectral (gross count) log because it is possible to convert them into quantitative logs of percent K, ppm U and ppm Th. This requires that the probe be calibrated in model boreholes with known concentrations of K, U and Th, such as the models constructed by the GSC at the Bells Corners Calibration Facility near Ottawa, Ontario (Killeen, 1986).

Because gamma rays can be detected through steel, logging can be done inside drill rod or casing with just a slight decrease in sensitivity.

A1.3 Spectral Gamma-Ray Logging Equipment

The GSC logging system utilizes gamma-ray spectral data acquisition equipment similar to that found in modern airborne gamma-ray spectrometers. Full 256 channel gamma-ray spectra over an energy range of approximately 0.07 to 3.0 MeV are recorded from a scintillation detector in the probe. The storage media is a 9-track magnetic tape. Scintillation detectors of different materials and of different sizes are used by the GSC. These include:

Name	Composition	Density (g/cm^3)
Cesium Iodide	CsI (Na)	4.0
Sodium Iodide	NaI (Tl)	3.67
Bismuth Germanate (BGO)	$Bi_4 Ge_3 O_{12}$	7.0

Probe housings of outside diameter 1.25" (32 mm), 1.5" (38 mm) or 2" (50 mm), contain detectors of sizes ¾" x 3", 1" x 3", and 1.25" x 5", for use in AQ, BQ, and NQ holes, respectively. The selection of probe (and detector) is determined by the hole diameter. The largest diameter probe that will safely fit into a borehole is selected to maximize the count rate and provide good counting statistics. For smaller probes, the high density (and thus higher efficiency) materials are chosen. These are also associated with higher costs. If the count rate is too low due to extremely low concentrations of K, U and Th, such as is often the case in limestones for example, it may not be possible to produce K log, U log and Th logs. In that case only the Total Count log is produced, which is the count rate of all gamma rays above a preselected threshold energy (usually 100 KeV or 400 KeV). A number of factors determine the logging speeds and sampling times during the acquisition of gamma-ray data. The critical factors considered are the anticipated levels of radioactivity and the size of detector in the probe. Gamma-ray spectral logging is usually done at 3 m/minute but can be done as fast as 6 m/minute or as slow as 0.5 m/minute for more detailed information. At each measurement, the volume sampled is about 0.5 cubic metres of rock surrounding the detector (i.e. 10 to 30 cm radius depending on the rock density).

A2. SPECTRAL GAMMA-GAMMA (SGG) DENSITY LOGGING

A2.1 Geological Interpretation of Density and SGG Logs

The density of rock is affected by porosity, water content and chemical composition. Most of the density variations within igneous and metamorphic rocks are due to variations in mineralogical composition. Rocks with higher percentages of mafic minerals (Fe, Mg silicates) have higher densities than those with higher percentages of felsic minerals (Ca, Na, K, Al silicates). The presence of minerals containing heavy elements such as base metals tends to increase the overall density of the host rock. In sedimentary rocks, density variations may be the result of differing degrees of compaction (induration) rather than changes in elemental composition.

The density/SGG logging tool measures rock density and SGG ratio. The SGG ratio (defined below) is related to the effective atomic number of the rock, which depends on the chemical composition of the rock. The SGG ratio log is particularly useful for detecting base metals since these elements have higher atomic numbers than most rock forming minerals, and can occur in high enough concentrations to significantly increase the effective atomic number of the host rock. The SGG ratio log may also be useful for lithology mapping in areas where the iron content differs significantly between the different rock types.

In ore tonnage and reserve computations, one of the parameters used is the specific gravity and hence knowledge of in-situ densities of the rocks may provide valuable information for ore reserve estimations. The density log is also useful for locating fractures since open fractures intersected by the borehole often appear as low density zones on the density log (Wilson et al, 1989).

A2.2 Principle of Spectral Gamma-Gamma (SGG) Density Logging

A gamma-ray source (e.g. ^{60}Co) emits gamma-rays (1.173 and 1.332 MeV) that interact with the rock formation. The detector counts gamma-rays that are backscattered toward the probe. With a spectral gamma-ray probe, these gamma-rays are sorted into an energy spectrum similar to a natural gamma ray spectral system. The gamma-ray intensity in the energy window from 200 to 500 keV (see A1.2), where the source gamma-ray interaction within the rock mass is predominantly by Compton scattering, is used to determine the densities.

The backscattered gamma-rays contain information about the density as well as the heavy element content that is closely related to the effective atomic number, Z, of the rock formation. A ratio of the high-energy gamma-ray intensities (energy window, 200 – 500 keV) to low-energy intensities (energy window, 50 – 100 keV) (the SGG ratio) of the backscattered gamma-ray spectrum is currently used to determine the heavy element content (ore distribution and estimate base metal concentration) along the borehole.

A2.3 Spectral Gamma-Gamma Density Logging Equipment

The density and SGG ratio (or heavy element indicator) logs are derived from the spectral gamma-gamma probe (Killeen and Mwenifumbo, 1988). The density/SGG tool is essentially a spectral gamma-ray logging tool with the addition of a weak (10 millicurie = 370 MBq) gamma-ray source (e.g. ^{60}Co) on the nose of the probe. The tool has a 23 mm by 76 mm (0.9" x 3") cesium iodide detector which measures gamma rays from the source that are backscattered by the rock around the borehole.

Complete backscattered gamma-ray spectra are recorded in 1024 channels over an energy range of approximately 0.03 to 1.0 MeV. Density information is determined from the count rate in an energy window above 200 keV. Information on the elemental composition or heavy element content is derived from the ratio of the count rates in two energy windows (spectral gamma-gamma ratio, SGG): one at high energy (above 200 keV) and one at low energy (below 200 keV). When there is a change in the density of the rock being measured, the count rates recorded in both windows will increase or decrease due to the associated change in Compton-scattered gamma rays reaching the detector. However, if there is an increase in the content of high Z

(atomic number) elements in the rock, the associated increase in photoelectric absorption (which is roughly proportional to Z^5) will cause a significant decrease in count rate in the low energy window with relatively little change in the high energy window. Since the low energy window is affected by both density and Z, while the high energy window is mainly affected by density, the ratio of the counts in the high energy window to the counts in the low energy window can be used to obtain information on changes in Z. This ratio increases when the probe passes through zones containing high Z materials. Thus the log can be considered as a heavy element indicator, and can be calibrated to produce an assay tool for quantitative determination of the heavy element concentration in-situ along the borehole, without resorting to chemical assaying of the core (Killeen and Mwenifumbo, 1988).

The sample volume is smaller than for natural gamma ray logging since the gamma rays must travel out from the probe, into the rock and back to the detector. A 10 to 15 cm radius around the probe is "seen". Because gamma rays can be detected through steel, logging can still be done inside drill rod or casing with just a slight decrease in sensitivity.

A3 RESISTIVITY LOGGING

A3.1 Geological Interpretation of Resistivity Logs

The electrical resistivity of rocks depends on several factors including the presence of conductive minerals such as base metal sulphides or oxides and graphite in the rock. Most rocks without these minerals are usually poor conductors and their resistivities are governed primarily by their porosity, degree of fracturing, salinity of pore water, degree of saturation of the pore spaces, and to a lesser extent by the intrinsic minerals that constitute the rock. Some alteration processes such as silicification and carbonatization tend to reduce the porosity and hence increase the resistivity of the rock. In igneous and metamorphic rocks, the resistivity log is useful mainly in mapping conductive minerals and fracture zones. In sedimentary rocks, the resistivity log is frequently used in lithologic mapping because changes in lithology are often associated with changes in porosity.

A3.2 Principle of Resistivity Logging

In resistivity logging, two current electrodes are used to inject current into the rock formation and two potential electrodes measure the resulting potential distribution. Several electrode array configurations are used to measure formation resistivity. The resistivity is determined as the ratio of measured voltage to the amount of the injected current multiplied by the geometric factor, a function of the electrode array configuration. Current flow in the formation is dependent on a number of variables including porosity, formation fluid salinity and presence of conductive minerals.

A3.3 Resistivity Logging Tool Description

Resistivity data are acquired with two electrode arrays; 1) a normal array with a current-potential electrode spacing of 40 cm and 2) a 120 cm three-electrode (pole-dipole) array with the potential

dipole spacing equal to 85 cm (Mwenifumbo, 1989). The downhole current and potential electrodes are made of brass, 25-mm long and 38-mm in diameter. Both electrode arrays use a surface return current electrode consisting of a 1-m long steel rod that is generally located approximately 100 m from the drillhole collar. The transmitter on this system is a constant current source, capable of supplying currents up to 20 mA. The volume of investigation depends on the array type and the electrode spacing, but it is larger for the three-electrode array than for the normal array.

Since resistivity measurements are made galvanically, they must be done in uncased, water-filled holes.

A4 MAGNETIC SUSCEPTIBILITY LOGGING

A4.1 Geologic Interpretation of Magnetic Susceptibility Logs

The magnetic susceptibility (MS) of a volume of rock is a function of the amount of magnetic minerals, mainly magnetite and pyrrhotite, contained within the rock. MS measurements can provide a rapid estimate of the ferromagnetism of the rock. These measurements can be interpreted to reflect lithology changes, degree of homogeneity and the presence of alteration zones in the rock mass. During the process of hydrothermal alteration, primary magnetic minerals (e.g. magnetite) may be altered (or oxidized) to weakly or non-magnetic minerals (e.g. hematite). Anomalously low susceptibilities within an otherwise homogeneous high susceptibility (ferromagnetic) rock unit may be an indication of altered zones.

Basic flows and diabase dykes containing higher concentrations of magnetic minerals can be easily outlined from magnetic susceptibility measurements when they occur within a sedimentary sequence that normally contains little or no magnetic minerals.

A4.2 Principle of Magnetic Susceptibility Logging

The magnetic sensor is a coil that is in an electrical bridge circuit energized at a frequency of 1400 Hz. When the probe passes through a magnetically susceptible material the coil inductance changes and causes the bridge to become unbalanced. The bridge is balanced automatically by changing the energizing frequency. The change in frequency is a function of the magnetic susceptibility of the rocks through which the probe passes and is converted into SI susceptibility units (Bristow, 1985, Bristow and Bernius, 1984).

A4.3 Magnetic Susceptibility Logging Tool Description

The magnetic susceptibility parameter is one of the components of the IFG multiparameter probe. The magnetic susceptibility tool consists of a 40-cm long, 38-mm diameter sensor coil. The measured values from the coil are transmitted digitally together with other parameters along the logging cable at a rate of 2 per second. Logging is generally done at 6 m/minute, providing a sample depth interval of 5 cm. Since the measurements are made inductively, this sensor operates inside plastic casing and in dry holes. Susceptibilities within the range from about 100

□SI to 1.0 SI can be measured with this tool. The volume of investigation or `sample volume' is roughly a sphere of 30 cm radius, surrounding the sensing coil in the probe.

A5 INDUCTIVE CONDUCTIVITY LOGGING

A5.1 Geological Interpretation of Conductivity Logs

The electrical conductivity of rocks depends on several factors, including the presence of conductive minerals, such as base metal sulphides or oxides and graphite in the rock. Most rocks without these minerals are usually poor conductors and their conductivities are governed primarily by their porosity, degree of fracturing, salinity of the pore water, degree of saturation of the pore spaces, and to a lesser extent by the intrinsic minerals that constitute the rock. The conductivity log is, therefore, useful mainly in mapping conductive minerals and fracture zones.

A5.2 Principle of Inductive Conductivity Logging

The same principle employed in the measurement of magnetic susceptibility is used for the conductivity measurement.

A5.3 Conductivity Logging Tool Description

Conductivity is also one of the parameters from the IFG multiparameter probe. The sensor design is a single induction coil, similar to the magnetic susceptibility coil, operating at a frequency of 400 Hz. The sensor coil is 40-cm long and 38-mm in diameter. Its response has been optimized for the measurement of the conductivity signal and minimized for the magnetic susceptibility interference.

The measured values from the coil are transmitted digitally together with other parameters along the logging cable at a rate of 2 per second. Logging is generally done at 6 m/minute, providing a sample depth interval of 5 cm. The conductivity measurements are not calibrated into conductivity units and are recorded and presented as volts.

A6 TEMPERATURE LOGGING

A6.1 Geological Interpretation of Temperature Logs

Temperature measurements are used to detect changes in thermal conductivity of the rocks along a borehole or to detect water flow through cracks or fractures. Fractures or shear zones may provide pathways for groundwater to flow if hydrologic gradients exist within the rock mass. Groundwater movements produce characteristic anomalies and their detection may provide information on the location of the fractured rock mass and hence aid in the structural interpretation of the area. The temperature gradient log amplifies small changes in the temperature log, making them easier to detect.

Large concentrations of metallic sulphides and oxides may perturb the isothermal regime locally

since metallic minerals have very high thermal conductivities. This perturbation may be delineated with the high sensitivity temperature logging system (Mwenifumbo, 1993). However, this would be observed only in a thermally ‘quiet’ environment. In areas where there are numerous fracture zones with ground water movements, thermal anomalies due to ground water movements are much larger than those that would be observed due to perturbation caused by the presence of metallic minerals.

A6.2 Principle of Temperature Logging

The IFG temperature sensor consists of a thermistor bead with a 1 second time constant and an equivalent temperature sensitivity of 0.0001 degrees Celsius. The thermistor is located at the bottom of the multiparameter probe so that it enters undisturbed water as the probe moves down the hole. Changes in temperature are recorded as changes in the thermistor electrical resistance that is then converted into true temperatures.

A6.3 Temperature Logging Tool Description

The ultra-high sensitivity temperature probe designed at the GSC has a 10 cm long tip of thermistor beads with sensitivity of 0.0001 degrees Celsius (Bristow and Conaway, 1984). Changes in temperature of the fluid in the borehole are measured and sent as a digital signal to the surface. The signal is then converted into true temperature after correcting for the effect of the thermistor time constants; the temperature gradients are then computed from the temperature data. All temperature logging is carried out during a downhole run so the sensor is measuring the temperature of the undisturbed fluid. The usual logging speed is 6 m/minute with data sampled every 1/5 of a second (approximately every 2 cm). This high spatial resolution of data is necessary if accurate temperature gradients are to be determined from the temperature data.

A7 ACOUSTIC LOGGING

A7.1 Geological Interpretation of Acoustic Logs

The acoustic logging tool can be used to determine compressional (P) and shear (S) wave velocities which can be combined with data from the density logging tool to calculate acoustic impedance, Poisson's ratio, Young's modulus, bulk modulus and shear modulus. These parameters are important to any mining operation. An acoustic tool requires a water-filled hole to make good acoustic 'contact' with the walls of the hole. Some special modifications to the probe are possible (e.g., clamping the probe against the borehole wall - still experimental) for use in air-filled holes.

The physical characteristics of the acoustic velocity probe are described by Pflug et al (1994). The 45 mm diameter probe consists of 2 sections: the transmitter section, and the receiver section, separated by a flexible acoustic isolator 0.5 m long. The manufacturer recommends a logging speed of less than 40 ft/minute (12 m/minute).

A7.2 Principle of Full Waveform Acoustic Logging

In full waveform sonic logging, the full acoustic waveform from a downhole source is recorded by two or more receivers located at different positions on the probe (Pailet and Cheng, 1991). Logs of the velocity of the first arrival in the waveform (P-wave) are determined from the full waveform data. Since P-wave velocities are dependent on lithology they can be useful in lithology mapping. Decreased velocities and amplitudes may indicate the presence of fractures.

The Borehole Geophysics Section of the GSC conducts acoustic velocity logging using a tool with a piezoelectric transducer for an energy source, and two piezoelectric transducer receivers. The difference in arrival times of the compressional waves (P-waves) at the two fixed receivers is converted to a velocity measurement. In addition, the amplitude of the first arrival is recorded as an amplitude log that can be used to give a qualitative measurement of the attenuation factor (Q). The equipment records the full sonic waveform. This makes it possible to reprocess the field data to improve the precision of the first arrival picks, or in some cases, to pick the arrival time of the slower S waves that will provide additional information on the mechanical properties of the rocks.

A7.3 Full Waveform Logging Equipment

The full waveform sonic logging equipment used in the acquisition of the data in the Flin Flon mining camp was manufactured by Mount Sopris Instrument Company (model CLP-4681). The probe is 2.8 metres long, 45-mm in diameter and consists of a single piezoelectric transducer transmitter, with a centre frequency of about 28 kHz, and two piezoelectric transducer receivers separated by about 300 mm. The transmitter-receiver spacings are 0.9 m and 1.2 m (3 ft and 4 ft). The transmitter is separated from the receivers by a flexible acoustic isolator to prevent acoustic energy from travelling directly to the receivers through the probe.

By pulsing the energy source every half second and recording alternately with the two receivers, an average velocity is obtained every second, which, at a logging speed of 3 m/minute, represents a sample every 5 cm in the borehole.

9.2 APPENDIX B – Flin Flon geophysical logging data

The lithology intersected in each of the drillholes is superimposed on the geophysical logs. A lithology legend is presented before each of the geophysical logging data.

The following is a list of the acronyms used for the geophysical log titles.

GAM - Total count natural gamma ray
K - percentage potassium in percent
eU - equivalent uranium in ppm
eTh - equivalent thorium in ppm
MS - magnetic susceptibility in SI
DEN - Density in g/cm^3
VEL - P-wave velocity in kilometres/second
IMP - acoustic impedance, (g/cm^3 * km/s)
RES - 40-cm normal resistivity in Ohm-m
TMP - temperature in degrees Centigrade
TMG - temperature gradient in milli Kelvin/m (degree/cm)

B1 Drillhole FFM001

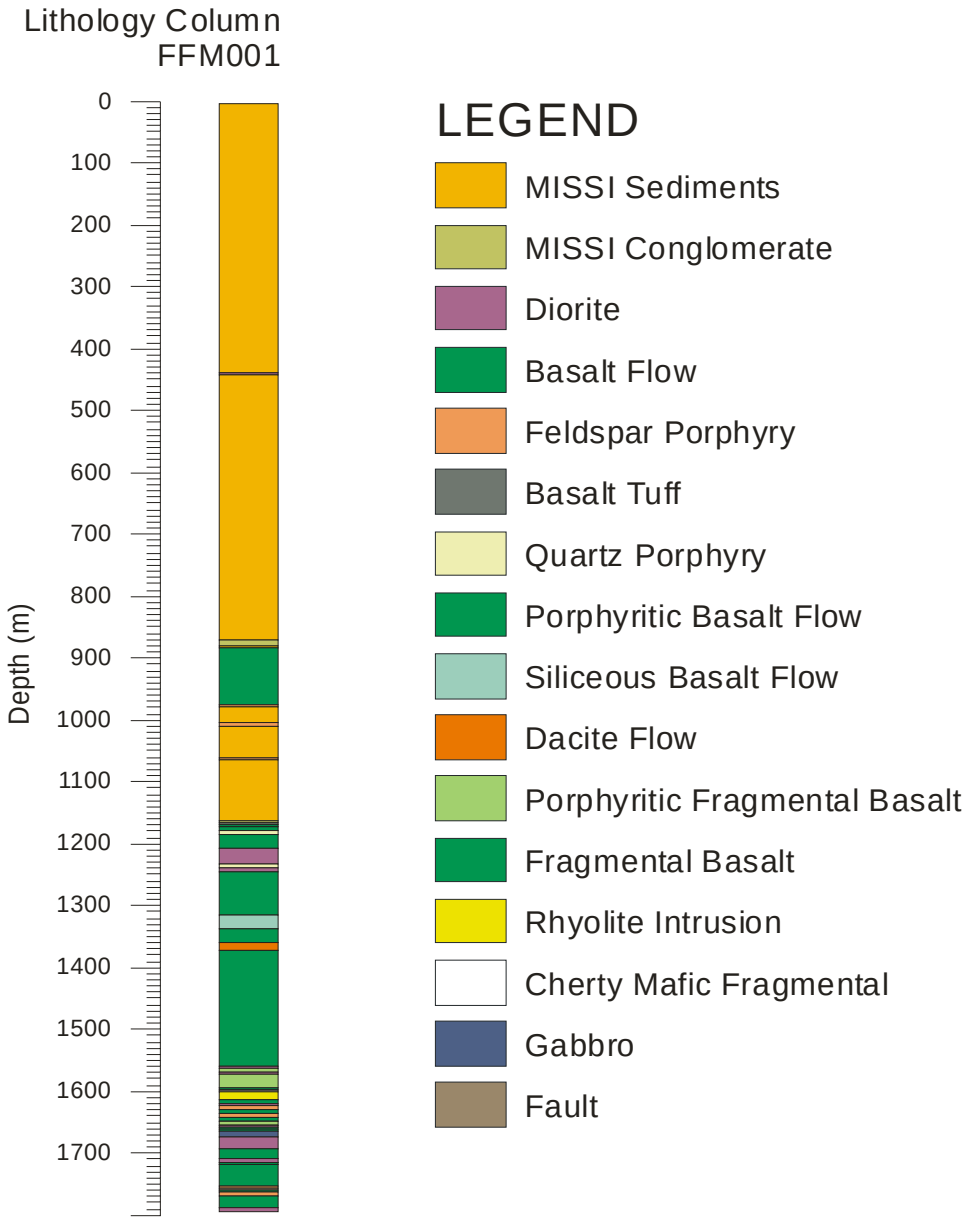

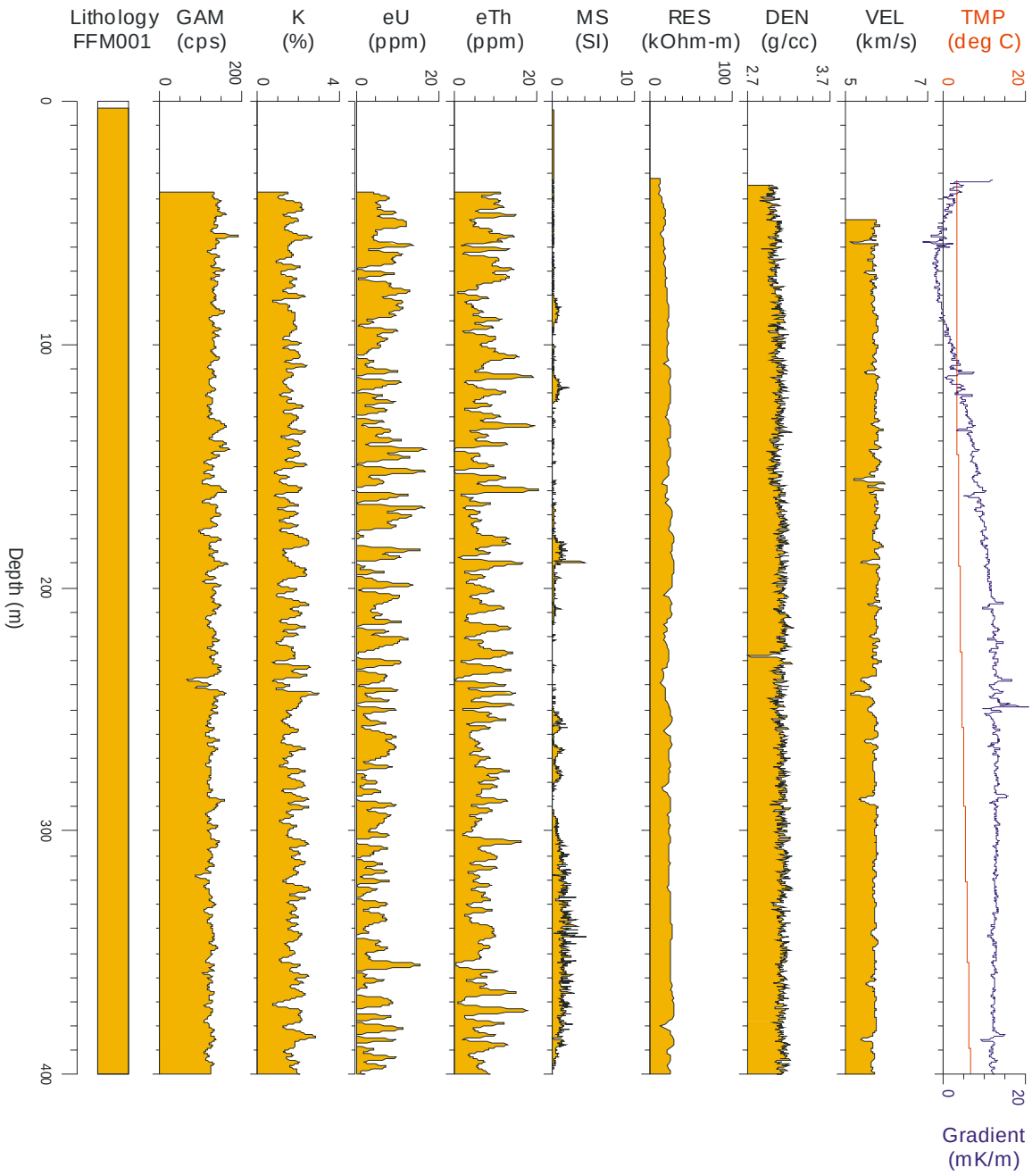
Lithology
FFM001
GAM
(cps)
K
(%)
eU
(ppm)
eTh
(ppm)
MS
(SI)
RES
(kOhm-m)
DEN
(g/cc)
VEL
(km/s)
TMP
(deg C)
Depth (m)
Gradient
(mK/m)

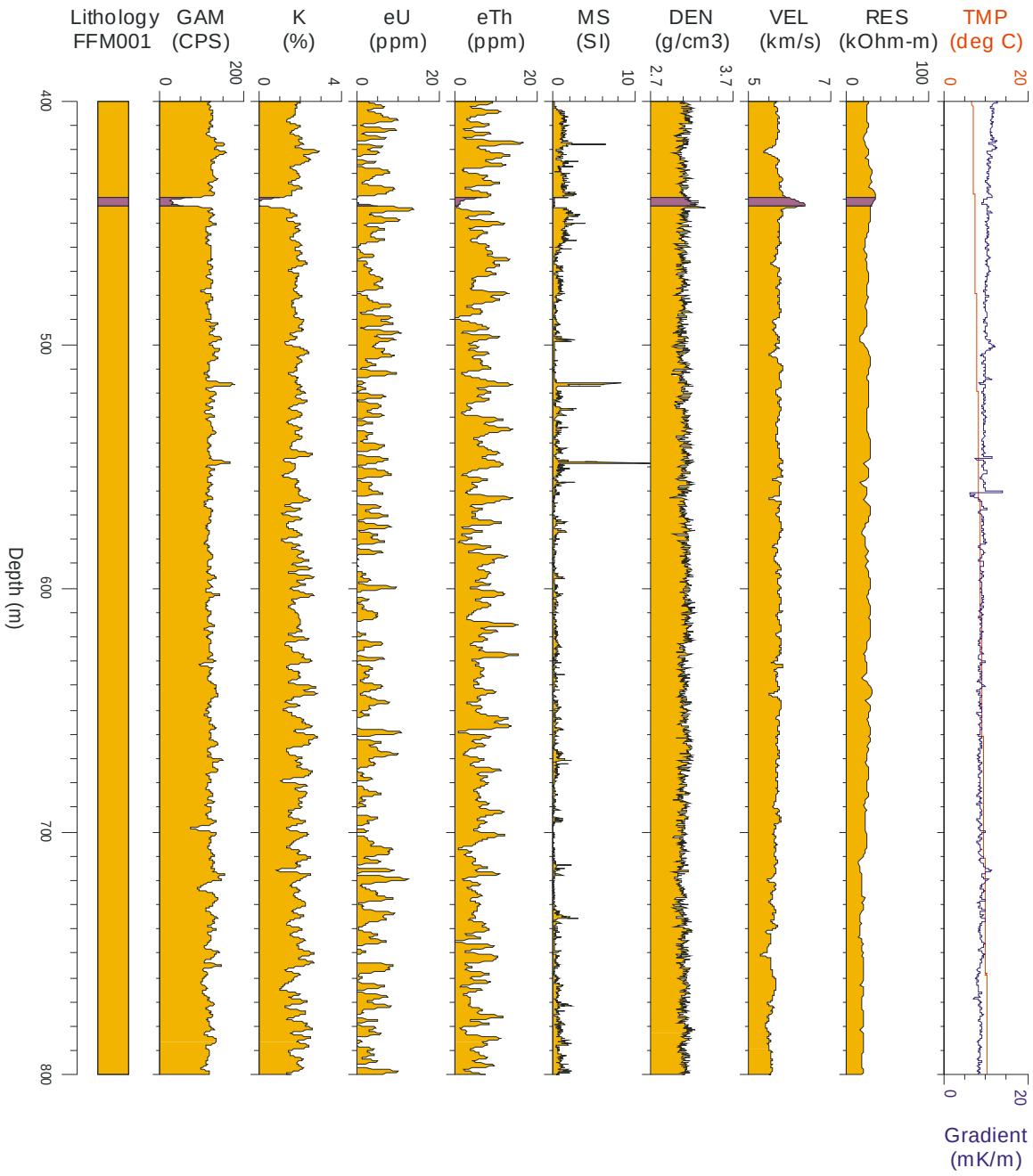
Lithology
FFM001
GAM
(CPS)
K
(%)
eU
(ppm)
eTh
(ppm)
MS
(SI)
DEN
(g/cm3)
VEL
(km/s)
RES
(kOhm-m)
TMP
(deg C)
Depth (m)
Gradient
(mK/m)

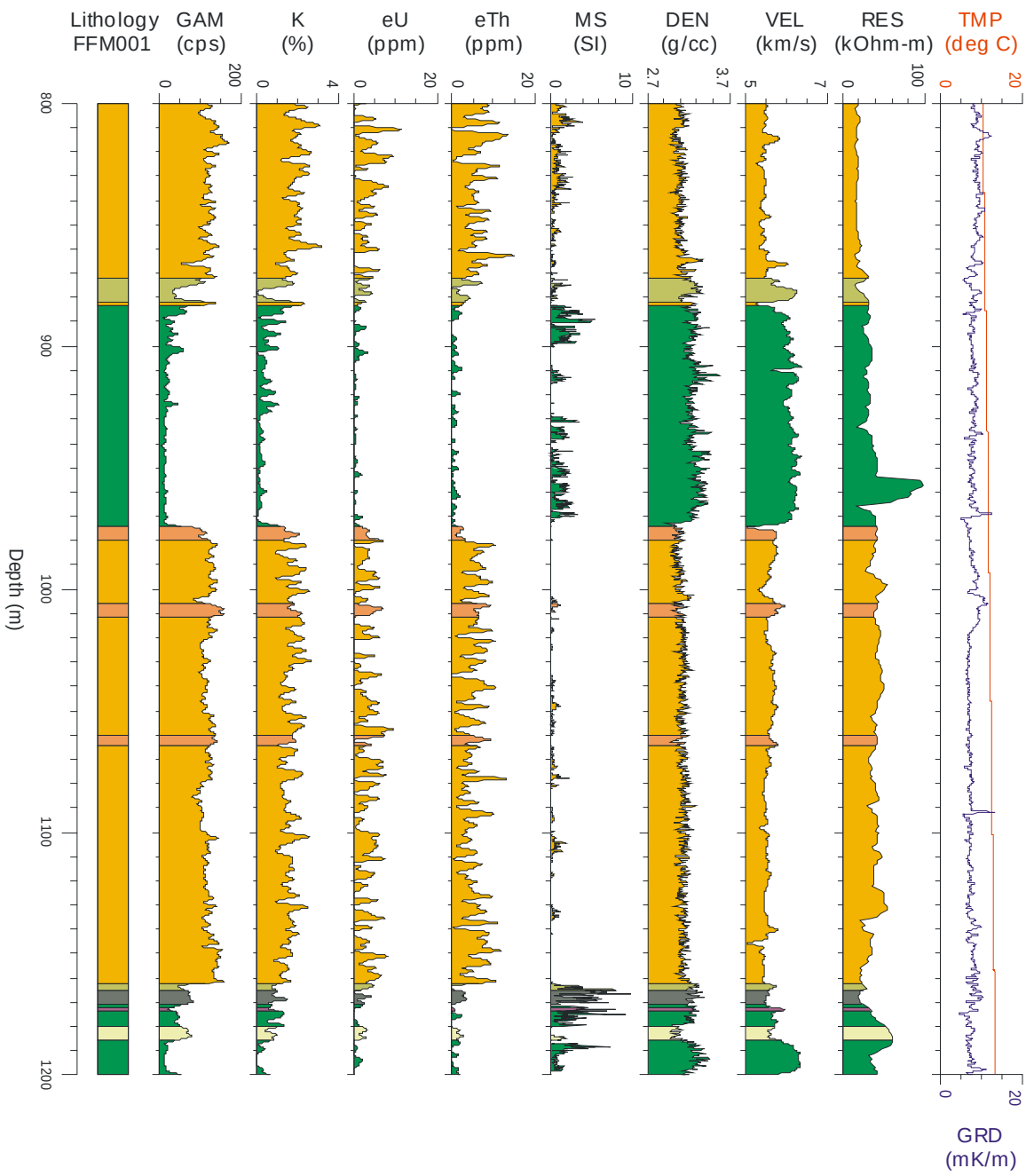
Lithology
FFM001
GAM
(cps)
K
(%)
eU
(ppm)
eTh
(ppm)
MS
(SI)
DEN
(g/cc)
VEL
(km/s)
RES
(kOhm-m)
TMP
(deg C)
GRD
(mK/m)
Depth (m)
800
900
1000
1100
1200
0
200
4
20
10
2.7
3.7
5
7
100
20

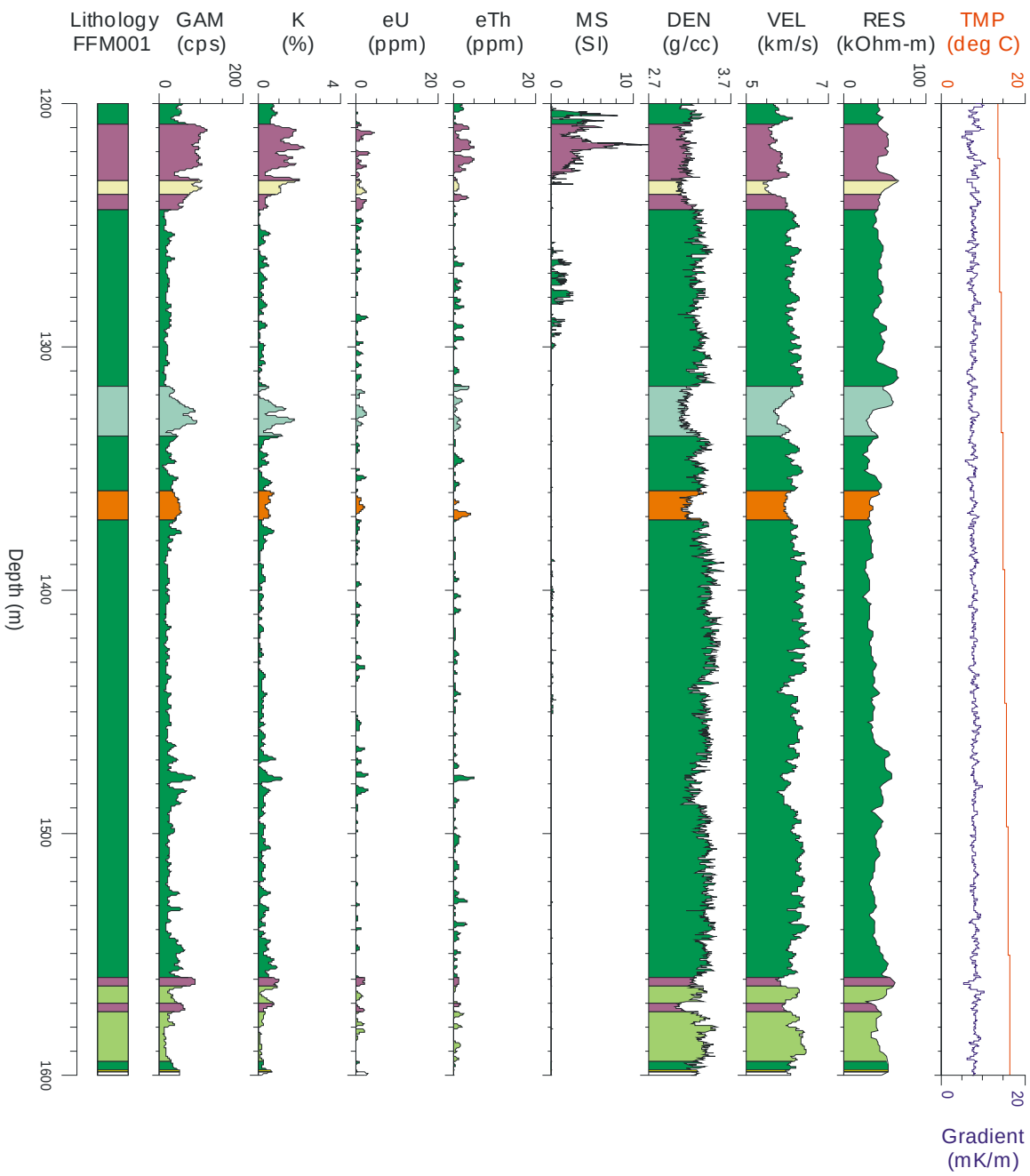
Lithology
FFM001
GAM
(cps)
K
(%)
eU
(ppm)
eTh
(ppm)
MS
(SI)
DEN
(g/cc)
VEL
(km/s)
RES
(kOhm-m)
TMP
(deg C)
Gradient
(mK/m)
Depth (m)
1200
1300
1400
1500
1600

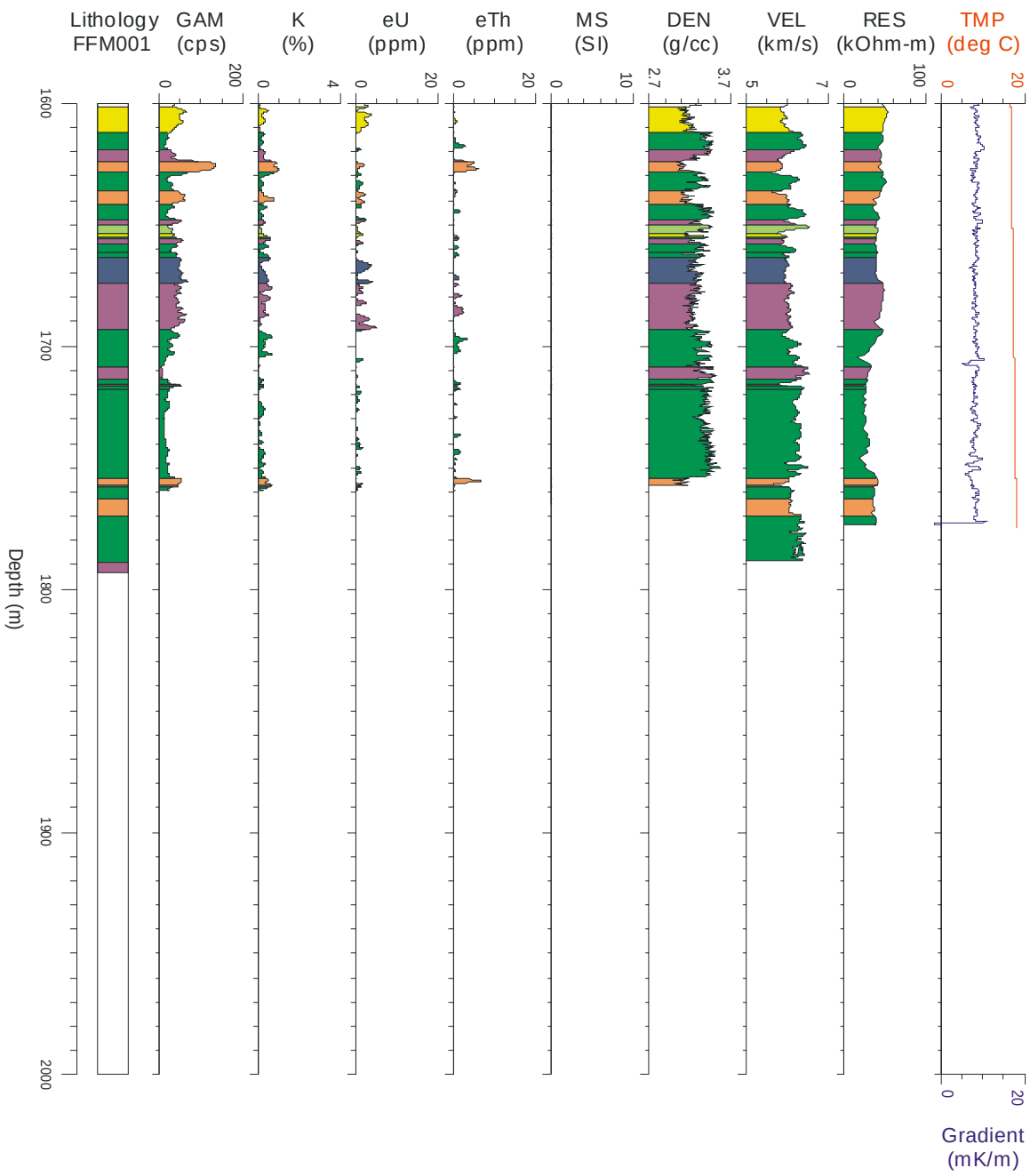
Lithology
FFM001
GAM
(cps)
K
(%)
eU
(ppm)
eTh
(ppm)
MS
(SI)
DEN
(g/cc)
VEL
(km/s)
RES
(kOhm-m)
TMP
(deg C)
Gradient
(mK/m)
Depth (m)
1600
1700
1800
1900
2000

B2 Drillhole 4Q66W3

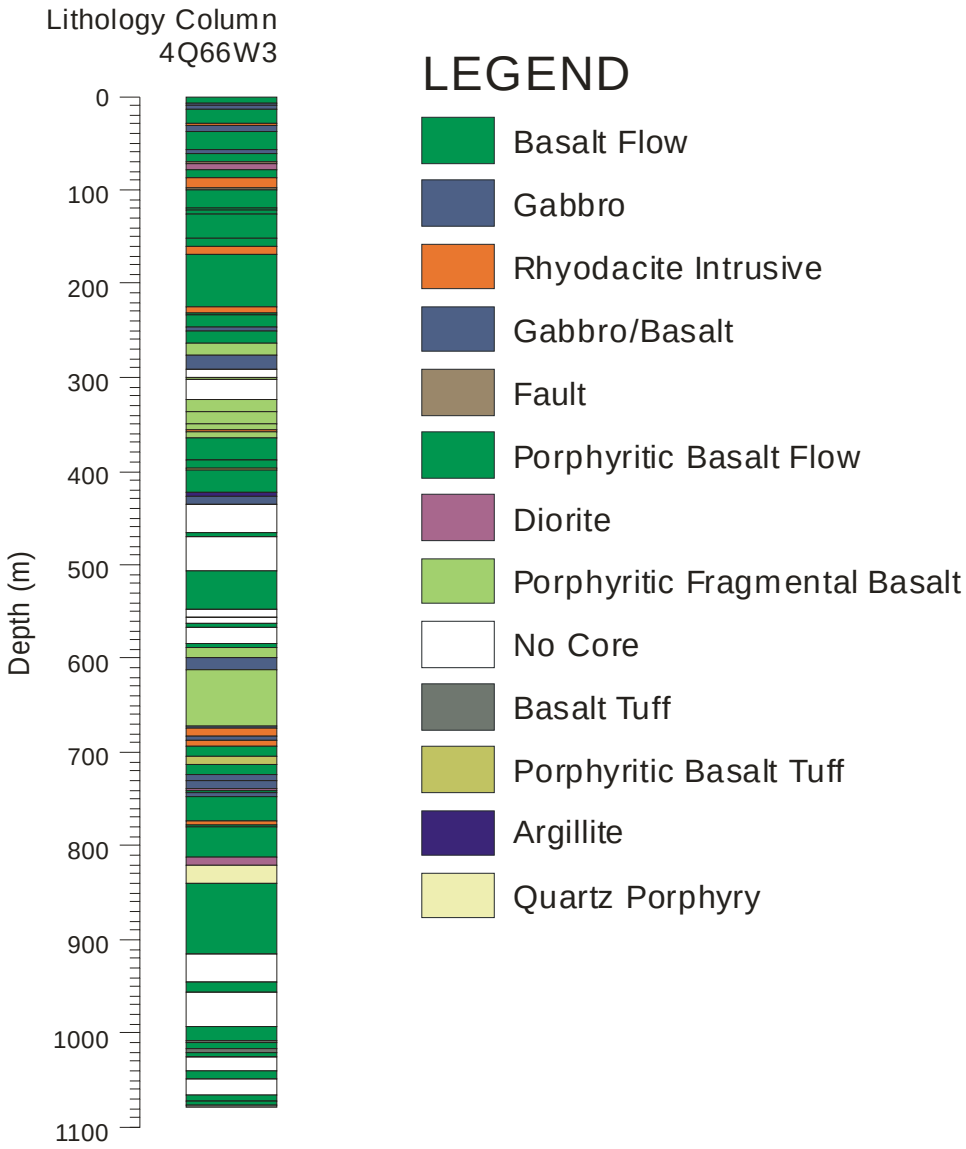

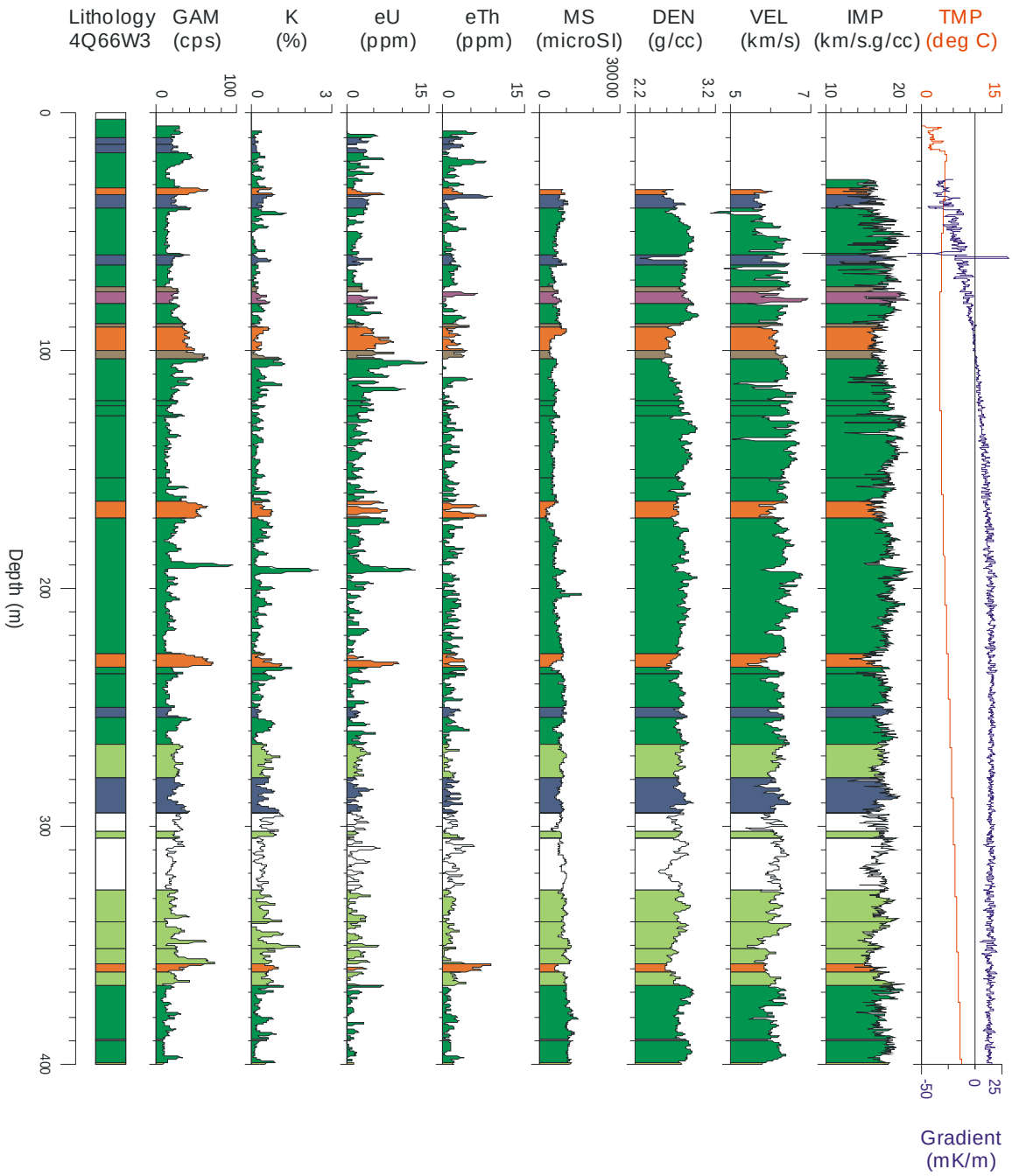
Lithology
4Q66W3
GAM
(cps)
K
(%)
eU
(ppm)
eTh
(ppm)
MS
(microSI)
DEN
(g/cc)
VEL
(km/s)
IMP
(km/s.g/cc)
TMP
(deg C)
Depth (m)
Gradient
(mK/m)

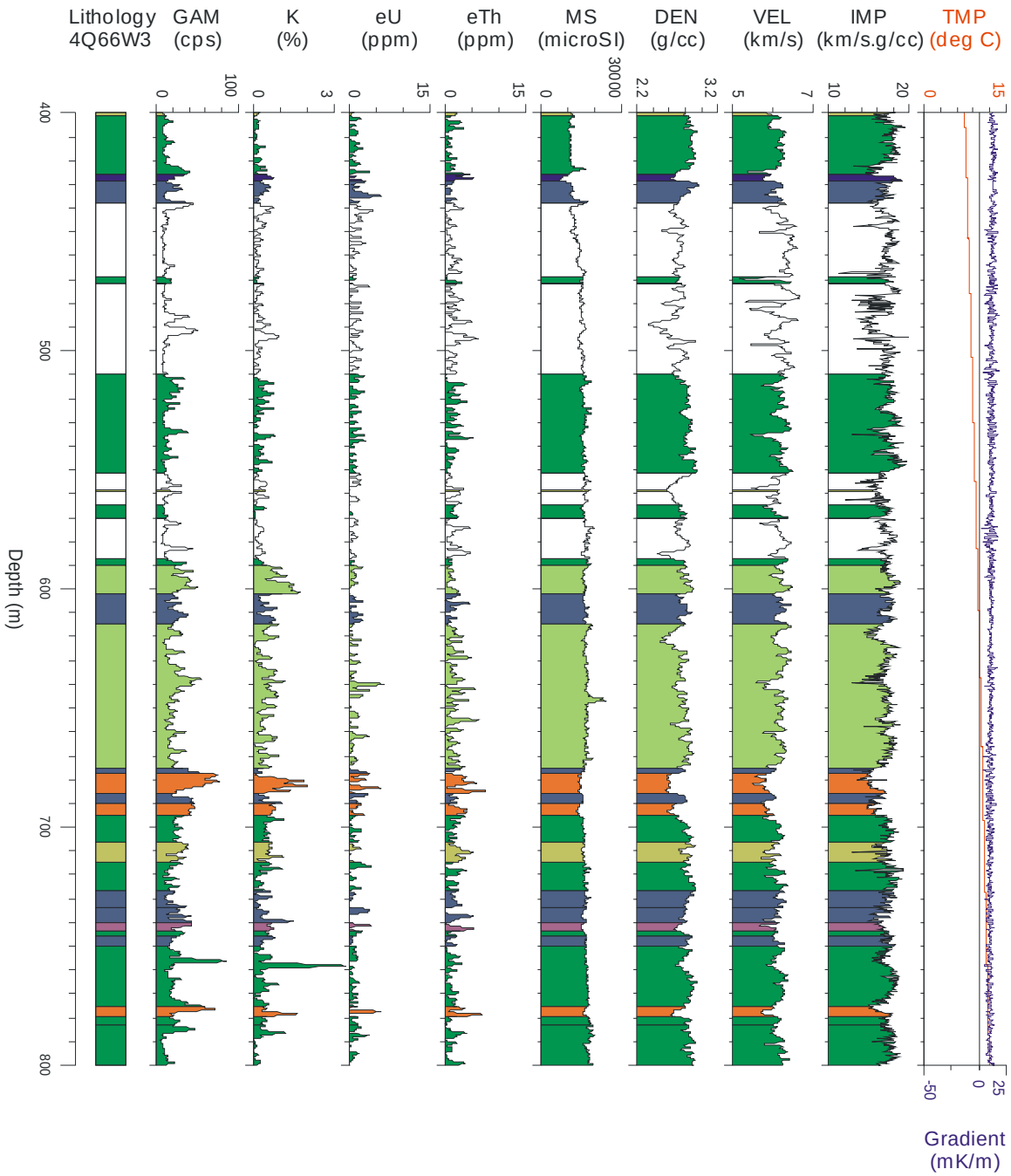
TMP (deg C)
IMP (km/s.g/cc)
VEL (km/s)
DEN (g/cc)
MS (microSI)
eTh (ppm)
eU (ppm)
K (%)
GAM (cps)
Lithology 4Q66W3
Depth (m)
Gradient (mK/m)

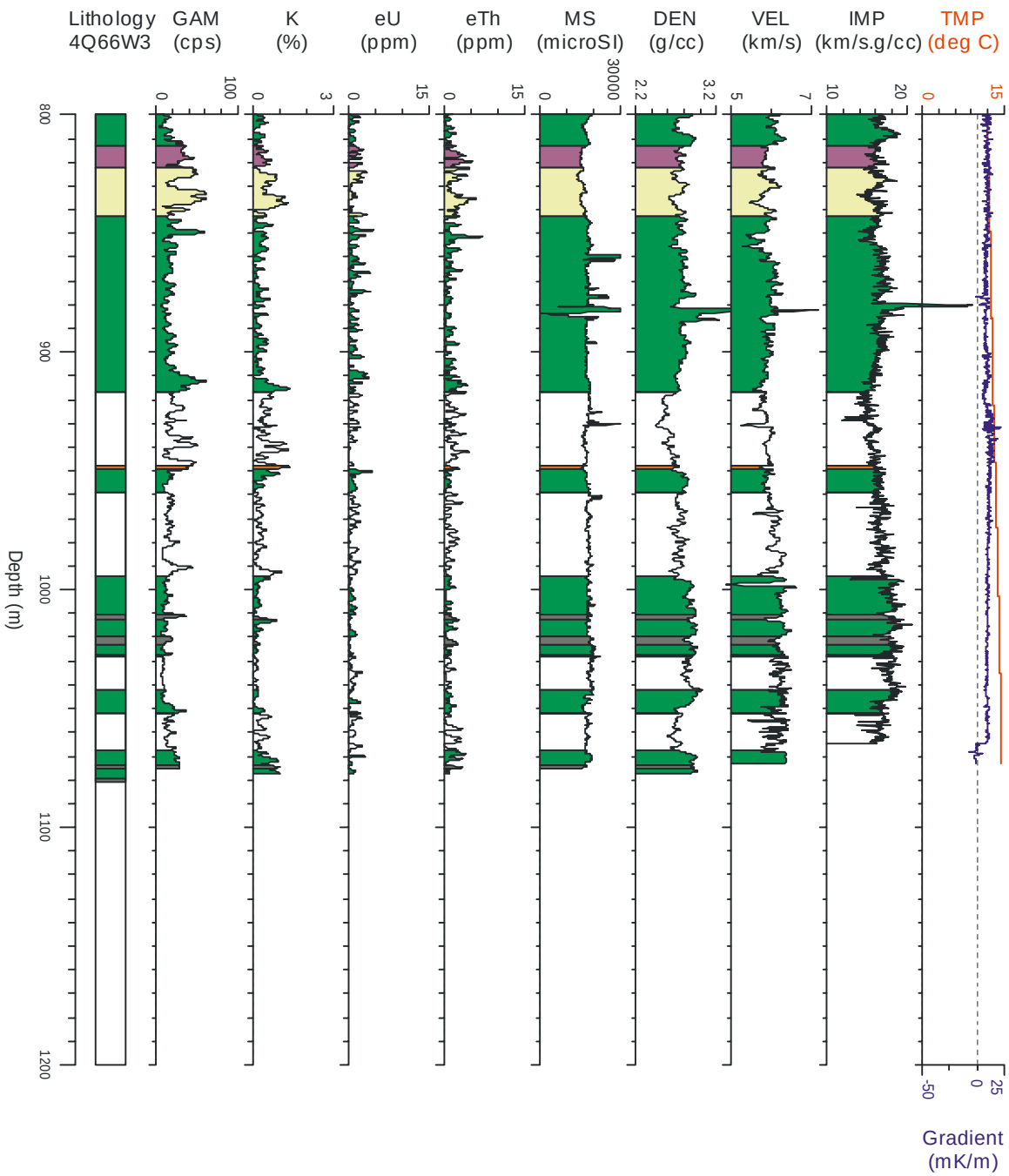
Lithology
4Q66W3
GAM
(cps)
K
(%)
eU
(ppm)
eTh
(ppm)
MS
(microSI)
DEN
(g/cc)
VEL
(km/s)
IMP
(km/s.g/cc)
TMP
(deg C)
Gradient
(mK/m)
Depth (m)
800
900
1000
1100
1200

B3 Drillhole FFS039

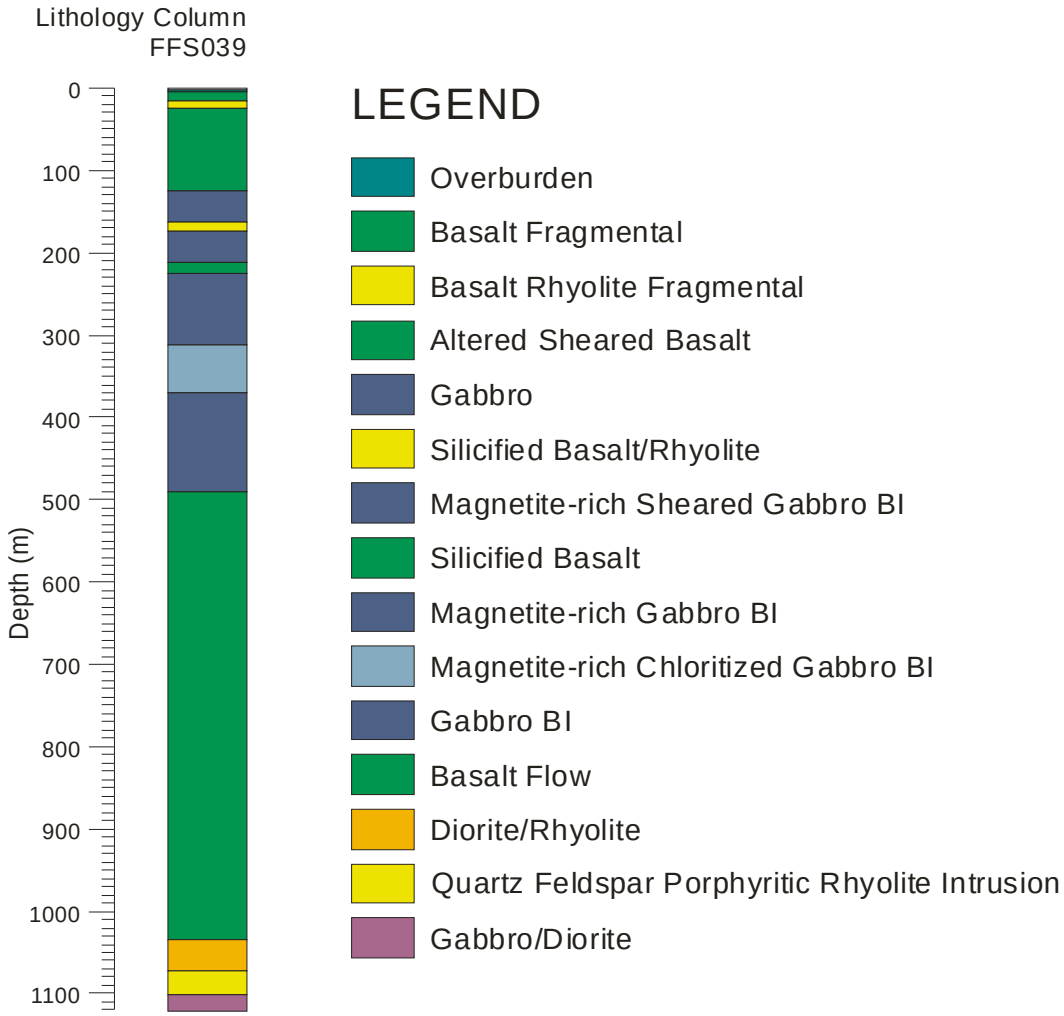

There are three pages of the geophysical logs for drillhole FFS039 plotted in sections of 400 m depth intervals

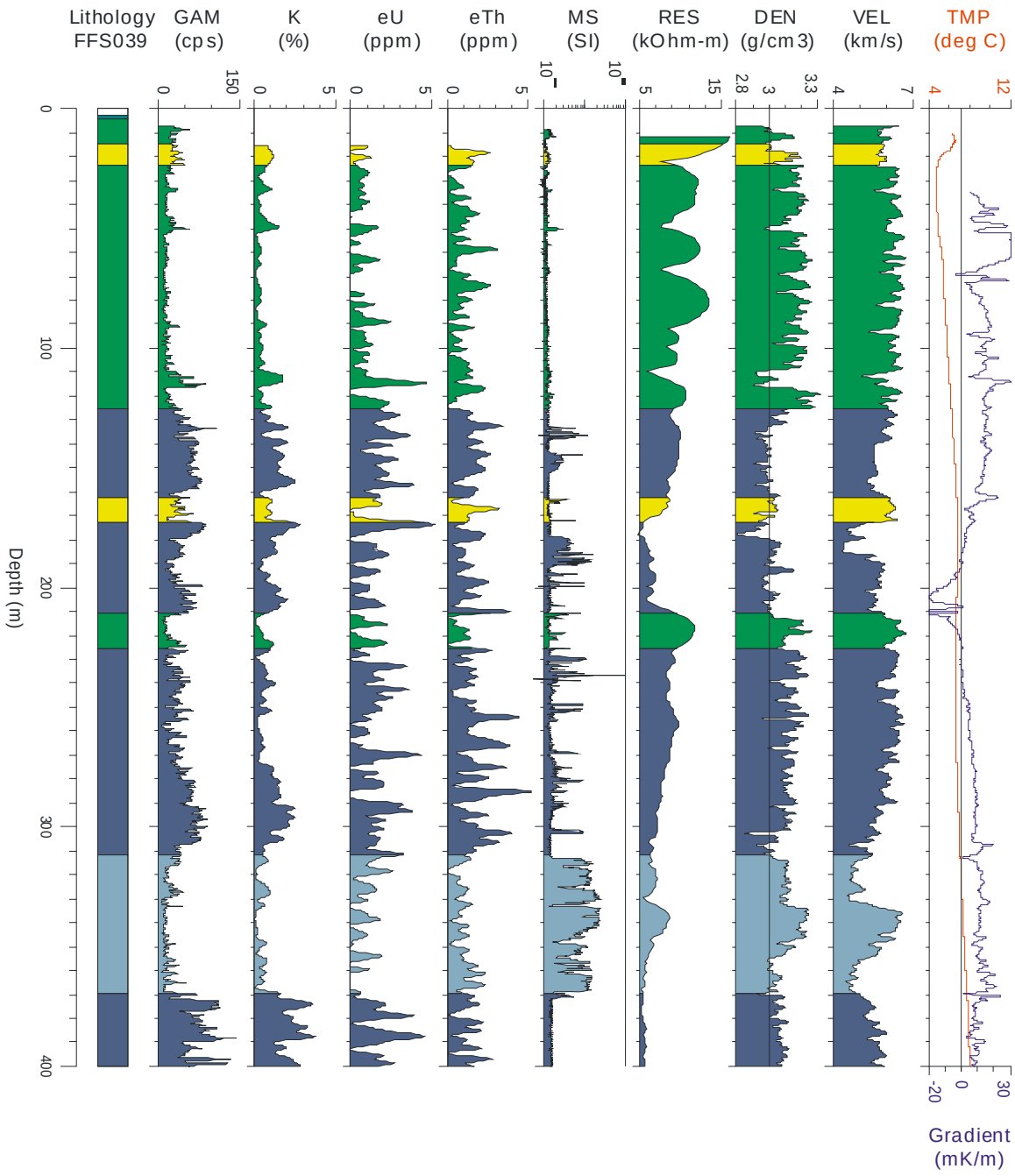
Lithology
FFS039
GAM
(cps)
K
(%)
eU
(ppm)
eTh
(ppm)
MS
(SI)
RES
(kOhm-m)
DEN
(g/cm3)
VEL
(km/s)
TMP
(deg C)
Depth (m)
Gradient
(mK/m)

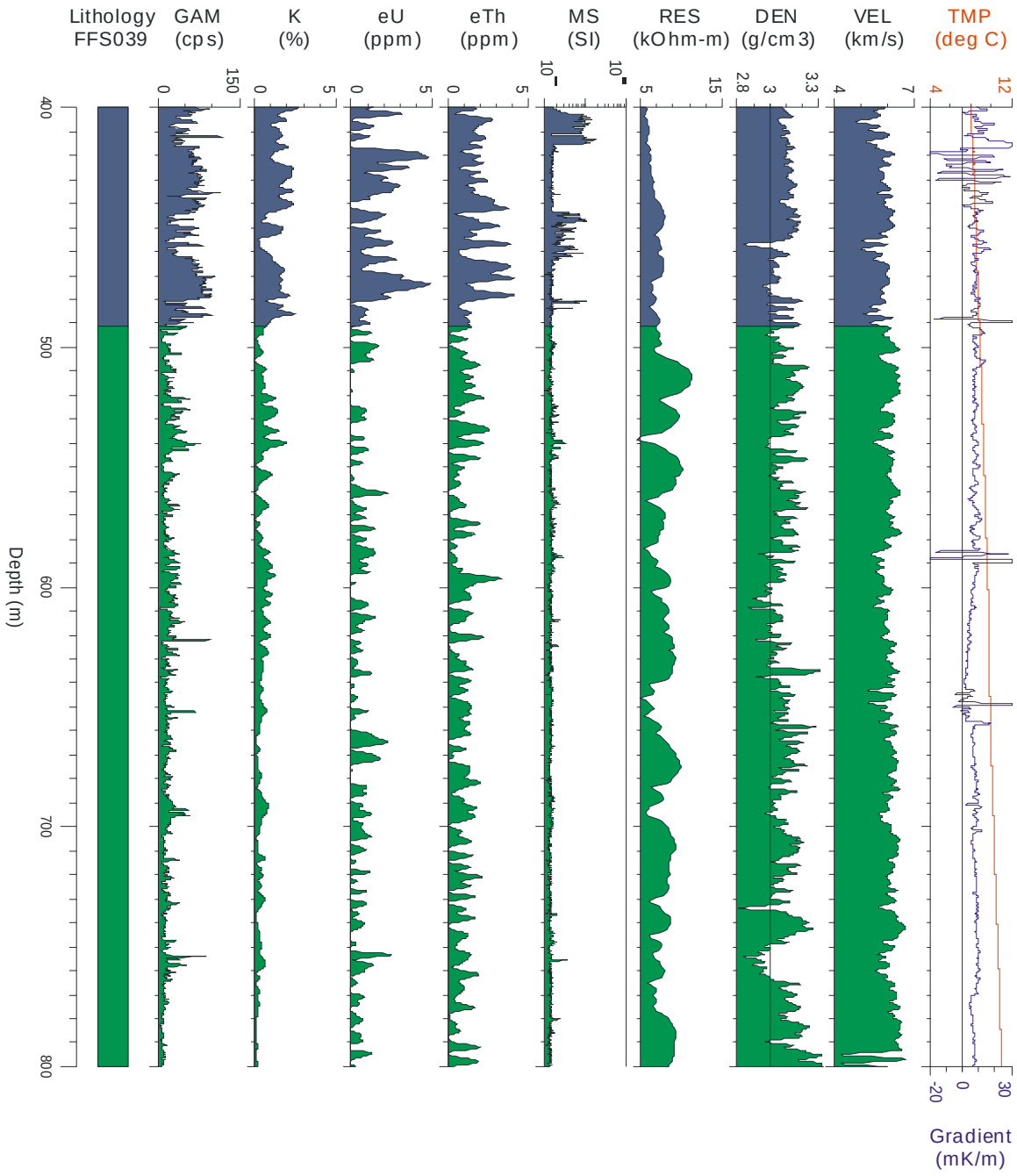
Lithology
FFS039
GAM
(cps)
K
(%)
eU
(ppm)
eTh
(ppm)
MS
(SI)
RES
(kOhm-m)
DEN
(g/cm3)
VEL
(km/s)
TMP
(deg C)
Depth (m)
Gradient
(mK/m)

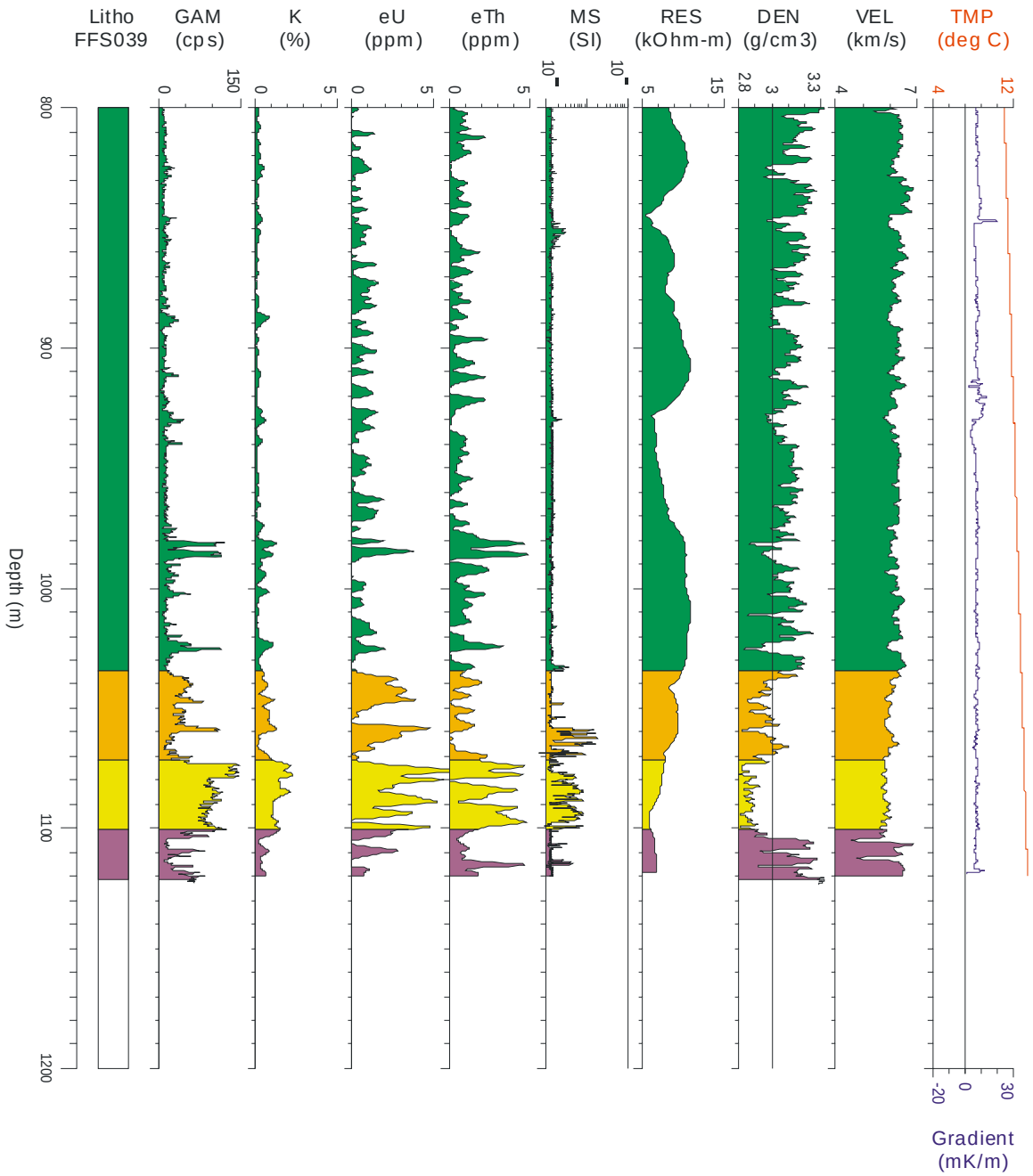
TMP
(deg C)
VEL
(km/s)
DEN
(g/cm3)
RES
(kOhm-m)
MS
(SI)
eTh
(ppm)
eU
(ppm)
K
(%)
GAM
(cps)
Litho
FFS039
Depth (m)
Gradient
(mK/m)

B3 Drillhole 4Q62

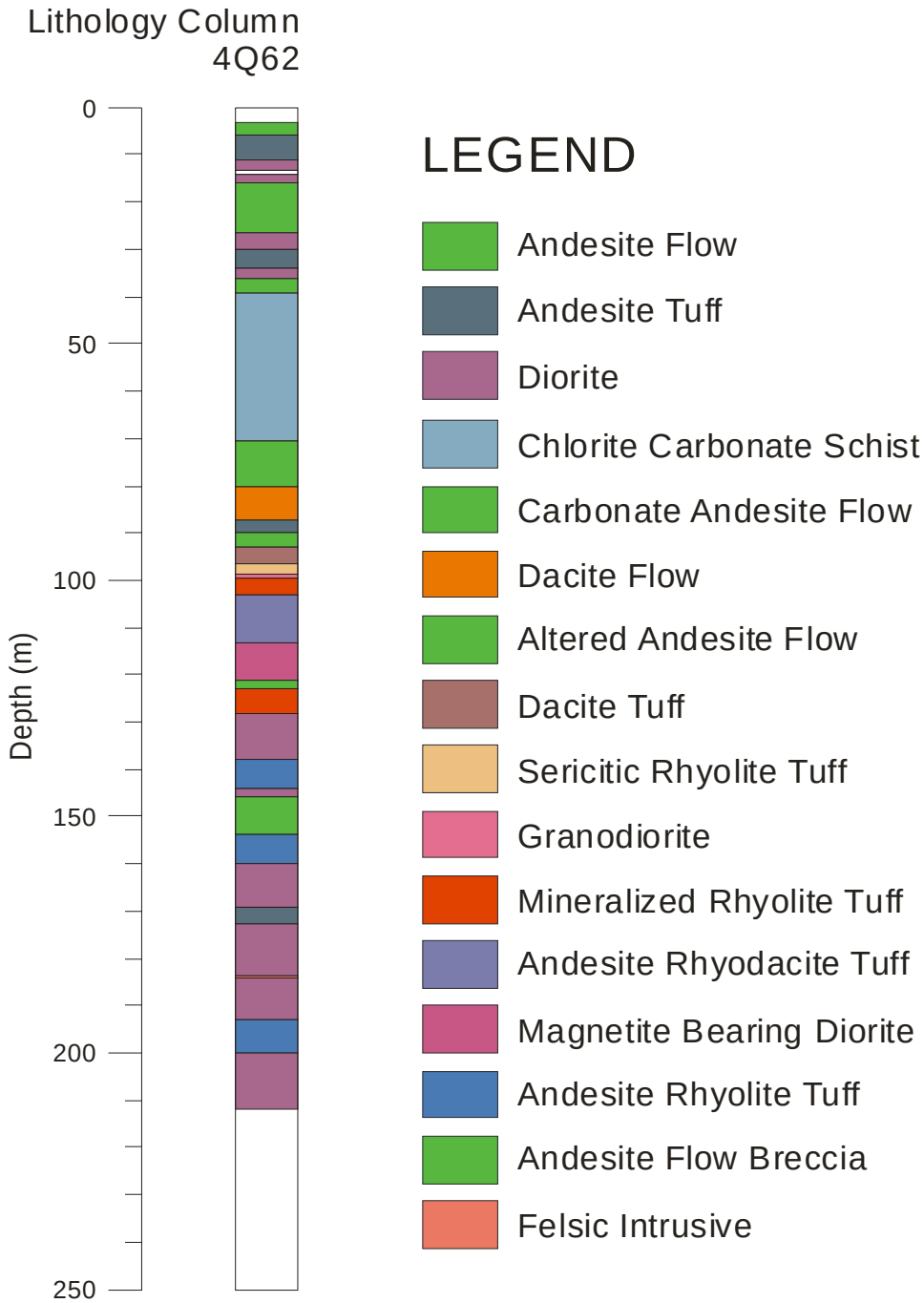

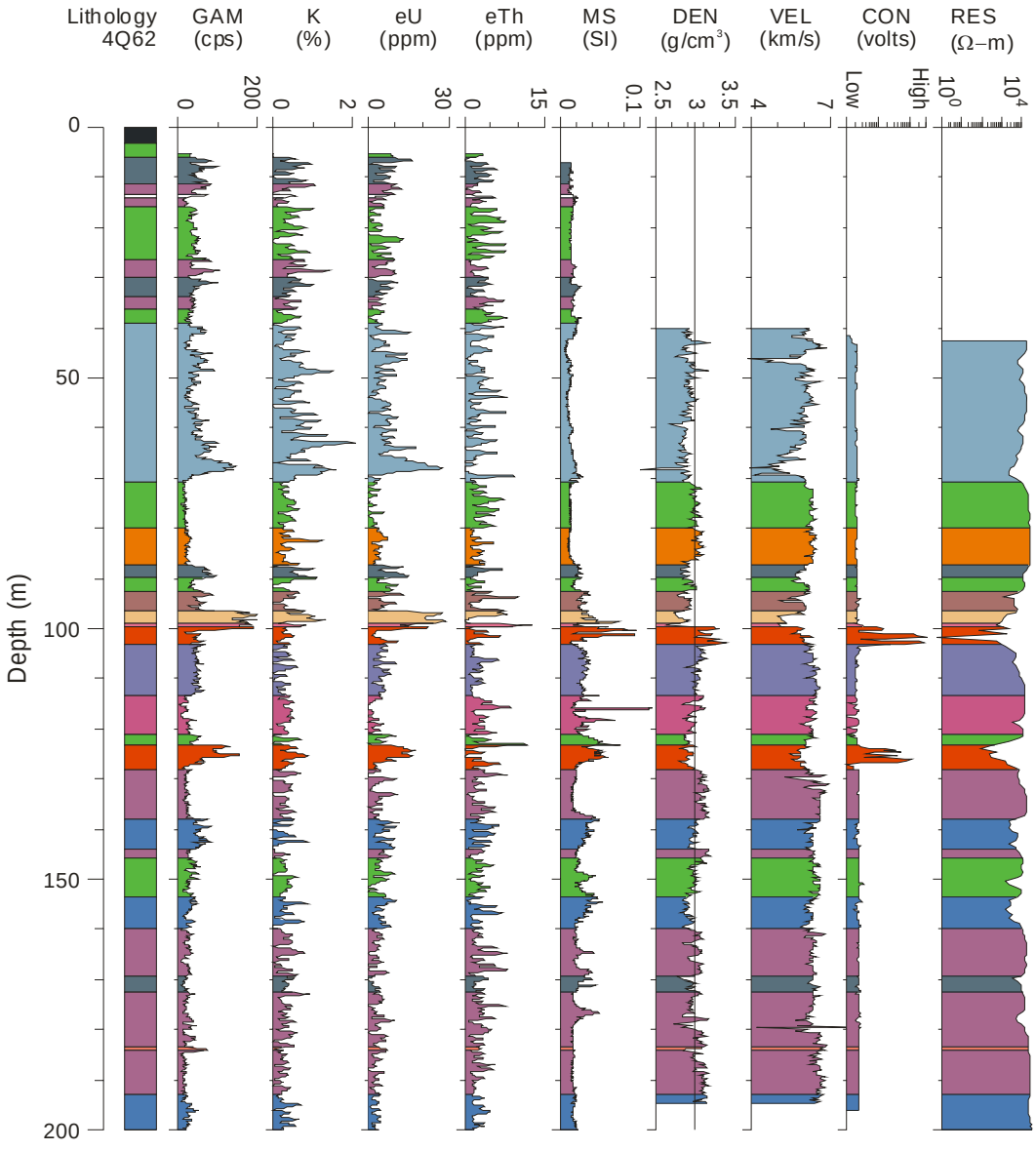
Lithology
4Q62
GAM
(cps)
K
(%)
eU
(ppm)
eTh
(ppm)
MS
(SI)
DEN
(g/cm3)
VEL
(km/s)
CON
(volts)
RES
(Ω–m)
Low
High
Depth (m)
0
50
100
150
200
0
200
0
2
0
30
0
15
0
0.1
2.5
3
3.5
4
7
10^0
10^4